CHARACTERIZATION OF PROTEINS INVOLVED IN THE PRODUCTION OF β-AMYLOID PEPTIDES AND TAU HYPERPHOSPHORYLATION IN FAMILIAL ALZHEIMER'S DISEASE

DISSERTATION

Submitted to the Department of Biology
Faculty of Mathematics, Informatics and Natural Sciences
University of Hamburg, Germany

In Fulfillment of the Requirements
for the Degree of
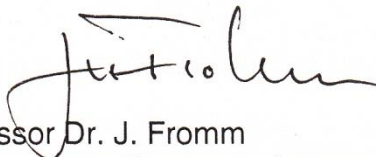
Doctor rerum naturalium

(Dr. rer. nat.)

Alvaro Andres Barrera Ocampo

from Medellin, Colombia

Hamburg, 2012

Genehmigt vom Fachbereich Biologie
der Fakultät für Mathematik, Informatik und Naturwissenschaften
an der Universität Hamburg
auf Antrag von Professor Dr. M. GLATZEL
Weiterer Gutachter der Dissertation:
Professor Dr. C. LOHR
Tag der Disputation: 25. Mai 2012

Hamburg, den 10. Mai 2012

Professor Dr. J. Fromm
Vorsitzender des Promotionsausschusses
Biologie

Universitätsklinikum Hamburg-Eppendorf

Zentrum für Molekulare Neuro-biologie

Research Group:
Neuronal Translational Control

Falkenried 94
20251 Hamburg

Dr. Kent Duncan
Telefon: +49(0)40 7410-56274
Telefax: +49(0)40 7410-53436

Kent.Duncan@zmnh.uni-hamburg.de
www.zmnh.uni-hamburg.de

Hamburg, 04.04.2012

To whom it may concern:

Alvaro Andres Barrera Ocampo is submitting his doctoral dissertation in English.

The title of his thesis is: 'CHARACTERIZATION OF PROTEINS INVOLVED IN THE PRODUCTION OF β-AMYLOID PEPTIDES AND TAU HYPERPHOSPHORYLATION IN FAMILIAL ALZHEIMER'S DISEASE'.

I hereby certify as a native speaker that the English language used in this thesis is correct.

Kent Duncan, Ph.D.

Universität Hamburg
Universitätsklinikum Hamburg-Eppendorf
Zentrum für Molekulare Neurobiologie
AG Duncan
Falkenried 94 · D-20251 Hamburg

to my wife, my son and my mother,

who offered me unconditional love and support

throughout the course of this thesis

TABLE OF CONTENTS

LIST OF FIGURES

SUMMARY

Alzheimer's disease (AD) is the most prevalent neurodegenerative disease afflicting currently 35 million people worldwide. The two basic variants of AD are sporadic (SAD) and familial (FAD). SAD is characterized by absence of inheritance pattern, while FAD is characterized by autosomal dominant heritability and it is caused by genetic mutation in the genes coding for APP, PS1 or PS2. Mutations in PS1 cause the most severe forms of AD with an early onset of ~45 years. More than 390 families carrying PS1 mutations have been identified, including the worldwide largest group of individuals bearing a missense PS1 mutation consisting of around 5000 members of a Colombian kindred carrying the E280A mutation. The most important pathological hallmarks of AD are senile plaques and neurofibrillary tangles (NFTs). The first are extracellular aggregates of Aβ peptides produced by the proteolytic processing of APP made by secretases, and the latter are intracellular aggregates of hyperphosphorylated Tau protein as consequence of altered activity of Tau-protein kinases.

The main goal of this work was to establish the expression profile of proteins involved in the production of Aβ and Tau hyperphosphorylation as potential biomarkers for different variants of AD. We have found that in FAD the expression of APP was altered as consequence of its increased processing. Although no major changes were observed in the expression profile of α- and β-secretases, variations in PS1 indicated that this protein is a determinant for the development of the disease in both AD variants. We also observed that in FAD the expression of PrP^c was modified, while in SAD no changes were observed. The differential expression of this protein in FAD and SAD is another point of divergence between both forms of AD and may help to explain the dynamic of the Aβ accumulation and the production of Aβ plaques. In FAD the activation level of GSK3β was decreased in the analyzed areas, while in SAD the activation of this kinase was elevated. This activation profile indicates that the steady-state of this enzyme is regulated in a differential fashion in both AD forms. The activation profile of Erk1/2 was increased in both forms of AD. Based on these facts we propose that Erk1/2 may be involved in the hyperphosphorylation of Tau and the formation of NFTs in FAD and SAD, while GSK3β contributes to this process in SAD, but not in FAD.

Testican-1 is a novel molecule that seems to be involved in the pathogenesis of AD as seen in CSF of affected cases. We show that it associates with Aβ plaques and *in vitro* analysis revealed that Testican-1 decreases Aβ levels in HEK293T cells expressing the APP Swedish mutation. Further analysis showed that neither APP expression nor canonical processing was affected. Also, secretases and Aβ-degrading proteins were unaffected. However, subcellular

localization of APP was altered by Testican-1 transfection and their subcellular localization modified. We conclude that this proteoglycan could regulate the β-secretase activity of cathepsin L and in this way modulate the production of Aβ. The results generated from this study can be used to create new methodologies for diagnosis and eventually treatment of the disease.

1. INTRODUCTION

1.1. Alzheimer's Disease

Alzheimer's disease (AD) is the most prevalent neurodegenerative disease of adult-onset, characterized by progressive impairment in cognition and memory. AD is also the most common type of dementia afflicting currently 35 million people worldwide with projections of increasing fourfold by 2050 (1;2). The largest number of affected individuals can be found in developed countries or regions like the USA, western Europe and China, and developing regions like western Pacific and Latin America (3).

The causes of the AD are still unknown, but the scientific community agrees that multiple factors are involved in disease progression and that a simple cause is improbable. Several risk factors have been shown to be related with the disease. Advanced age is the greatest risk factor for AD and most of the patients are aged 65 or older (4). Other risk factors include family history, being an Apolipoprotein E-ε4 (APOE-ε4) allele carrier, mild cognitive impairment (MCI), cardiovascular disease risk factors (high cholesterol, type 2 diabetes, high blood pressure, smoking, obesity, etc), head trauma and traumatic brain injury (5-10).

The early clinical symptoms include difficulty to remember names and recent events, apathy and depression. Impaired judgment, disorientation, confusion, behavioral changes and speech impairment could be present during disease

progression. Finally, swallowing and walking impairment are often late symptoms (11). These clinical features contribute to the diagnosis of the disease and include the revision of the medical and family history (psychiatric history and history of cognitive and behavioral changes), accompanied by cognitive tests and neurological examinations (12). All this may be complemented by imaging studies (MRI or PET) and the measurement of biomarkers such amyloid-β (Aβ) species and Tau protein in cerebrospinal fluid (CSF) (13).

1.1.1. Sporadic and Familial Alzheimer's Disease

The two basic variants of AD are sporadic (SAD) and familial (FAD). The sporadic AD is characterized by absence of inheritance pattern and according to the age of onset can be classified as either *early-onset* (before 60 years of age) or *late-onset* (after 60 years of age). Familial AD is characterized by autosomal dominant heritability; accounts for probably less than 1% of the AD cases, and the disease tends to develop before 60 years of age (*early-onset*) (14;15). In FAD the cause of the disease is a genetic mutation in the genes coding for the amyloid precursor protein (APP), presenilin-1 (PS1) or presenilin-2 (PS2) (16).

Currently over 32 different missense mutations have been found in APP. Mutations in APP account for 10% to 15% of FAD and most of the cases have an age of onset 45 years. An important number of the mutations occur at the secretase cleavage site or in the transmembrane domain. Examples of this are

the "Swedish" (K670N>M671L) and the "London" (V717I) mutations which are among the most studied APP mutations that lead to the increased production of Aβ and development of AD (15).

Regarding PS1, more than 180 mutations have been identified and are responsible for around 80% of FAD cases. These mutations cause the most severe forms of AD; they have complete penetrance and an early onset of ~45 years (16;17). Mutations in PS1 seem to increase the ratio of Aβ42 to Aβ40 as a result of an increased Aβ42 and decreased Aβ40 production (18). So far more than 390 families carrying PS1 mutations have been identified. However, the worldwide largest group of individuals bearing a missense PS1 mutation is consisting of around 5000 members of a Colombian kindred carrying the E280A mutation (19;20).

In contrast to the mutation in the PS1 gene, missense mutations in PS2 rarely cause early-onset FAD. The onset age among affected members of a family varies highly (21). Currently 18 mutations have been identified in 6 families (22). One of them results in the substitution of a valine for a methionine at the residue 393 (V393M) located within the seventh transmembrane domain (23).

1.1.2. Neuropathogenesis of Alzheimer's Disease

The most important pathological hallmarks of AD are senile plaques and neurofibrillary tangles (NFTs). The first are extracellular aggregates of Aβ peptides and the latter are intracellular aggregates of hyperphosphorylated Tau

protein, a microtubule associated protein (24). Whereas in the amyloid cascade hypothesis genetic, pathologic, and biochemical evidence implicate aggregation of Aβ as a critical early trigger in the chain of events that lead to tauopathy, neuronal dysfunction, and dementia (25), the degree of Tau deposition correlates with the cognitive decline in AD (26;27) questioning the role of Aβ deposition as the trigger for Tau pathogenesis. Initially, the amyloid hypothesis stated that the neuronal dysfunction and death was produced by the toxic effects of the total Aβ load. However, recently it has been suggested that not only Aβ elimination, but also its production can be altered in AD patients. Moreover, new studies indicate that not only Aβ peptides (Aβ40 and Aβ42) contribute to the neuronal dysfunction, but that the oligomeric forms of the protein (small aggregates of two to 12 peptides) are actually more deleterious to brain functions than the Aβ aggregates such as senile plaques (28;29). Aβ peptides can also grow into fibrils, which arrange themselves into β-pleated sheets to form insoluble fibers of amyloid plaques (30).

Postmortem analyses of human brains reveal a characteristic progression of Aβ plaques and a regular pattern of appearance of NFT. The progression of Aβ plaques appearance is correlated functionally and anatomically with affected brain regions (31;32). Aβ aggregation affects first the neocortex, followed by the allocortex and then the subcortex. While the NFTs arise first in the locus coeruleus and enthorinal cortex/limbic brain areas, and then spread to interconnected neocortical regions (27;33). The incidence of plaques and tangles correlates positively in AD, but until now there is no anatomical relationship between lesions. The development of compounds that bind

selectively to protein deposits *in vivo*, such as the Aβ ligand PIB (Pittsburg compound B), will enable the analysis of lesions spreading in AD brains (34;35).

1.2. Molecular mechanism of Amyloid Precursor Protein (APP) processing

The proteolytic pathway involved in the processing of APP has been well characterized using several *in vitro* and *in vivo* models (36;37). APP is produced in large amounts in neurons and metabolized very rapidly (38). After sorting in the endoplasmic reticulum (ER) and Golgi, APP is transported to the axon and synaptic terminals. The processing of APP takes place in the trans-Golgi network (TGN) and from there can be transported to the cell surface or to endosomal compartments. Both steps are mediated by clathrin-associated vesicles. Once on the cell surface, APP can be proteolyzed by α-secretases and the γ-secretase complex in a process that does not generate Aβ and which is known as the *Non-amyloidogenic pathway* (Figure 1). The other possibility is that APP can be reinternalized in clathrin-coated pits in endosomal compartments containing β-secretases and the γ-secretase complex. The result of the interaction with these enzymes is the production of Aβ, which is then released to the extracellular space or is degraded in lysosomes. This process is known as the *Amyloidogenic pathway* (Figure 1)(39-41).

The α-secretase cleavage is mediated by members of the family of desintegrin and metalloproteinase domain proteins (ADAM), with ADAM-9, -10, -17 and -19 being the most likely candidates (42;43). The α-secretase cleavage site lies

within the Aβ sequence and, thus, avoids Aβ formation (44). The α-secretase enzymatic activity generates two fragments. The N-terminal fragment is called secreted APP alpha (sAPPα) and the C-terminal fragment (CTF) is called CTF83 due to the amount of amino acid residues of this peptide (Figure 1). The corresponding cleavage of CTF83 by the γ-secretase complex generates a small peptide known as p3 (Figure 1)(45).

The beta-site APP cleaving enzyme 1 (BACE1) is the most important β-secretase in the brain and is responsible for production of the sAPPβ and the CTF99 fragments (Figure 1). The subsequent processing of CTF99 by the γ-secretase complex leads to the formation of Aβ and the amino-terminal APP intracellular domain (AICD)(Figure 1)(45;46).

A group of proteins constitutes the γ-secretase complex. Four proteins are required for this complex: PS1 or PS2, nicastrin (Nct), presenilin enhancer 2, and anterior pharynx defective 1. γ-secretase cleaves APP in its transmembrane region to create Aβ40/Aβ42 or p3 and AICD59/57, a second cut at the ε-cleavage site produces the AICD50 fragment (Figure 1)(47;48).
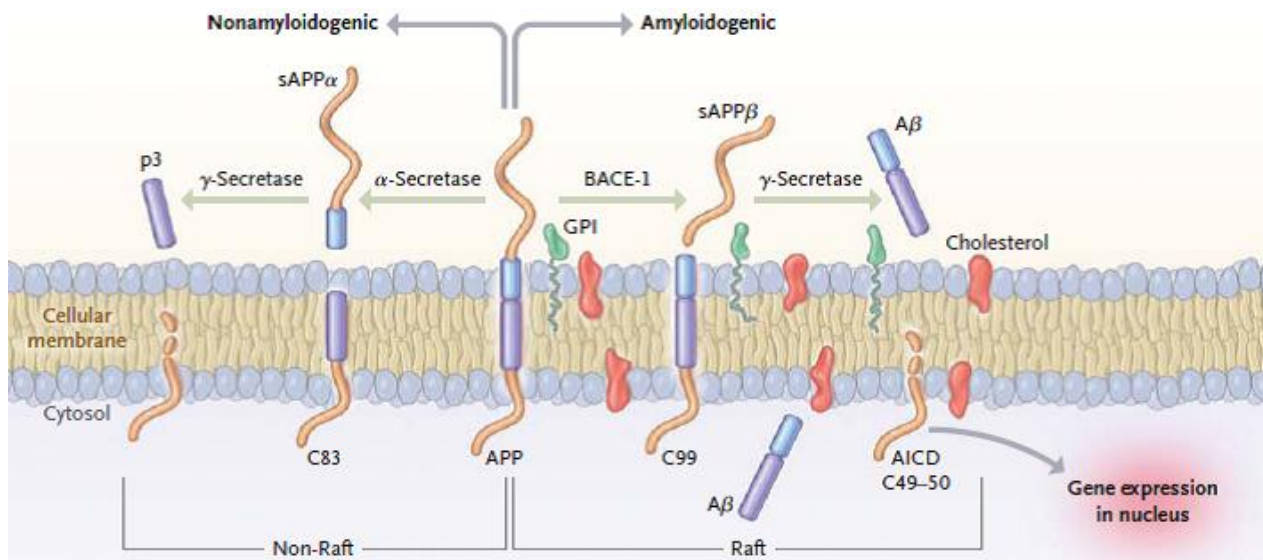
Figure 1. Processing of APP: Non-amyloidogenic and Amyloidogenic pathways. In the Non-amyloidogenic pathway APP is first cleaved by α-secretase (ADAM-10) producing two fragments, sAPPα and C83, the late is cleaved by the γ-secretase complex generating the p3 and AICD peptides. The Amyloidogenic pathway involves the cleavage of APP by β-secretase (BACE1) producing the sAPPβ and C99 fragments; C99 is then processed by the γ-secretase complex producing Aβ and AICD peptides. Source: Querfurth HW, LaFerla FM. Alzheimer's disease. N Engl J Med. 2010 Jan 28;362(4):329-44.

1.2.1. Proteins involved in the processing of APP

Great progress has been made in characterizing the molecules involved in APP processing and the functions of APP cleavage products. As a result, a complex picture has emerged for the physiological and pathological roles of APP. Due to the importance of these molecules for the pathogenesis of AD, they are the target of several therapeutic substances developed to regulate their function and in this way the production of Aβ. For this reason the study of their structure and function has been an active research field during the last 20 years.

1.2.1.1. Structure and function of APP

APP is a single transmembrane protein with a long N-terminal domain and a short cytoplasmatic tail. APP is member of a family of related members that include the amyloid precursor-like proteins (APLP1 and APLP2) which also have a large extracellular domain, but lack the Aβ domain. Human APP is coded by a single gene of 19 exons located on the chromosome 21q21.3; eight isoforms are generated by alternative splicing, out of which there are three main isoforms: the 695 amino-acid form is exclusively expressed in neurons, while the 751 and 770 forms are ubiquitously expressed (41).

APP undergoes post-translational modifications including, *N-* and *O-*glycosylations, sulfations, and phosphorylations (49). The precise physiological function of the protein is unknown; however, some of its processing products have shown to be important for different cellular functions. In this regard, it has been established that sAPPα stimulates neurite outgrowth from mouse hippocampal neurons (50), stimulates proliferation of neural stem cells from embryonic cells (51), increases synaptic density, memory retention and long-term potentiation (LTP) (52;53) and it may function as metallochaperone regulating copper and zinc homeostasis (54). Despite all studies, the function of APP and some of its processing products remains elusive.

1.2.1.2. Structure and function of ADAM-10

Several members of the ADAM family have been involved with constitutive and regulated α-secretase activity responsible for the processing of APP into sAPPα and CTF83 (43). Recently it could be demonstrated *in vitro* that ADAM-10 is the genuine constitutive α-secretase and constitutes a valuable therapeutic target for AD (55). ADAM-10 is a single pass type I membrane protein; in humans the gene is located at chromosome 15q22 and encodes a 748 amino acids protein. Like other ADAMs, ADAM-10 is characterized by the presence of an N-teminal signal sequence; a prodomain, important for the proper folding; a metalloprotein domain; a desintegrin domain; a cystein domain; a transmembrane domain; and a cytoplasmatic domain. ADAM-10 is synthesized in the rough ER and matured in the late Golgi compartment. In the cell surface ADAM-10 is processed and thus becomes catalytically active (56).

ADAM-10 plays an important role during development. Deficiency of this protein leads to embryonic lethality in mice (E9.5) and severe defects in central nervous system (CNS) and heart (57). This protein mediates the cleavage of Notch, a cell surface receptor critical for transcription control during development (58); classic cadherins, a family of homotypic cell-cell adhesion proteins that participates in tissue morphogenesis during development (59;60); and EphrinB2, receptor protein-tyrosine kinase involved also in tissue morphogenesis and vascular development (61). ADAM-10 also interacts with the Prion protein (PrP^c) (62), a glycosylphosphatidylinositol (GPI)-anchored membrane protein involved in neurogenesis and myelin maintenance as well as

in neurodegeneration as the principal agent in spongiform encephalopaties (63;64). Recent evidence suggests that ADAM-10 may be the sheddase of PrP^c, but does not perform the α-cleavage of this. Using ADAM-10 conditional knock-out mice, it could be shown that the lack of this protein increases the amount of PrP^c due to its retention within the early secretory compartments (65). However, more studies are necessary to clarify the physiological impact of this finding. In addition to the already mentioned functions, ADAM-10 has a central role in inflammatory vascular diseases, atherosclerosis and cancer (66).

1.2.1.3. Structure and function of BACE1

BACE1 is a type I transmembrane aspartic protease related to the pepsins and retroviral proteases. The BACE1 gene is located at chromosomal region 11q23.3 and encodes a 70 kDa protein. The protein is synthesized as a 501 amino acid pro-enzyme in the ER, where it is glycosylated and transiently acetylated. Subsequently, it is translocated to the Golgi apparatus, where complex carbohydrates are attached. The subcellular localization of BACE1 is within the TGN and endosomal compartment. Although BACE1 reaches the plasma membrane due to the vesicle traffic, it is recycled quickly. Only limited amount of APP cleavage mediated by BACE1 takes place at the plasma membrane; the primary BACE1-mediated APP processing takes place in endocytic vesicles (67).

The past decade has shown significant progress in the understanding of the molecular and cellular BACE1 function. While the majority of the reports focus

on BACE1 function in the proteolysis of APP, the identification of other substrates indicates that there are more physiological functions of this protein that still are unknown. These substrates include APLP1 and APLP2 (68), voltage gate sodium channel β2-subunit (69), low density lipoprotein receptor-related protein (70) and neuroregulin-1 (71) among others. On the other hand, it has been found that some proteins interact with BACE1 producing an inhibition of its proteolytic activity. Recently it has been reported that BACE1 is inhibited by PrP^c and hence the production of Aβ can be decreased (72).

BACE1 is highly expressed in neurons and its biological relevance has been demonstrated using knock-out mice. Initially, no phenotype was found in the $BACE1^{-/-}$ mice (73). Hence, BACE1 was considered to be a good therapeutic target for AD. However, new reports have shown that these mice exhibit some abnormal phenotypes including electrophysiological dysfunction and cognitive deficits (74;75). These findings raise concerns about the use of BACE1 inhibitors for the treatment of AD.

1.2.1.4. Structure and function of Presenilin-1

Presenilin-1 is an integral membrane protein and one of the members of the γ-secretase complex. The PS1 gene is located on chromosome 14q24.3 and encodes a 467 amino acids protein with a molecular weight of 57 kDa. The full length protein contains nine transmembrane regions and is cleaved in the cytoplasmic loop between the 6th and 7th transmembrane region to generate N-terminal and C-terminal fragments. These fragments represent the active form

of the protein and stay in association with the membrane. PS1 is primarily located in ER and Golgi membranes, nevertheless, it has been demonstrated that endogenous PS1 localizes in the plasma membrane as an active molecule (47;48). However, the subcellular localization of PS1 may not overlap with subcellular compartments involved in Aβ production. This phenomenon is called "spatial paradox", in reference to the fact that PS1 is predominantly located in ER and the intermediate compartment. In 2002, Kaether and colleges reported that PS1 binds to mature, cell surface-located Nct (76). These data suggested that the complex formed by PS1 and Nct was necessary for the release of PS1 from the ER and subsequent distribution to Golgi and the plasma membrane, where it is biologically active.

Different functions have been ascribed to PS1, including a role regulating the susceptibility of neurons to apoptosis (77), modulating intracellular calcium signaling (78) and calcium-mediated apoptosis (79). Other well studied functions of PS1 are the regulation of β-catenin stability (80), trafficking of membrane proteins (81) and the processing of various type I membrane proteins including Notch1, N- and E-cadherins, low density lipoprotein receptor-related protein and nectin 1a among others (82).

1.2.2. Other proteins involved in the processing of APP

An alternative explanation for Aβ accumulation in the elderly would be an alteration in the cleavage of APP. Earlier studies indicate that Aβ is likely to be produced in the endosome and lysosome system where, cathepsins S, B and L

are located, and the use of cathepsin inhibitors in cellular and animal models reduces the levels of Aβ (83). Recent studies have shown that cathepsins could process APP to form the Aβ peptide in a β-secretase fashion by cleaving the β-site sequence of APP much faster than BACE1 (84). These findings make cathepsins an interesting target for compounds with therapeutic relevance for AD.

1.2.2.1. Structure and function of Cathepsin L

The cysteine cathepsin L participates in protein degradation in lysosomes and the production of active secretory vesicle peptides required for cell-cell communication in the nervous and endocrine system (85). The cathepsin L gene is located at chromosome 9q21.33 and encodes a 42 kDa protein which is processed to obtain the mature form with a molecular weight of 25 kDa. The protein is synthesized with an N-terminal signal that directs it to the lumen of the ER where is glycosylated. Afterwards, cathepsin L is processed in the Golgi apparatus by modification of mannose residues to mannose-6-phosphate (M6P) which induces the binding with the M6P receptor and the subsequent transport to the lysosome (86).

It has been shown that cathepsin L cleaves APP at $k$cat/Km: $3460 M^{-1} S^{-1}$ while BACE1 does the cleavage slower at $k$cat/Km: $46.6\ M^{-1} S^{-1}$. This cleavage seems to take place at the K-M bond of the β-site sequence of APP (84). More studies are necessary to establish the relevance *in vivo* of cathepsin L as β-secretase and its role in the pathogenesis of AD. However, these results indicate that

cathepsin L is a promising target to develop inhibitors that could modify the course of the disease by slowing down the progression of the neurodegeneration if AD patients.

1.2.3. Prion protein (PrP^c) and Alzheimer's disease

Prion (*proteinaceous and infectious particle*) is a 209-residues protein with two glycosylation sites and a GPI anchor. An abnormal isoform of PrP^c, denoted as PrP^{Sc}, stimulates the conversion of PrP^c in new PrP^{Sc} leading to neurodegeneration. Over 40 mutations in the gene PRNP located at chromosome 20p13 have been shown to segregate with heritable human prion diseases. However, prion diseases also occur as sporadic and transmissible disease in humans; with the sporadic forms being the most frequent in humans (87).

Infectious prion diseases are rare, but the mechanism of tissue destruction by aggregation of proteins via their beta-pleated sheets seems to also apply to other diseases like AD. The action of oligomeric Aβ on neuronal cells suggests the presence of one or more neuronal high-affinity receptors for Aβ. One of the major candidates to accomplish this function is PrP^c. This hypothesis arises from the fact that PrP^c has shown experimentally to have high affinity and specificity for Aβ oligomers (88). The exact binding site of Aβ oligomers has been found between the amino acids 95 and 110 of PrP^c and corresponds to a region implicated in neuronal toxicity and neurodegeneration in mice (89).

Prion protein has been also reported to regulate APP processing by modulating BACE1 activity. Nevertheless, these findings are still a matter of discussion. *In vitro*, the coexpression of APP and PrP^c reduces the levels of Aβ secreted compared to controls expressing only APP (90). Conversely, the overexpression of PrP^c in transgenic APP mice produces an increase in the number of Aβ plaques found in the brain (91). Although different studies support the function of PrP^c as putative coreceptor for Aβ oligomers, it is still unclear whether this interaction might affect the ability of PrP^c to regulate BACE1. The relevance of these mechanisms for a therapeutic approach in AD requires further investigation and more data to decipher the molecular puzzle offered by interactions.

1.3. Molecular mechanism of Aβ degradation

New evidence indicates that while in the brain the concentration of Aβ increases due to the continuously processing of APP, the concentration of Aβ decreases in CSF (92;93). These findings suggest decreased Aβ transport from the brain and are supported by reports that found defects of Aβ clearance in AD patients compared with healthy individuals (94).

One mechanism to eliminate Aβ in the brain includes its degradation by proteases such as insulin degrading enzyme (IDE) and neprilysin among others (95). These proteases regulate the steady-state levels of Aβ. IDE, a thiol metalloendopeptidase, degrades small peptides such insulin and monomeric Aβ

(96). The deletion of this enzyme in mice reduces Aβ degradation by more than 50% (97); and conversely, its overexpression prevents plaque formation (98). Neprilysin, a membrane-anchored zinc endopeptidase, degrades Aβ monomers and oligomers and the reduction of its expression leads to Aβ accumulation in the brain (99).

1.3.1. Insulin degrading enzyme (IDE) and Alzheimer's disease

IDE is a neutral thiol metalloprotease with a molecular weight of 118 kDa. The gene encoding IDE is located on chromosome 10q23-q25 and contains 24 exons that code for a protein well conserved during the evolution from *E. coli* to humans. The active site of IDE is formed by a His-Glu-aa-aa-His sequence in which two histidines coordinate the binding of the zinc atom and the glutamate plays an important role in catalysis (100). IDE is abundant in the cytosol and peroxisomes (100), and it is also found in rough ER, plasma membrane and the extracellular space (96). Several small peptides have been shown to be degraded by IDE, including insulin (101), insulin-like growth factors I and II (102), Aβ (96) and others . IDE is secreted at high levels from microglial cells, and degrades Aβ extracellularly (96). In brain homogenates from AD patients, IDE degrading activity was found to be decreased when it was compared with controls and the expression levels of this protein were reduced in the hippocampal region of AD patients (103). The deficiency of IDE might lead to increased Aβ and thus AD pathology. This offers a new scenario where approaches like gene therapy, enzymatic induction and control of type 2 diabetes may contribute to the prevention and treatment of AD.

1.4. Role of Tau hyperphosphorylation in Alzheimer's disease

Tau pathology is one of the factors that contribute the most to the neurodegenerative process in AD. In parallel to Aβ deposition, the cell body of neurons and their processes develop NFTs, neuropil threads, and neuritic dystrophy which are composed mainly by an aggregated form of the microtubule-associated protein, Tau. This protein is synthesized in neurons and glia and its principal function is to bind to tubulin and stabilize microtubules. In AD Tau becomes hyperphosphorylated thus dissociating from microtubules and tending to aggregate to form NFTs (Figure 2). Tau monomers first bind together to form oligomers, which then aggregate into a β-sheet before forming NFTs. Filamentous Tau can be transported to other brain regions spreading the neurodegeneration (104;105). In human CSF it has been found that high levels of Tau phosphorylation correlate with cognitive decline and elevated levels of phosphorylated Tau amino acids in CSF are biomarkers for predicting AD in patients with MCI (106).

Several kinases have been involved in Tau phosphorylation including glycogen synthase kinase 3β (GSK3β), extracellular signal-related kinase 1 and 2 (Erk1/2), cyclin dependent kinase 5 (CDK5) and cAMP-dependent protein kinase (PKA). Tau phosphorylation has different effects on its biological function. It has been demonstrated that Tau phosphorylation at threonine 231, serine 235 and serine 262 inhibits its binding to microtubules (107). Further phosphorylations at threonine 231, serine 396 and serine 422 induce self-aggregation of Tau into filaments; and phosphorylations of Tau near to the

microtubule-binding region decrease its activity and disrupt microtubules (Figure 2)(108). Consequently, these phosphokinases represent potential targets to reduce the damage caused by aberrant Tau phosphorylation and its subsequent aggregation.
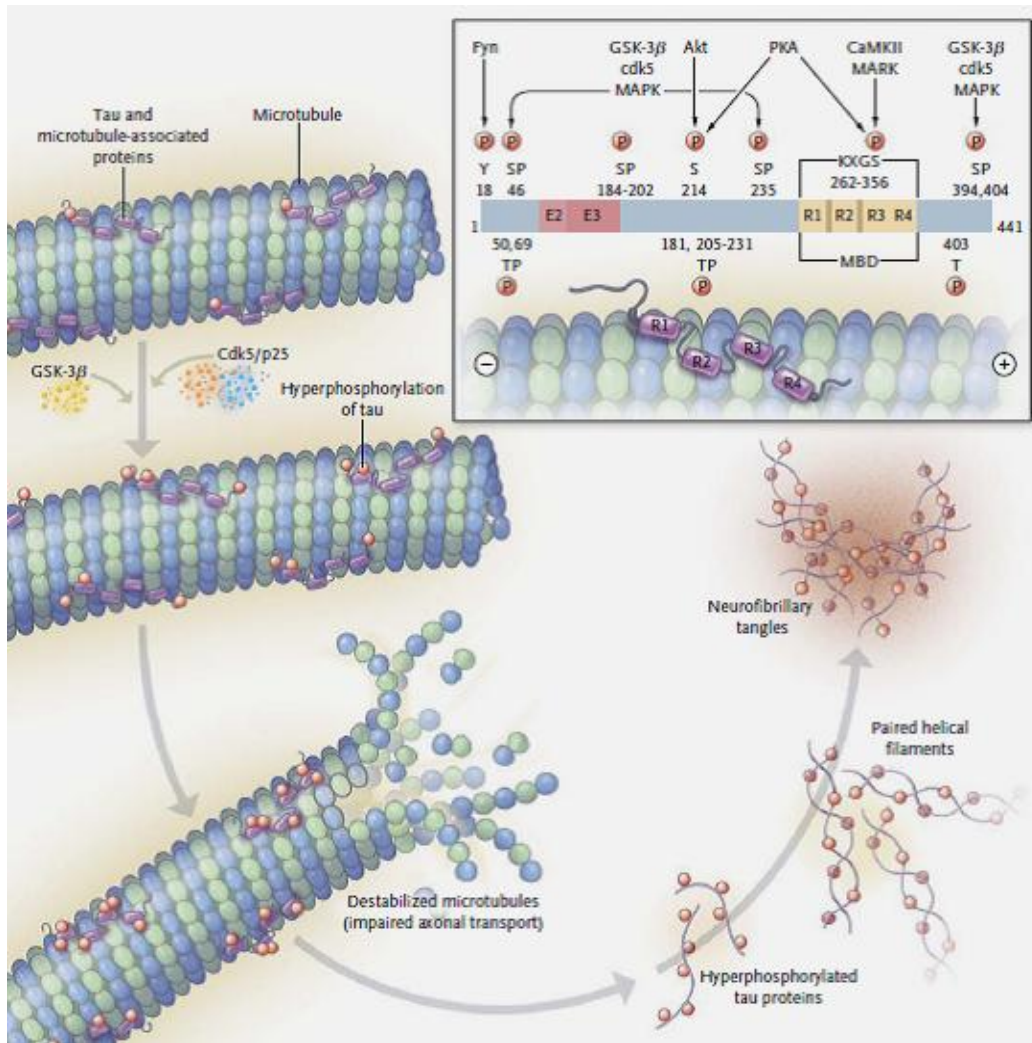
Figure 2. Tau hyperphosphorylation. The microtubule-associated protein Tau is phosphorylated by several kinases (GSK3β, Erk, CDK5, etc) at different amino acid residues. Tau phosphorylations modulate the binding to microtubules and their stability. The hyperphosphorylation of Tau prevents its binding to microtubules leading to their destabilization. This process induces the formation of Tau aggregates forming PHF and NFTs. Source: Querfurth HW, LaFerla FM. Alzheimer's disease. N Engl J Med. 2010 Jan 28;362(4):329-44.

1.4.1. Glycogen synthase kinase 3β (GSK3β) and Tau hyperphosphorylation

Initially GSK3β was recognized as one regulating enzyme in glycogen metabolism. However, later studies demonstrated that it was also involved in different cellular process (gene transcription, apoptosis and microtubule stability) and was critical in neurodegeneration. GSK3β has two isoforms, GSK3α and GSK3β encoded by distinct genes located on chromosomes 19q13.2 and 3q13.3 respectively. They are highly expressed in hippocampus, neocortex and cerebellum; however the hippocampal expression of GSK3β is higher than the expression of GSK3α and for this reason has been more related to AD (109;110).

The activity of GSK3β is modulated by insulin and Wnt signaling. Insulin signaling leads to the activation of PI3K and subsequently the activation of Akt which phosphorylates GSK3β at serine 9 inducing its inhibition. In addition to the negative regulation, GSK3β can be phosphorylated at tyrosine 216 increasing its activity (109;110).

Many GSK3β substrates require a priming phosphorylation by another kinase. Some phosphorylation sites of GSK3β require priming by CDK5 which has been also linked to Tau hyperphosphorylation in AD (111). Under pathological conditions GSK3β becomes more active due to the permanent phosphorylation of tyrosine 216 which leads to Tau hyperphosphorylation. In AD brains, active GSK3β colocalizes with NFTs and sites of granulovacuolar degeneration (112).

GSK3β is central for AD pathogenesis and there is evidence to support this role; however, more studies are necessary to reveal the details of the contribution of GSK3β to neurodegeneration.

1.4.2. Extracellular signal-related kinase 1 and 2 (Erk1/2) and Tau hyperphosphorylation

Erk1 and 2 belong to the mitogen-activated protein kinases (MAPKs) superfamily. They are serine/threonine protein kinases that promote a large diversity of cellular functions. Other members of this family are the c-Jun NH2-terminal kinases (JNK) and p38 kinases (113). Erk1 and 2, also known as p44 and p42 MAPKs, can be activated by survival or death signals, but the mechanism of differential activation is still unclear. The activation of Erk1/2 is mediated by a dual phosphorylation at threonine and tyrosine residues (Erk1: threonine 202 and tyrosine 204; Erk2: threonine 185 and tyrosine 187). It is considered a proline-directed kinase since it phosphorylates serine or threonine residues followed by a proline. Erk1/2 has multiple activation targets including, several transcription factors, signaling mediators, cytoskeletal proteins and protein kinases (114).

Initially, localization of Erk1/2 in NFTs and senile plaques was reported and that its activation leaded to the production of Tau-based paired helical filaments (PHF) which are the core constituents of NFTs. Later on, these results were confirmed by the activation of Erk 1/2 associated with early Tau deposition in neurons and glial cells in AD and other dementias. Also its activation is

associated with the progression of neurofibrillary degeneration in AD (115). Recently, a study done using CSF samples from AD patients established that the amounts of basal Erk1/2 correlated with the levels of basal and phosphorylated Tau which supports the notion that Erk1/2 is a key participant of the neurodegeneration process caused by Tau accumulation in AD (116).

1.5. New molecules and their potential as biomarkers for Alzheimer's disease

Alzheimer's disease can only be definitively diagnosed postmortem, although earlier diagnosis is possible with the use of diagnostic techniques and clinical criteria, but this is too late because the degenerative progress has begun already and the symptoms become evident. For the development of future therapies it is necessary to consider in which stage treatments can be most effective. The aggregation process starts probably 10 to 20 years before the onset of clinical manifestations and many researchers state that this is the point when the treatment should be started. One of the strategies that has been used is the search for new molecules that could serve as early signals to recognize the disease before its onset. Several approaches have been used for this aim, including the development of new compounds and methods for diagnosis based on imaging, genomic and proteomic approaches.

The analysis of CSF in search of neuropathological AD-associated proteins or peptides has been already incorporated into the diagnosis of AD. Thousands of

candidate molecules have been found, however, not all of them match the requirements to be considered as biomarkers (117). Recently, one UKE collaborative group in which we take part performed a proteomic study using CSF from several dementias including AD. They created a differential peptide pattern for dementias to identify new potential biomarkers for AD. One of these molecules was the proteoglycan Testican-1, which showed high correlation between sensitivity and specificity (area under curve of the ROC curve = 0.973, SE = 0.020, CI = 95% and P=0.0001) becoming a good candidate as CSF biomarker for AD (118).

1.5.1. Structure and function of Testican-1

Testican-1 was initially isolated from the seminal plasma, but later was found also in human brain (cortex, hippocampus, thalamus, cerebellum and other regions). The gene is encoded on chromosome 5q31 and it is called SPOCK or more often TESTICAN. Testican-1 is highly conserved among species, suggesting that the function of this gene is important for survival. The protein has a signal sequence at the N-terminal region, followed by a sequence unique for Testican responsible for the inhibition of membrane-type matrix metalloprotease 1 and 2; then a Follistatin-like domain is found with a Kazal-like module associated with inhibition of serine proteases. It also has an extracellular calcium-binding domain, a thyroglobulin type-1 domain and the C-terminal region (119).

Biochemical and kinetic analysis have shown that Testican-1 inhibits the cysteine protease cathepsin L. Through its thyroglobulin type-1 domain, Testican-1 seems to stabilize cathepsin L, thereby increasing the duration of the activity, but reducing the proteolytic ability (120). These findings suggest that Testican-1 might serve as modulator of the activity of enzymes related to the processing of APP and therefore could be a modifying factor of the pathogesis of AD.

2. RESEARCH GOAL AND OBJECTIVES

The main goal of this work was to establish the expression profile of proteins involved in the production of Aβ and Tau hyperphosphorylation as potential biomarkers for different variants of AD.

To meet this goal, the following objectives were pursued:

- To determine the expression level of proteins involved in the processing of APP, aggregation and degradation of Aβ in frontal cortex, temporal cortex and cerebellum from AD patients and healthy individuals.

- To determine the expression and activation level of proteins involved in the hyperphosphorylation of Tau protein as a parallel neurodegenerative mechanism in frontal cortex, temporal cortex and cerebellum from AD patients and healthy individuals.

- To elucidate the role of a candidate biomarker, Testican-1, in the pathogenesis of AD using human samples and an *in vitro* approach.

3. MATERIALS AND METHODS

For detailed information about the equipment, reagents and other materials used during this study please refer to the Appendices section.

3.1. Human samples

Post mortem tissue was obtained after donor consent signed by relatives according to pertaining laws in Colombia, Germany and Netherlands. This study was approved by ethical boards in the University of Antioquia, Medellin, Colombia; University Medical Center Hamburg-Eppendorf, Hamburg, Germany; and Netherlands Brain Bank, Amsterdam, Netherlands. Formalin fixed and frozen brain tissue from AD patients and controls, was handled as previously described (121) and it was used for experimentation according to availability and sample status (Appendices 1 and 2).

3.2. Plasmid preparation for transient transfection

3.2.1. Cloning

Human Testican-1 cDNA was purchased from ImaGenes (GenBank: BC030691.2) and it was extracted from the shuttle vector (pBluescriptR) using *Sal*I (Fermentas) and *Acc65*I (Fermentas). The cDNA was subcloned into the pcDNA3.1-/Zeo vector (Invitrogen) using the *Xho*I (Fermentas) and *Acc65*I restriction sites. Enzymatic digestions were made using 1 μg plasmid DNA, 1 μL

restriction enzyme, 2 µL digestion buffer and sterile distilled water to obtain a final volume of 20 µL. The mixture was incubated for 1 h at 37ºC. The fragments were separated by agarose electrophoresis and purified using a gel purification kit (Appendix 3).

3.2.2. DNA purification from agarose gels

After electrophoresis the separated fragments (linearized vector and insert) were cut from the gel using a scalpel, put into a 1.5 mL sterile tube and purified using a DNA gel extraction kit (Fermentas). 100 µL of binding buffer were added to each tube and heated at 60ºC for 10 min. After the agarose melting the tubes were centrifuged at 13000 rpm for 1 min. The supernatant was added to a new tube containing a spin column and centrifuged at 13000 rpm for 1 min. The column was washed with washing buffer and the DNA was eluted with 50 µL sterile distilled water.

3.2.3. Ligation

The ligation between plasmid (pcDNA3.1-/Zeo) and insert (Testican-1 cDNA) was done in a molar ratio of 1:5 using the T4 ligase (Fermentas). For this a mixture of insert and vector were incubated with 2 µL enzyme, 2 µL ligation buffer and sterile distilled water in a final volume of 20 µL. The reaction was conducted at 22ºC overnight.

3.2.4. DNA agarose gels

DNA agarose gels were used to confirm the success of the different enzymatic treatments. To separate the DNA according to its size, horizontal electrophoresis with 1% agarose diluted in 1X TAE was performed. Therefore, the mixture of agarose and TAE was heated in a microwave until complete dilution of agarose was observed. After this the solution was cooled-down at 60ºC and cast in a sealed chamber with an inserted comb for loading the samples. Each sample (9 µL) was mixed with 10X loading buffer (1 µL) and loaded to the gel. A 1 kb DNA ladder (Fermentas) was used as size standard. The electrophoresis was performed at 110 V and after separation the gel was incubated for 10 min in a bath containing 0.5 µg/mL ethidiumbromide. The DNA was visualized using a gel documentation system.

3.2.5. DNA Sequencing

The plasmid DNA samples were sequenced to confirm the success of the cloning. For this, 1 µg of plasmid DNA was mixed with 1 µL sequencing primers (Appendix 4) at a concentration of 10 pmol/µL. Sequencing was performed by Eurofins MWG Operon.

3.2.6. Transformation of competent cells

The plasmid DNA containing the human Testican-1 cDNA was used for transformation of XL10-Gold competent cells (Stratagene). Therefore, 45 µL of ultracompetent cells were thawed on ice and 2 µL of β-mercaptoethanol were

added. After 2 min. incubation 2 μL of pDNA (100 ng) were added carefully and gently mixed by flicking. The mixture was incubated for 30 min. before being heat-shocked at 42ºC for 30 sec. and then placed on ice for 2 min. Afterwards 450 μL of sterile antibiotic-free NZY$^+$ broth was added and incubated for 1 h at 37ºC with agitation at 300 rpm. Approximately 200 μL of each transformation was plated on ampicillin containing HSG agar plates under sterile conditions and incubated for 16 h overnight at 37ºC. Transformation efficiency was estimated from the number of colonies found on each plate against control transformation.

3.2.7. Mini purification of plasmid DNA

Colonies were selected from HSG agar plates with a sterile toothpick and grown at 37ºC for 16 h with agitation at 300 rpm in HSG medium containing 100 μg/μL ampicillin. The plasmid DNA was purified using DNA purification kit (Invitek) following the manufacturer manual. Cells were pelleted by centrifugation at 13000 rpm for 1 min. The supernatant was discarded and the cells were resuspended in 250 μL solution A supplemented with RNase A, then 250 μL lysis solution B was added and mixed by inverting 6 times. The whole homogenate was centrifuged at 13000 rpm for 1 min. The clarified supernatant was transferred to a spin filter, incubated for 1 min. and centrifuged at 13000 rpm for 1 min. After the flow-through was discarded, 750 μL wash buffer was added followed by centrifugation twice at 13000 rpm for 2 min. The column was then placed into a sterile 1.5 mL microcentrifuge tube and DNA was eluted by

addition of 50 µL sterile distilled water, incubation at room temperature for 5 min. and centrifugation at 13000 rpm for 1 min.

3.2.8. Midi purification of plasmid DNA

The plasmid DNA was obtained in large amounts using a silica-based anion-exchange purification kit (Macherey-Nagel). 20 µL of transformed cells were used to inoculate 200 mL of HSG media supplemented with 100 µg/µL ampicillin and incubated at 37ºC for 16 h with agitation at 300 rpm. The cultured bacterial cells were pelleted by centrifugation at 6000 x g for 30 min. at 4ºC. After centrifugation the supernatant was discarded and the cells were resuspended in 8 mL of resuspension buffer containing RNase A by vortexing until no clumping was observed. Then 8 mL of lysis buffer were added and mixed gently by inverting the tube 5 times and incubated for 5 min. After lysis, 8 mL of neutralization buffer were added and mixed by inverting the tube 15 times. NucleoBond columns with an integrated filter were equilibrated by applying 12 mL of equilibration buffer. The lysate was loaded on the column and cleared from cell debris. After washing with 8 mL of equilibration and washing buffer, the plasmid DNA was eluted using 5 mL of elution buffer. The plasmid DNA was precipitated with 3.5 mL of isopropanol for 2 min. before being pelleted at 6000 x g for 1 h at 4ºC. The pellet was washed with 2 mL of 70% ethanol and centrifuged at 6000 x g for 10 min at room temperature. The supernatant was discarded and the pellet was air-dried for 10 min. under a hood and diluted in 500 µL sterile distilled water and incubated at 37ºC for 30 min.

3.2.9. DNA quantification

To determine the DNA concentration, samples were diluted 1:100 in water. The absorbance of the diluted sample was measured at 260 nm and 280 nm in a cuvette with a spectrophotometer. Water was used as blank. The reading at 260 nm allows for calculation of the nucleic acids in the sample. An optical density of 1 corresponds to approximately 40 µg/mL for RNA and 50 µg/mL for double-stranded DNA. The concentration can be calculated in this way:

$$RNA \ (\mu g/mL) = OD_{260} \ x \ 40 \ \mu g/mL \ x \ dilution \ factor$$
$$DNA \ (\mu g/mL) = OD_{260} \ x \ 50 \ \mu g/mL \ x \ dilution \ factor$$

The purity of the nucleic acid is indicated by the ratio OD_{260}/OD_{280} where values between 1.8 and 2.0 represent clean nucleic acids.

3.3. Cell line culture

Human Embryonic Kidney cells (HEK293T) were purchased from ATCC collection (ACC 305, Leibniz Institute DSMZ-German Collection of Microorganisms and Cell Cultures) and stably transfected with human wild type form of APP (APPwt) or APP variant bearing the swedish double mutation K670N>M671L (APPsw) (Appendix 5). These were grown in DMEM (PAA) supplemented with 10% fetal bovine serum (PAA) at 37ºC and 5% CO_2. For protein isolation 2 x 10^6 cells were plated in 6-well plates (Falcon) and for

immunocytochemistry 2 x 10^5 cells were plated on cover slips in 6-well plates 24 h before to begin the experiment to reach approximately 90 - 95% confluence.

3.4. Cell line transfection

Wild type, APPwt and APPsw HEK293T cells were grown in supplemented DMEM to confluence (90 - 95%) and transfected with 8 µg of pcDNA3.1-/Neo empty vector (Mock) or pcDNA3.1-/Neo + Testican-1 using Lipofectamine 2000 (Invitrogen) for 24 h. After transfection the expression of Testican-1 was analyzed by western blot and immunocytochemistry (Appendix 6).

3.5. Protein isolation

Human brain tissue

Human frontal cortex, temporal cortex and cerebellum (vermis) were cleared of meninges and only grey matter was used for the procedure. 500 mg of tissue were cut in small pieces, poured into a glass Dounce tissue grinder type B and homogenized with ten even strokes in 1 mL of lysis buffer containing 150 mM NaCl, 20 mM Tris pH 7.4, 1 mM EDTA, 10% Glycerol, 1% NP40 and a cocktail of phosphatase and protease inhibitors (Roche). The homogenate was centrifuged at 14000 rpm for 10 min at 4ºC and the proteins present in the supernatant were quantified using the bicinchoninic acid method (BCA Protein

Assay Kit, Thermo). The protein extracts were stored at -80ºC for further experiments.

Cell cultures

HEK293T cells were washed with PBS and incubated for 20 min at 4ºC with buffer lysis (see above). The cell extracts were centrifuged at 14000 rpm for 10 minutes and the proteins present in the supernatant were quantified by the BCA method (Thermo). The protein extracts were stored at -80ºC for further experiments.

3.6. Western blot

Sodium dodecyl sulfate polyacrylamide gel electrophoresis (SDS-PAGE)

Once proteins were quantified, SDS-PAGE was carried out using a miniprotean system (BioRad) with a molecular weight marker of standard range (Fermentas). Proteins (25 - 30 µg) were loaded into each well with loading buffer (0.375 M Tris pH 6.8, 50% glycerol, 10% SDS, 0.5 M DTT and 0.002% bromophenol blue) and heated to 95ºC for 5 minutes before loading on the gel. After electrophoresis, proteins were transferred to nitrocellulose membranes (BioRad) using an electrophoretic transfer system (Mini Trans-blot Electrophoretic Transfer Cell, BioRad) at 300 mA for 2 h. The membranes were incubated for 1 h in 5% non-fat milk dissolved in TTBS (100 mM Tris pH 7.5, 500 mM NaCl, 0.02% Tween-20). Then, the membranes were incubated overnight at 4°C with primary antibody (Appendix 10). Subsequently, the

membranes were washed with TTBS and incubated with secondary antibody (Appendix 11) coupled to peroxidase for 1 h at room temperature. Immunoreactive signal was developed with the ECL Western Blotting chemiluminescence system (SuperSignal West Pico Chemiluminiscent Substrate, Thermo) and detected with a ChemiDoc system (BioRad). The images were analyzed using the quantification software QuantityOne (BioRad). The results of each sample were normalized with respect to the values of β-actin or glyceraldehyde 3-phosphate dehydrogenase (GAPDH) and compared between groups. To minimize interassay variation, the samples from all experimental groups were processed in parallel.

Tricine gel electrophoresis

Protein extracts were loaded into each well with loading buffer (0.15 M Tris pH 6.8, 36% Glycerol, 12% SDS, 0.3 M DTT, 0.002% Coomasie Blue) and heated to 95ºC for 5 minutes before loading on precast 10%-20% Tricine gels (Invitrogen). The gels were run using cathode buffer (1 M Tris base, 1 M Tricine and 1% SDS), anode buffer (1 M Tris base and 0.225 M HCl) and transferred to nitrocellulose membranes (BioRad) using an electrophoretic transfer system (BioRad) at 300 mA for 80 min. The membranes were blocked, incubated in primary and secondary antibodies (Appendices 10 and 11) and detected as described above.

3.7. Tissue microarray (TMA) and immunohistochemistry

Selected anatomically defined areas (frontal cortex, gryrus frontalis medius, temporal cortex at the level of the lateral corpus geniculatum and entorhinal cortex) from a total of 72 formalin-fixed (buffered neutral aqueous 4% solution), paraffin-embedded tissue specimens were used for TMA generation. Tissue cylinders with a diameter of 0.6 mm were punched from anatomically defined areas of a "donor" tissue block using a semiautomatic robotic precision instrument and brought into 3 different recipient paraffin blocks, each containing 356 individual samples. Multiple 4 μm sections of the resulting TMA block were cut, mounted to an adhesive-coated slide system and further processed for histological staining according to standard protocols.

Immunohistochemistry was performed using appropriate antigen retrieval methods with internal controls. For the detection of neuritic plaques, the primary antibody 6E10 directed against Aβ was used (Appendices 7 and 10). An affinity-purified polyclonal antibody against Testican-1 was used at a dilution of 1:100. Primary antibodies were visualized using a standard diaminobenzidine streptavidin-biotin horseradish peroxidase method (Sigma). Quantification of diffuse plaques, neuritic plaques, and Testican-1 positive deposits was accomplished by counting positive signals for Aβ and Testican-1 on consecutive sections. The average of positive signals was determined for each region of patients/controls by calculating the mean value of all assessed tissue specimens. In average 6.9 out of 8 tissue specimens in one row were analyzable. A region was considered analyzable if at least two tissue specimens

could be assessed. A total of 5 regions had to be excluded from analysis due to poor quality.

3.8. Immunofluorescence

Human tissue

Unfixed snap frozen tissue was cut at a thickness of 5 µm, fixed in acetone, blocked with donkey serum and incubated with 6E10 and Testican-1 primary antibodies (Appendix 7) overnight at 4ºC. Subsequently, sections were washed with PBS and incubated with secondary antibody (Alexa Fluor 555 and FITC respectively)(Appendix 7) for 1 h at room temperature. Nuclei were counterstained with 4',6-diamidino-2-phenylindole (DAPI; Sigma).

Cell lines

After transfection the HEK292T cells were washed with PBS 3 times, fixed with 4% paraformaldehyde for 20 min. and permeabilized with ice-cold acetone (-20ºC) for 5 min. The cells were washed 3 times with PBS and incubated overnight with primary antibody (Testican-1, 6E10, KDEL, GM130, EF-1α, Adaptin-γ and cathepsin L)(Appendix 10) diluted in incubation buffer (PBS, 0.3% Triton X-100, 1% BSA) at 4ºC in a wet chamber. Then the cells were washed 3 times with PBS and incubated with FITC and Alexa Fluor 555 secondary antibody diluted in incubation buffer for 1 h (Appendix 11). After that the cells were washed 4 times with PBS and mounted in slides using Fluoromount-G (Southern Biotech). Cells were examined under a confocal

microscope (Leica TCS SP2, Wetzlar). Confocal images were analyzed individually to confirm the transfection and expression of Testican-1 and to observe its subcellular distribution. Cells incubated only with secondary antibodies were used as negative control.

3.9. Antibody generation against Testican-1/CTF

A polyclonal antibody against the C-terminal region of Testican-1 was created by the company BioGenes. Before antibody generation, pre-immune serum from rabbits was obtained. The animals that did not show reaction with the antigen were selected for the antibody production. Animals were immunized 5 times with a synthetic peptide containing the sequence CAVTEDDEDEDDDKEDEVGYIW and then were bled. 25 mL of immune serum was obtained per animal and titred.

3.10. Enzyme-linked immunosorbent assay (ELISA)

3.10.1. ELISA for Testican-1/CTF

Synthetic Testican-1/CTF peptide was diluted in 0.05 M carbonate buffer, pH 9.5 and used to coat 96-well plates overnight at room temperature. Then the wells were emptied and incubated with TBS containing 1% FBS for 30 min. at room temperature. The plates were washed three times with TBS-Triton (0.05%

Triton X-100) and incubated with 100 µL of preimmune sera (1:100, 1:500 and 1:1000) or immune sera (1:100, 1:500 and 1:1000) for 1 h at room temperature. After that the wells were washed four times with TBS-Triton and incubated with secondary antibody (Appendix 11) coupled to peroxidase for 1 h at room temperature. The plates were washed four times with TBS-Triton and developed with tetramethyl benzidine reagent (TMB kit, Thermo). After 15 min. the reaction was stopped with 0.2 M sulfuric acid and the absorption was read in a spectrophotometer at 450 nm.

3.10.2. ELISA for Aβ40 and Aβ42 peptides

The quantification of Aβ40 and Aβ42 levels in HEK293T cells transfected with Testican-1 was performed using ELISA kits and following the instructions of the manufacturer (Invitrogen). For this procedure 50 µL of primary antibody and 100 µL of conditioned medium were added to each well and incubated overnight at 4ºC. The plates were washed 4 times with 200 µL of washing buffer and incubated with secondary antibody coupled to peroxidase for 1 h at room temperature and the washed 4 times with 200 µL of washing buffer. Chromogen reagent was added to produce the coloration reaction which was stopped after 15 min. with stop solution. The absorbance of each well was read using an ELISA reader at 450 nm. For each assay a standard curve was generated using synthetic Aβ40 and Aβ42 peptides and a well without chromogen was used as blank.

3.11. Statistical analysis

Protein expression profile (Western blot)

Data collection was performed in Microsoft Excel 2007 (Microsoft, Seattle, WA) and the statistical analysis was carried out in GraphPad Prism 4 (La Joya, CA) and SPSS 17 for Windows (Chicago, IL). The use of parametric or no-parametric analysis was determined using Fisher's exact test for homogeneity of variances. *t*-test was used to determine significant differences between two independent groups. A probability of $P<0.05$ was adopted in a two tailed test to determine statistical significance. At least 4 independent experiments were conducted for each study. The data analyzed were expressed as mean ± SEM.

Protein distribution in tissue analysis

A descriptive analysis for protein distribution was devised in a radial graph for each protein. Data normalization as Z-values were calculated from obtained densitometry values in each brain area and for each protein. In these Z-values 0 represents the normalized mean for each grouped data, positive Z-values represent densitometry values higher than the mean and negative Z-values represent densitometry values lower than the mean.

Histological analysis

The data from the histological analysis were evaluated using a *t*-test and probabilities of $P<0.01$ and $P<0.05$ were adopted in a two tailed test to determine statistical significance.

4. RESULTS

4.1. Expression profile of the Amyloid Precursor Protein (APP) and its C-terminal fragments in Sporadic and Familial Alzheimer's Disease

The expression levels of APP and the APP-CTFs were analyzed in frontal cortex, temporal cortex and cerebellum of brain samples from patients with familial Alzheimer's disease (FAD), sporadic Alzheimer's disease (SAD) and compared with healthy individuals. First, the expression profile of APP was established. In the frontal cortex, decreased levels of APP were observed in FAD patients when compared to SAD cases (P=0.0343) (Figure 3A). This effect was also observed between healthy controls and SAD (Figure 3A). A slight decrease in APP expression was found in FAD samples relative to control samples; nevertheless, the difference was not statistically significant (Figure 4A). When the levels of APP were evaluated in temporal cortex a statistically significant decrease was observed in FAD cases compared with healthy controls (P=0.0180) (Figure 3A). Similarly, a tendency to decreased APP was found in FAD when compared to SAD. On the other side, levels of APP were unchanged between SAD patients and healthy individuals (Figure 3A). Cerebellum (vermis) homogenates were used to study the expression of APP. Decreased levels of APP were found in FAD and controls while in SAD samples increased amounts were observed, these changes were not statistically significant (Figure 3A). Regarding the distribution of APP in the different areas, both AD groups showed a similar pattern of higher APP distribution in frontal cortex and cerebellum compared with hippocampus (Figure 3D), however, FAD

showed lower Z values as derived from its expression level as seen in Figure 3A. The Normal distribution pattern of APP, as seen on healthy controls, showed higher Z values in temporal cortex.

In order to obtain an indirect measurement of the APP processing, the levels of APP-CTFs (C83 and C99) were analyzed in our sample. In frontal cortex, a tendency towards increased presence of C83 and C99 was found in SAD cases with respect to FAD and control samples. This was also observed between FAD and healthy individuals; however, none of these changes reached statistical significance (Figure 3B). In temporal cortex decreased levels of APP-CTFs were found in FAD patients in comparison with SAD and healthy individuals. There was a slight decrement of APP-CTFs production in SAD cases compared with control individuals (Figure 3B). In the cerebellar region only low amounts of APP-CTFs were detectable which might reflect less proteolytic activity of APP in this brain area. In this region SAD samples presented slightly increased levels of these fragments when compared with FAD and controls (Figure 3B), while FAD and control showed the same expression (Figure 3B). However, no statistical difference was found. The distribution pattern of APP-CTF in AD cases showed higher Z values in SAD with increased cerebellar distribution, while FAD cases showed increased frontal cortex distribution (Figure 3D). APP-CTF distribution in healthy controls resembled full length APP distribution with higher Z values in temporal cortex.

The ratio APP-CTF/APP-FL was evaluated to determine the amount of APP that was processed by α-/β-secretases. This analysis showed that in frontal and temporal cortex from FAD patients the APP ratio was increased compared with SAD and healthy individuals (Figure 3C). The APP ratio between SAD and control samples was unchanged (Figure 3C). In the cerebellar tissue the APP ratio was slightly augmented in FAD and SAD cases compared with controls while in FAD and SAD patients the ratio was at same level (Figure 3C).
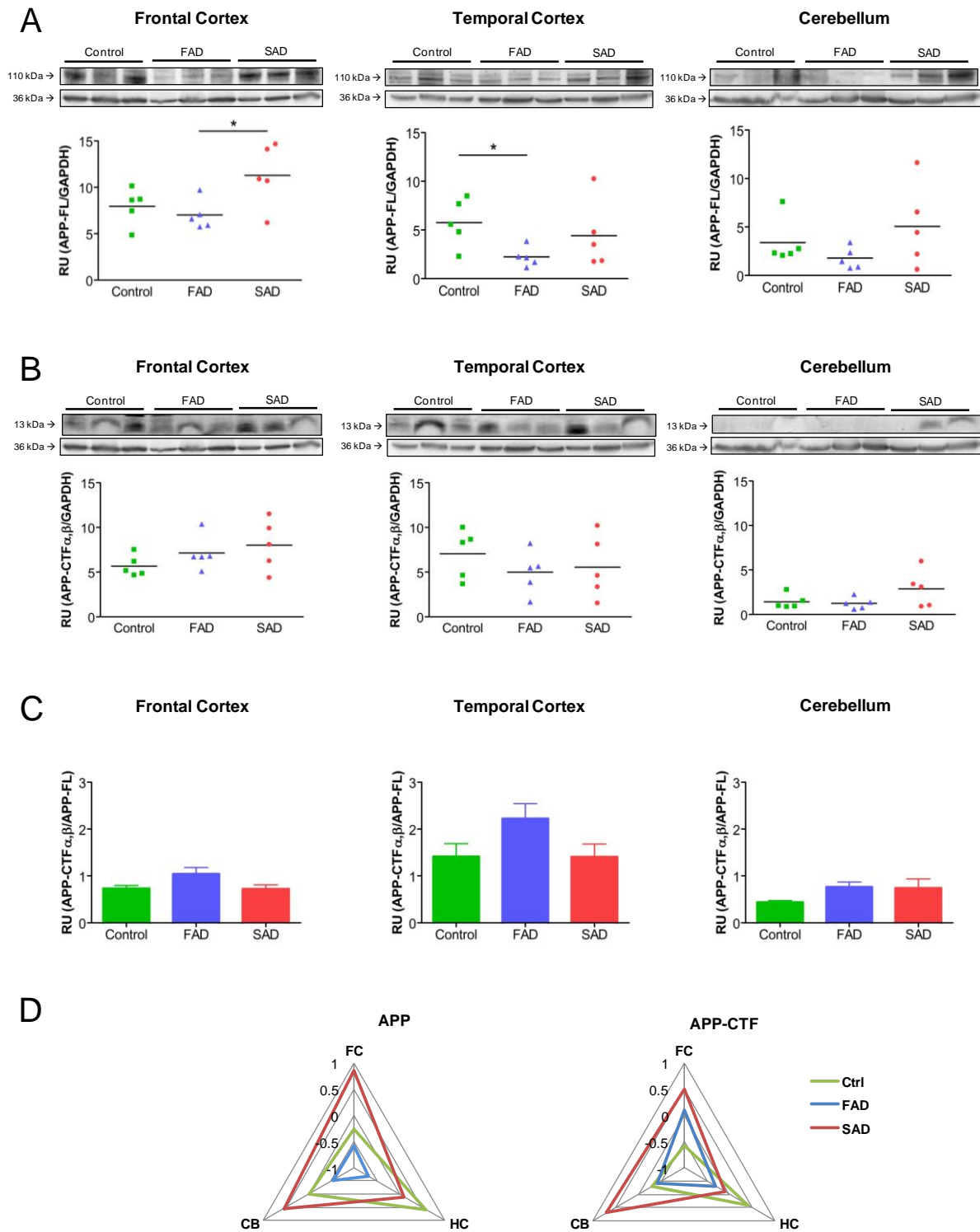
Figure 3. Expression profile of APP and its CTFs in Frontal Cortex, Temporal Cortex and Cerebellum from FAD, SAD and healthy individuals. A) APP-FL levels in three different brain regions from FAD, SAD and controls. **B)** Expression of APP-CTFs in three different brain regions from FAD, SAD and controls. **C)** APP-CTF/APP-FL ratio. **D)** Comparison of APP, APP-CTF and APP-CTF/APP-FL distribution profiles between brain regions calculated as Z values. Results were analyzed using a *t*-test and a *P*<0.05 was adopted for statistical significance. Data are shown as dot plots with horizontal bars indicating the mean and as bars showing mean ± SEM, *n*=5.

4.2. Expression profile of proteins involved in the processing of Amyloid Precursor Protein (APP) in Sporadic and Familial Alzheimer's Disease

The expression of ADAM-10, BACE1 and PS1, considered the most relevant proteins involved in the processing of APP, was analyzed by Western blot. The levels of these enzymes were evaluated in frontal cortex, temporal cortex and cerebellum of brain samples from AD patients compared with healthy individuals.

Initially we examined the expression profile of ADAM-10, an α-secretase responsible for sAPPα production and C83 fragments from APP. The analysis of the frontal cortex showed that the levels of this enzyme were increased in SAD cases compared with FAD and controls individuals. However, these changes were not significant (Figure 4A). In contrast, the amount of ADAM-10 in the temporal cortex of SAD patients was lower than the observed in FAD and controls and no statistical differences were found (Figure 4A). In the cerebellar region the expression of ADAM-10 remained unchanged among groups of individuals (Figure 4A). The comparison of the distribution profile between areas showed that while in SAD cases ADAM-10 was mainly expressed in frontal cortex and cerebellum, in FAD and controls the protein was more expressed in temporal cortex than in the other regions (Figure 4D).

The following step was to study the levels of BACE1, the enzyme responsible for the β-cleavage of APP and the production of sAPPβ, C99 and Aβ fragments, in three different brain regions. In the frontal cortex of SAD cases the

expression of BACE1 was increased compared with FAD and controls, and this difference was also observed between FAD and healthy individuals. These findings are consistent with other studies (122;123). However, in our case there is no statistically significant difference (Figure 4B). When the temporal cortex was evaluated it was found that the expression of BACE1 in SAD samples was higher relative to FAD patients and the difference became significant in comparison with the controls (P=0.4030). This tendency was also present when FAD and controls were compared, but there was no significant difference (Figure 4B).

In the same way the expression of BACE1 was determined in the cerebellum (vermis) homogenates from these samples and no changes were observed among the groups (Figure 4B). The protein expression profile indicates that in SAD patients the mean distribution of BACE1 is elevated in temporal cortex compared with frontal cortex and cerebellum. In contrast, in FAD cases, the analysis of the Z values showed increased BACE1 distribution in cerebellum relative to the media of the other areas. The comparison of the Z values from healthy individuals showed that BACE1 is distributed mainly in cortex (Figure 4D). The expression prolife of PS1, one of the most important members of the γ-secretase complex, was evaluated in different brain areas. It was found that in frontal cortex the levels of PS1 were elevated in FAD (P=0.0267) and SAD (P=0.0268) cases relative to controls (Figure 4C). In contrast, no differences in the expression of PS1 were observed in the temporal cortex when the groups were compared (Figure 4C). Cerebellum reveals significantly decreased amounts of PS1 in FAD patients compared with controls (P=0.0404). This

tendency was also observed between FAD and SAD cases; however these changes were not statistically significant. The comparison between SAD samples and controls did not show statistically significant differences (Figure 4C). The analysis of PS1 distribution revealed that in SAD patients this protein has an uniform pattern with a slight increase in cerebellum. FAD cases showed higher distribution in cortices relative to cerebellum Z values. In healthy individuals higher distribution was found in temporal cortex and cerebellum (Figure 4D).
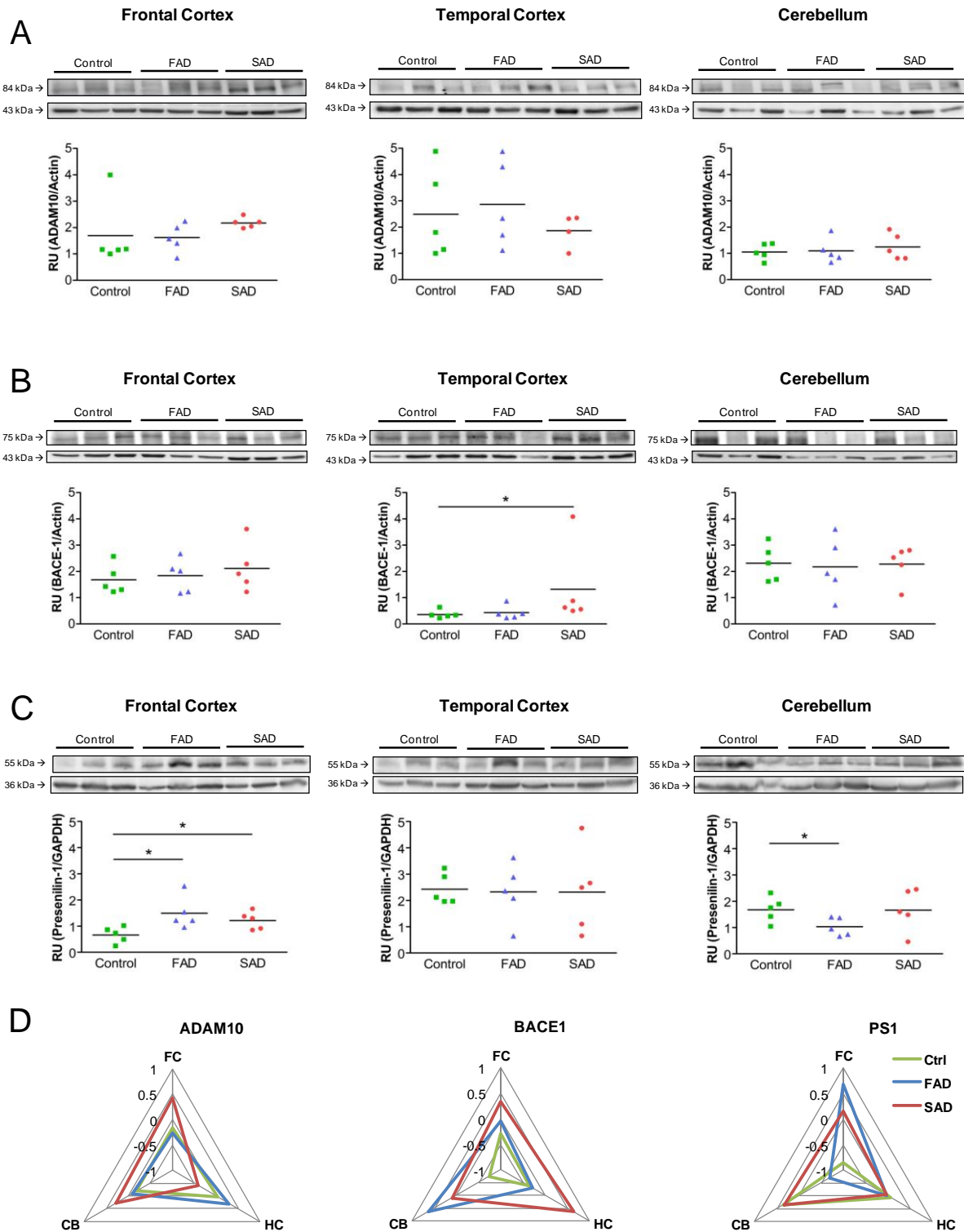
Figure 4. Expression profile of ADAM-10, BACE1 and PS1 in Frontal Cortex, Temporal Cortex and Cerebellum from FAD, SAD and healthy individuals. A) Levels of ADAM-10 in three different brain regions from FAD, SAD and controls. **B)** Expression of BACE1 in three different brain regions from FAD, SAD and controls. **C)** Expression of PS1 in three different brain regions from FAD, SAD and controls. **D)** Comparison of ADAM-10, BACE1 and PS1 distribution profiles between brain regions calculated as Z values. Results were analyzed using a *t*-test and a *P*<0.05 was adopted for statistical significance. Data are shown as dot plots with horizontal bars indicating the mean, *n*=5.

4.3. Expression profile of cathepsin L in Sporadic and Familial Alzheimer's Disease

Several studies have proposed that independent of canonical enzymes involved in the production of Aβ, there are other proteins that can regulate directly or indirectly the levels of Aβ. Proteins with α- or β-secretase activity that are able to process APP in the same way that the classical enzymes have been identified (124). In addition, there are enzymes which can modulate the α-/β-secretase activity and in consequence the production of Aβ. This is the case of cathepsins, specifically cathepsin L and cathepsin B which have shown both properties, α-/β-secretase activity and the modulation of the activity of the classical enzymes (84;125).

Cathepsin L acts as β-secretase and is related with the processing of APP and the production of Aβ (84). Given that Aβ levels in FAD and SAD cases were elevated, we evaluated cathepsin L in order to find possible dysregulations in the expression of this enzyme. In the frontal cortex, a trend towards increased presence of cathepsin L in SAD samples when compared to either FAD samples or healthy controls was observed. This tendency was also seen in FAD relative to control individuals. However, none of these changes showed statistical significance (Figure 5). The temporal cortex samples of SAD cases also have a slight increase in the levels of cathepsin L compared with FAD cases and control individuals. This increase was observed too when the FAD sample were compared with the controls. Nevertheless, all these variations were tendencies and no statistical significance was reached (Figure 5). When

the cerebellar tissue was analyzed, SAD patients showed decreased levels when compared with FAD and healthy controls, but when FAD cases were compared with controls more cathepsin L was expressed by FAD patients (Figure 5). The modification of the cathepsin L expression in the cerebellar region among groups was not statistically significant. The distribution analysis of cathepsin L in SAD cases showed an uniform pattern among brain regions, while in FAD samples there was prevalence for cerebellum compared with frontal and temporal cortices. In controls a distribution pattern similar to that of FAD cases was observed (Figure 5).

Figure 5. Expression of cathepsin L in FAD, SAD and healthy individuals. Levels of cathepsin L in frontal cortex, temporal cortex and cerebellum from FAD, SAD and controls. Comparison of cathepsin L distribution profiles between brain regions calculated as Z values. Data are shown as dot plots with horizontal bars indicating the mean, *n*=5.

4.4. Expression profile of Prion protein (PrP^c) in Sporadic and Familial Alzheimer's Disease

During the last years there has been an increasing interest in the role of PrP^c in the pathogenesis of Alzheimer's disease. There is accumulating evidence that BACE1 and ADAM-10 are involved in the processing of PrP^c and there are also some reports showing the interaction of this protein with Aβ forms which has led to the theory that PrP^c could serve as scaffolding for the formation of Aβ oligomers and fibrils (62;72;89). We decide to evaluate the expression pattern of PrP^c in our samples in order to obtain new information that could be used as starting point for further studies.

The levels of PrP^c in frontal cortex from FAD and SAD cases were compared with healthy controls. The expression of this protein was significantly diminished in FAD samples compared to controls (P=0.0107) and SAD patients (P=0.0040). No difference between SAD and controls was found (Figure 6). The Prion protein showed the same expression profile in the temporal cortex than in frontal cortex. The levels of the protein were decreased in FAD cases relative to controls (P=0.0423) and SAD cases (P=0.0053) and no statistical difference was observed when control and SAD individuals were analyzed (Figure 6).
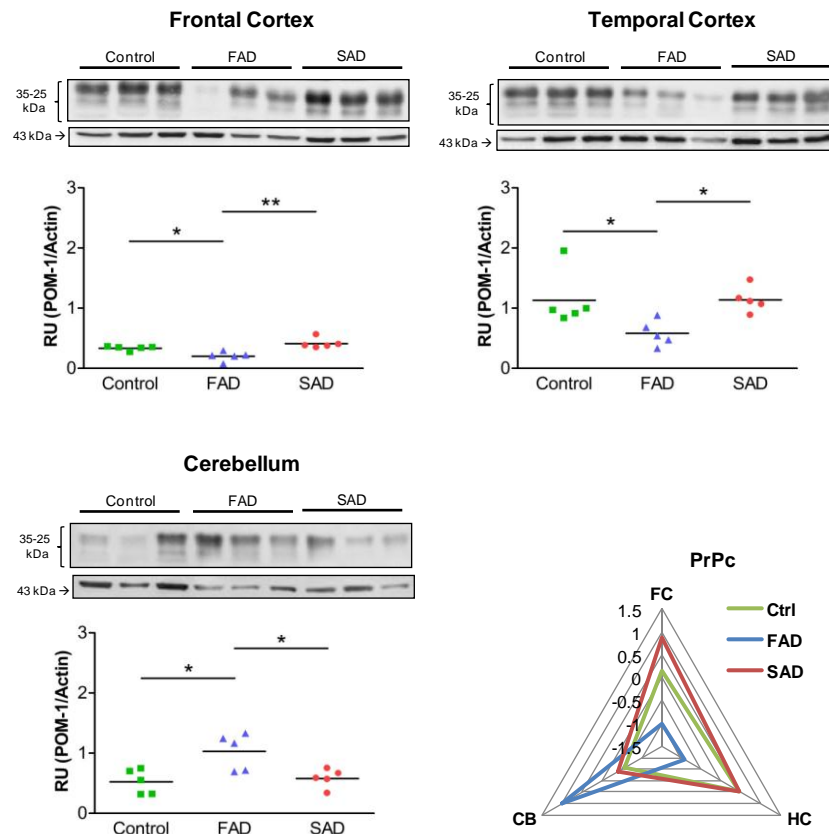
Figure 6. Expression of PrP^c in FAD, SAD and healthy individuals. Levels of PrP^c in frontal cortex, temporal cortex and cerebellum from FAD, SAD and controls. Comparison of PrP^c distribution profiles between brain regions calculated as Z values. Results were analyzed using a *t*-test and a *P*<0.05 was adopted for statistical significance. Data are shown as dot plots with horizontal bars indicating the mean, *n*=5.

Interestingly, the amount of PrP^c found in the cerebella from FAD cases was significantly higher that that observed in controls (*P*=0.0146) and SAD samples (*P*=0.0181). No differences were observed between controls and SAD patients (Figure 6). The comparison of PrP^c distribution among brain areas showed that in SAD and control individuals this protein was mainly found in frontal and temporal cortex, while in FAD cases there was a clear preference for the cerebellar region as indicates the mean Z value (Figure 6).

4.5. Expression profile of Amyloid-beta (Aβ) degrading enzymes in Sporadic and Familial Alzheimer's Disease

One of the most active research fields in Alzheimer's disease is the analysis of molecules related to the modulation of the degradation of Aβ. The insulin-degrading enzyme (IDE), a relevant protease for the metabolism of the insulin, has been linked to the degradation of Aβ. In a previous study, this peptidase was found colocalizing with Aβ40 in frontal cortex from SAD and FAD samples carrying the E280A presenilin-1 missense mutation (126). Based on these results, we evaluated the levels of IDE in our study group using Western blot. The expression profile of this enzyme was determined in the frontal cortex, temporal cortex and cerebellum from FAD and SAD cases and compared to healthy individuals (Figure 7). The statistical analysis did not show any difference when the groups comparison was done. The comparison of IDE Z values among brain regions showed that both SAD and controls were mainly found in cerebellum while FAD cases were mainly distributed in frontal and temporal cortex (Figure 7).
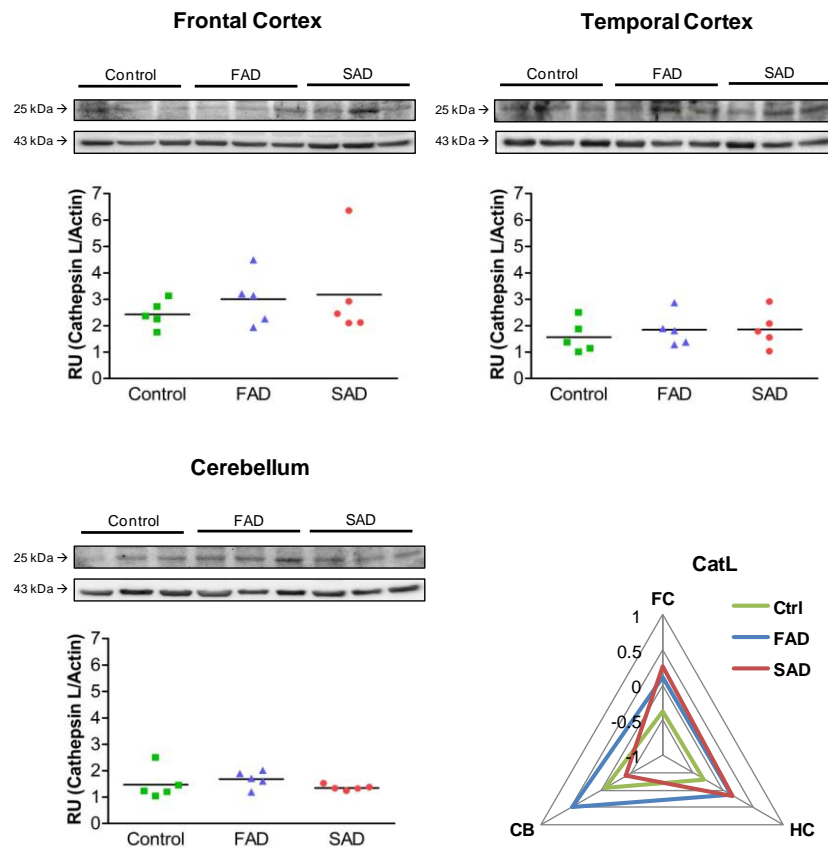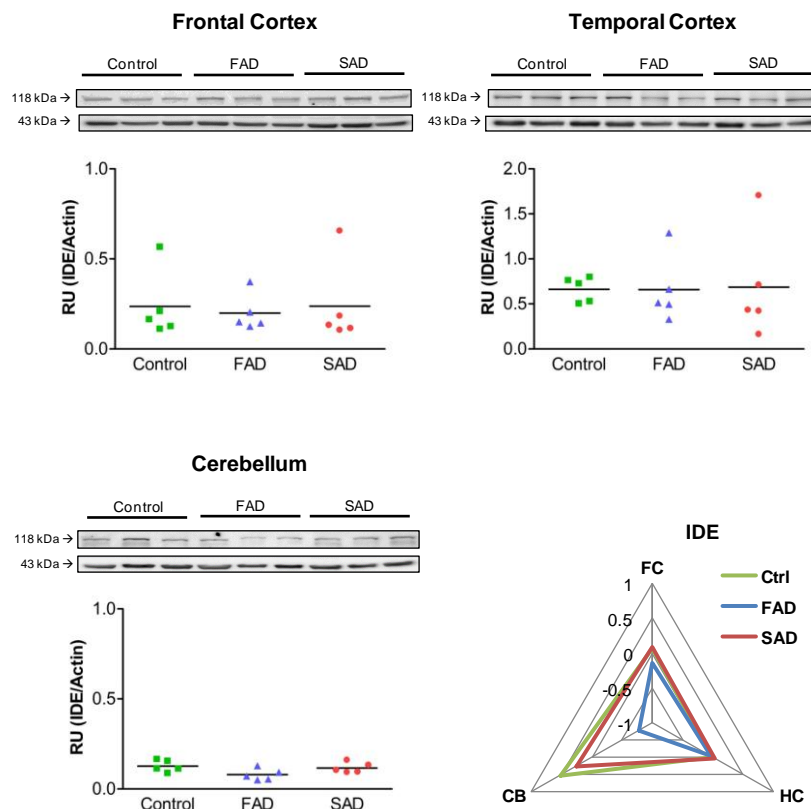
Figure 7. Expression of IDE in FAD, SAD and healthy individuals. Levels of IDE in frontal cortex, temporal cortex and cerebellum from FAD, SAD and controls. Comparison of IDE distribution profiles between brain regions calculated as Z values. Data are shown as dot plots with horizontal bars indicating the mean, *n*=5.

4.6. Expression profile of Glycogen synthase kinase 3β (GSK3β) and Erk in Sporadic and Familial Alzheimer's Disease

The formation of intracellular Tau protein aggregates is a well characterized neuropathological hallmark in brains from patients with Alzheimer's disease. The neurofibrillary tangles are aggregates of hyperphosphorylated Tau protein which are the product of an uncontrolled activity of kinases like GSK3β or Erk (109;113).
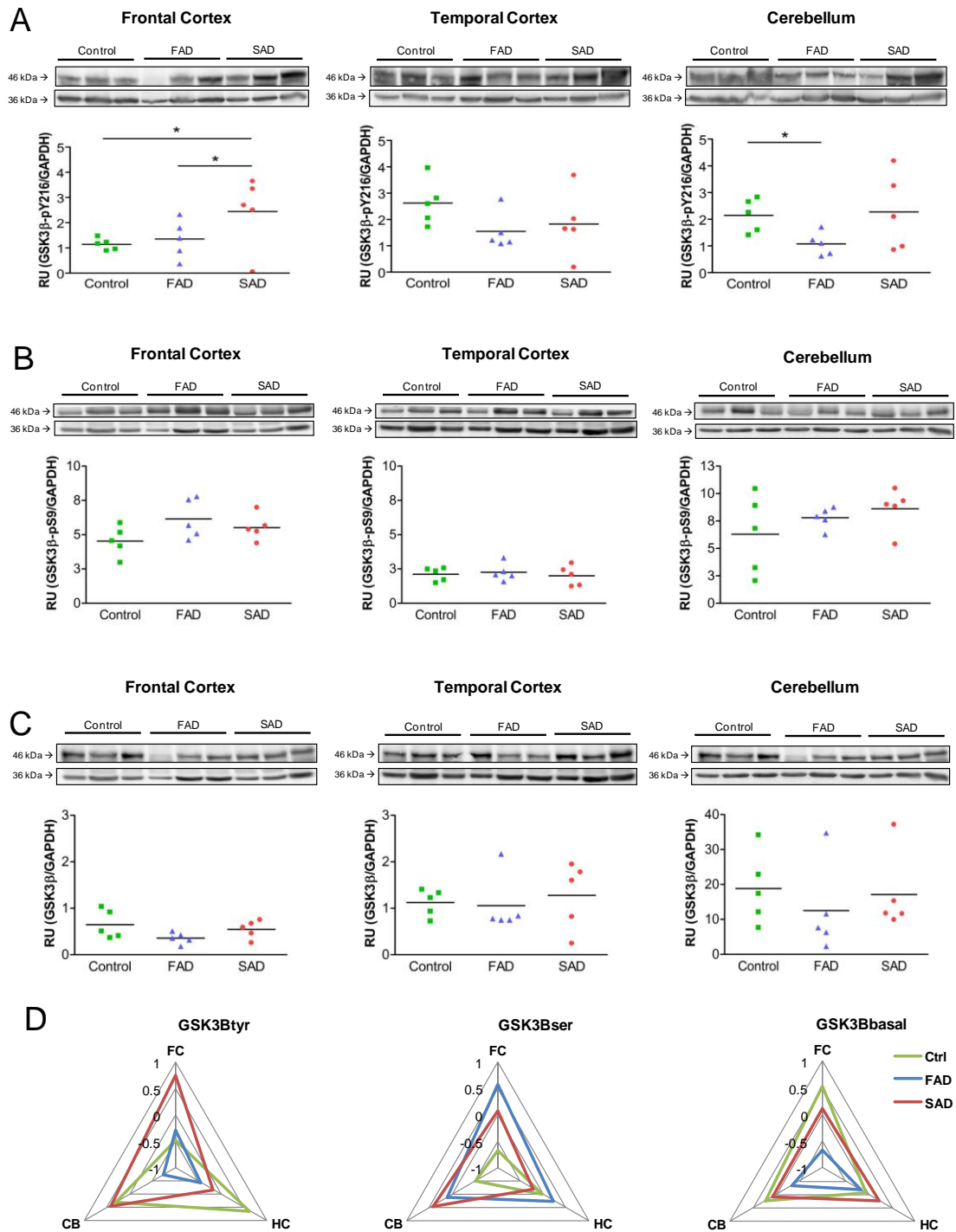
Figure 8. Activation profile of GSK3β in Frontal Cortex, Temporal Cortex and Cerebellum from FAD, SAD and healthy individuals. A) Phosphorylation levels of GSK3β in tyrosine 216 in frontal cortex, temporal cortex and cerebellum from FAD, SAD and controls. **B)** Phosphorylation of GSK3β in serine 9 in frontal cortex, temporal cortex and cerebellum from FAD, SAD and controls. **C)** Expression of GSK3β in three different brain areas of FAD, SAD and controls. **D)** Comparison of GSK3βpY216, GSK3βpS9 and GSK3β distribution profiles between brain regions calculated as Z values. Results were analyzed using a *t*-test and a $P<0.05$ was adopted for statistical significance. Data are shown as dot plots with horizontal bars indicating the mean, *n*=5.

We evaluated the activity state of GSK3β by analyzing its phosphorylation status. As mentioned above, GSK3β is inhibited when is phosphorylated at serine 9 and becomes active when is phosphorylated at tyrosine 216. The activation states are in equilibrium, but under pathological conditions the enzyme remains active and phosphorylates its substrates without control. Due to the importance of this phenomenon for the pathogenesis of the disease, we studied the phosphorylation and expression levels of GSK3β in our samples. The analysis of the frontal cortex showed that there were increased levels of active GSK3β in SAD individuals relative to FAD (P=0.0002) and controls (P=0.0073). The comparison of FAD and healthy individuals revealed that in both groups GSK3β had the same activation level (Figure 8A). It was also observed that in temporal cortex the phosphorylation of GSK3β in tyrosine 216 was decreased in FAD and SAD cases compared with healthy individuals. When FAD and SAD were compared, a slight increase of active GSK3β was found in SAD relative to FAD samples. However, no statistical significance was reached (Figure 8A). Interestingly, in the cerebellar tissue a significant decrease in the activation of GSK3β was observed in FAD samples (P=0.0141) compared with controls (Figure 8A). This effect was also observed when FAD and SAD cases were compared, but the change was not statistically significant (Figure 8A). When the activation levels of GSK3β was compared in SAD and control individuals a slight increase was observed in the first group (Figure 8A). The expression profile of GSK3β phosphorylated at tyrosine 216 showed that SAD patients had an increased presence of this kinase in frontal cortex, followed by cerebellum and temporal cortex. On the contrary, FAD samples had a relative

distribution that was elevated in temporal cortex and cerebellum while the controls were homogeneously distributed among brain areas (Figure 8D).

In the frontal cortex a slight increase in the phosphorylation of GSK3β on serine 9 was observed in FAD cases with respect SAD cases and controls. This trend was also seen between SAD and control individuals. However, the inhibition levels of this kinase were not statistically significant (Figure 8B). When the serine 9 phosphorylation was analyzed in the temporal cortex and cerebellum, no changes were observed among experimental groups (Figure 8B). The distribution pattern of inhibited GSK3β in AD cases showed higher Z values in SAD with increased cerebellar distribution, while FAD cases showed an uniform distribution pattern. The distribution of this enzyme in healthy controls showed a tendency to higher Z values in temporal cortex (Figure 8D).

The expression of the basal form of GSK3β was also determined. There was a tendency toward decreased levels of GSK3β in FAD and SAD cases relative to controls although this decrease was not significant. This was also true for the comparison between FAD and SAD individuals (Figure 8C). No differences in the expression of basal GSK3β were observed among samples when the temporal cortex was analyzed (Figure 8C). The evaluation of the cerebellar region showed that GSK3β was decreased in FAD and SAD patients relative to controls. This was also observed between FAD and SAD samples. None of the analysis resulted in statistical significance (Figure 8C). The protein expression profile indicated that in SAD and FAD patients the mean distribution of GSK3β was homogeneous among regions. The comparison of the Z values from

healthy individuals showed that GSK3β was distributed mainly in temporal cortex and cerebellum (Figure 8D).

An up-regulation in the activation of Erk1/2 has been found in brains from Alzheimer's disease patients and this finding correlates with the progressive sequence of development of NFTs (115). This supports the theory that the abnormal hyperphosphorylation of Tau could be carried out by Erk. With this in mind, we tested the phosphorylation of Erk1/2 in our experimental groups. It was observed that the activation levels of Erk1/2 were significantly elevated in FAD (P=0.0079) and SAD (P=0.0079) patients compared with control individuals (Figure 9A) while the phosphorylation between FAD and SAD cases was at the same level (Figure 9A). This pattern was also observed in the temporal cortex. Here it was found that the levels of activation of Erk1/2 were significantly higher in FAD (P=0.0079) and SAD (P=0.0079) cases in relation with controls (Figure 9A). Interestingly, the phosphorylation levels of this kinase in SAD patients was decreased in comparison with that of the FAD patients, however, this difference was not significant (Figure 9A). In the cerebellum, the phosphorylation pattern of Erk1/2 was also found to be increased in FAD (P=0.0159) and SAD (P=0.0080) samples compared with the control group and these changes were statistically significant (Figure 9A). In this particular region, it was observed that the activation of the kinase was more augmented in SAD individuals than in FAD, but without statistical relevance (Figure 9A). The distribution analysis reveals a contrasting pattern between SAD and FAD cases. In the first case there was an increased distribution in cerebellum while in the second a marked distribution in temporal cortex was observed. Healthy controls

showed uniform distribution and lower values (Figure 9C). We also studied the expression of basal Erk1/2 in our sample and no statistically significant difference was found among groups in the brain regions evaluated (Figure 9B). The distribution analysis demonstrated a similarly uniform expression pattern among brain areas in all groups (Figure 9C).
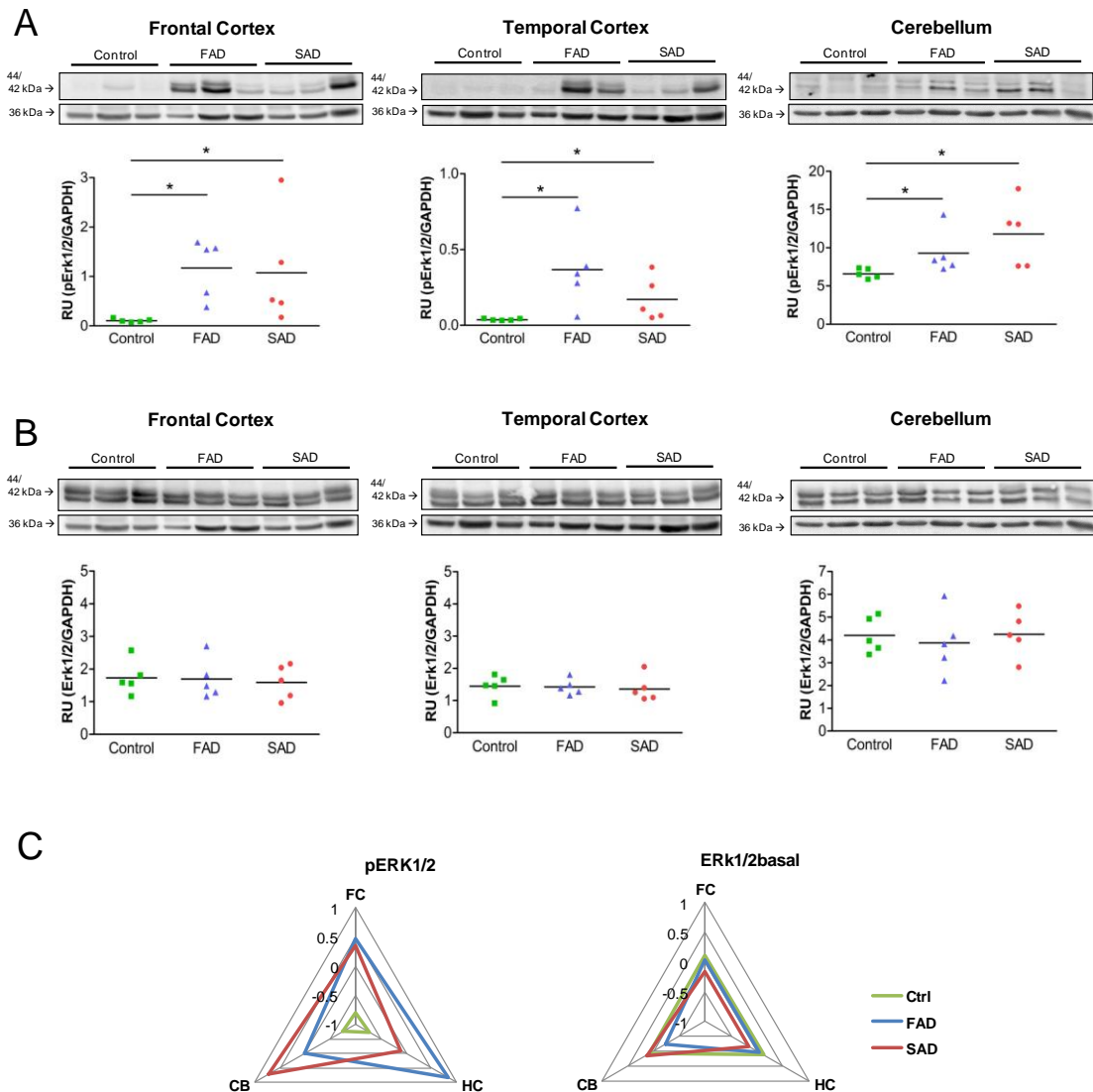
Figure 9. Activation profile of Erk1/2 in Frontal Cortex, Temporal Cortex and Cerebellum from FAD, SAD and healthy individuals. A) Phosphorylation levels of Erk1/2 in frontal cortex, temporal cortex and cerebellum from FAD, SAD and controls. **B)** Expression of Erk1/2 in three different brain areas from FAD, SAD and controls. **C)** Comparison of Erk1/2 and pErk1/2 distribution profiles between brain regions calculated as Z values. Results were analyzed using a t-test and a $P<0.05$ was adopted for statistical significance. Data are expressed as mean ± SEM, $n=5$.

4.7. Role of the Protease Inhibitor Testican-1 in Sporadic and Familial Alzheimer's Disease

Testican-1 is a proteoglycan containing protease inhibition domains with a wide expression in the human brain (127). In a recent proteomic study, it was found that in CFS of Alzheimer's disease patients the presence of the C-terminal fragment (CTF) of Testican-1 was increase with regard to age-matched controls (0.79% vs. 0.53%) and the correlation between sensitivity and specificity (AUC of the ROC curve = 0.973, SE = 0.020, CI = 95% and P=0.0001) was high enough to consider this protein as a new potential CSF biomarker for Alzheimer's disease (118). These results were used as starting point for our study.

First, we tried to develop a direct ELISA test to quantify the levels of Testican-1 CTF in CSF from FAD, SAD and controls. For this we generated an antibody targeting the sequence of the Testican-1 fragment with the best ROC value (0.015). During the standardization process it was noticed that the test was not sensitive enough to detect low concentrations of the fragment present in the CSF samples, reaching a detection limit in the range of ng/mL while the peptides should be detected at pg/mL levels (Figure 10A and B).
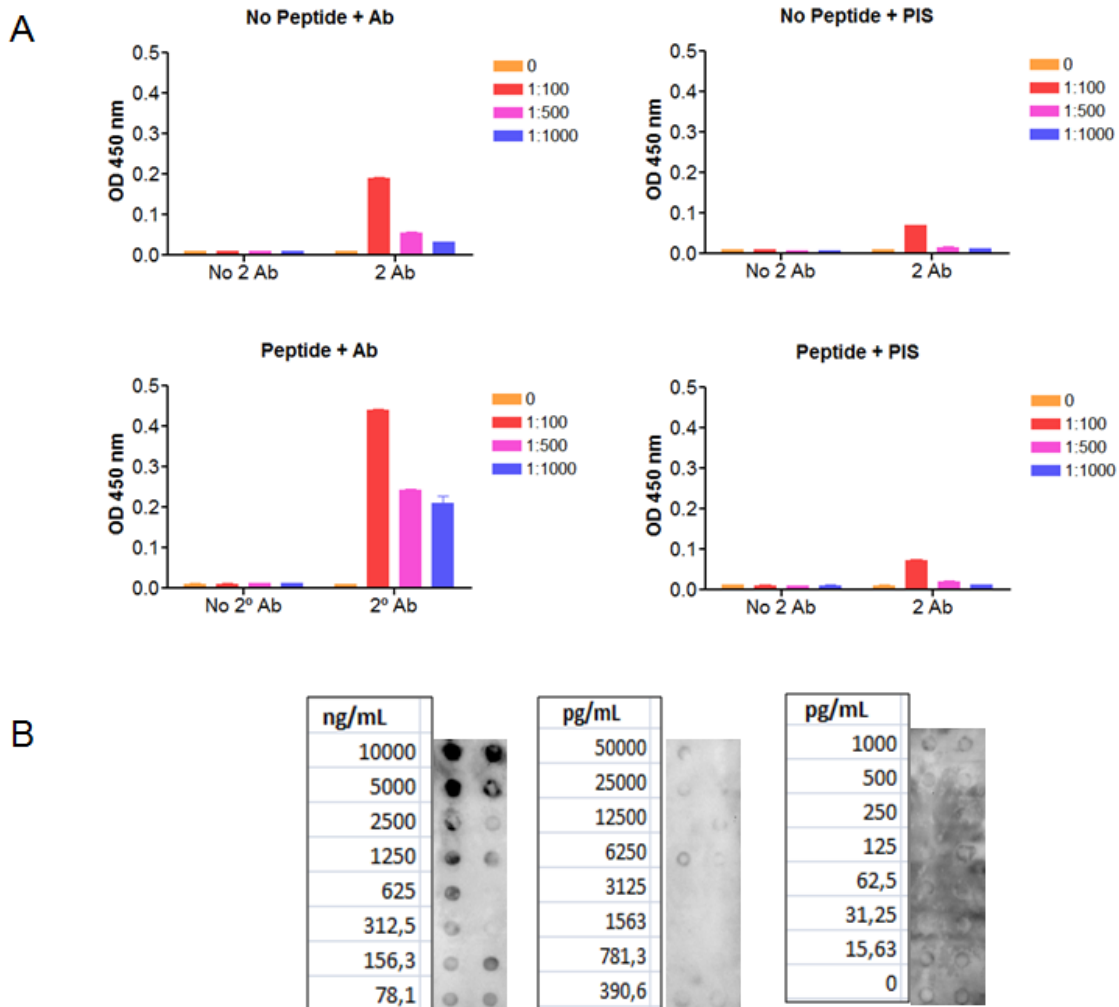
Figure 10. Standardization of the ELISA test for Testican-1/CTF. A) Specificity test for the antibody designed to detect Testican-1/CTF. **B)** Sensitivity test to detect Testican-1/CTF in human CSF.

As an alternative we tried to determine the levels of the Testican-1 CTF through Western blot using tricine gels to resolve small peptides. This method was even less sensitive and no signal was obtained during the assay. Finally, we opted for another strategy and decided to evaluate the level of full length Testican-1 in our groups of study. The expression of this protein in the frontal cortex remained at the same level in the three groups of individuals (Figure 11) while in the temporal cortex there was a trend to increased amounts of Testican-1 in FAD and SAD samples compared with controls failing to reach statistical

significance (Figure 11). The expression of this protein was not modified in the cerebellar region of either group of subjects (Figure 11).
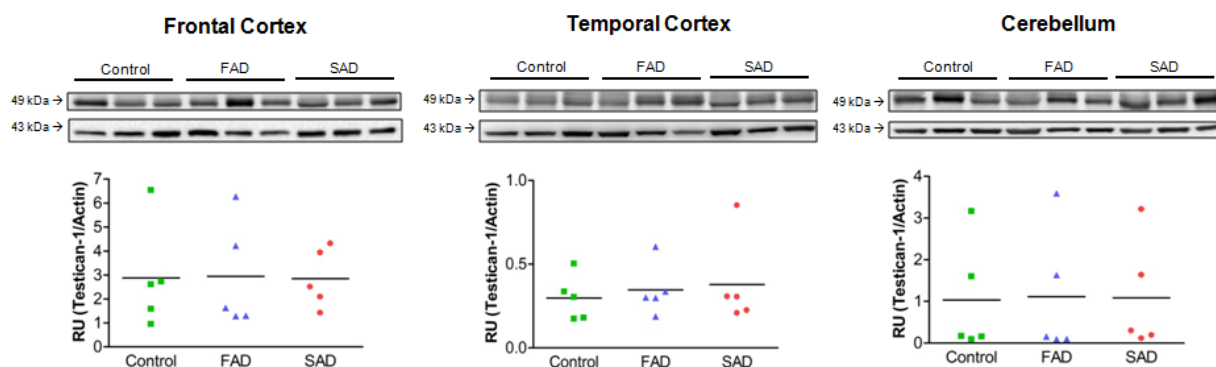
Figure 11. Expression profile of Testican-1 in FAD, SAD and healthy individuals. Levels of Testican-1 in three different brain areas of FAD, SAD and controls. Data are shown as dot plots with horizontal bars indicating the mean, *n*=5.

Testican-1 also forms part of the extracellular matrix and is secreted from neurons (119). We hypothesized that due to the extracellular localization, this protein could be found co-aggregating in amyloid plaques. To test this hypothesis, a new group of individuals consisting of 34 controls and 38 SAD patients (Appendices 2 and 7) was evaluated. A tissue microarray (TMA) was made and the frontal, temporal and entorhinal cortex of these cases were analyzed by mean of immunohistochemistry and immunofluorescence.

Immunohistochemical detection using a Testican-1 antibody revealed an extracellular plaque-like Testican-1 accumulation in the cerebral cortex of AD patients (Figure 12) and the immunofluorescence analysis showed co-localization of Testican-1 and amyloid plaques in the cerebral cortex of AD patients (Figure 12). For the TMA, tissue cylinders were punched from anatomically defined areas within paraffin blocks of gryrus frontalis medius,

temporal cortex at the level of the lateral corpus geniculatum and the entorhinal cortex. A total of eight tissue cylinders were punched from each region and punches were randomly taken from the six layers of the cortex.
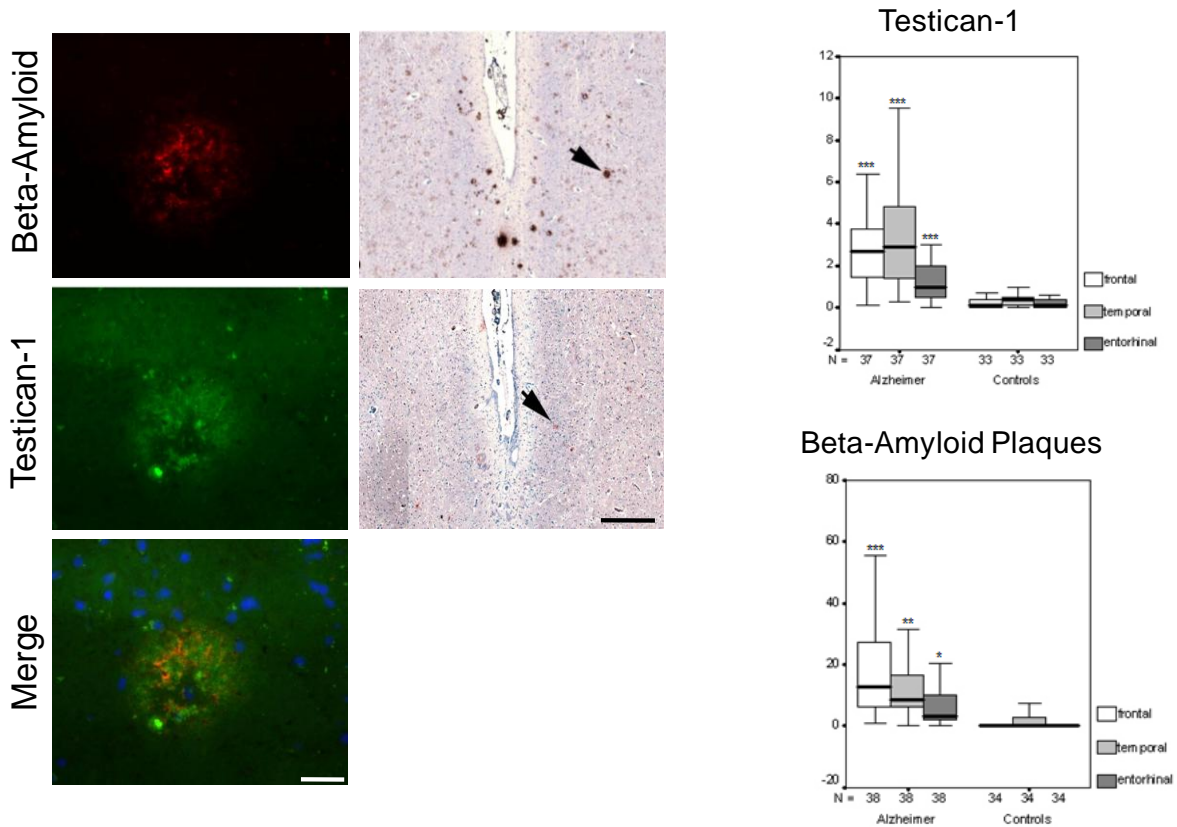
Figure 12. Colocalization of Testican-1 and Aβ plaques. Colocalization analysis reveals the presence of Testican-1 in Aβ plaques from AD patients. Number of Testican-1 and Aβ positive plaques per specimen in TMA-arrays of AD patients and controls using immunohistochemical analysis. The boxes encompass 25th and 75th distribution percentiles and the whisker indicates the range of values. *** p<0.001, ** p<0.005, * p<0.05. Scale bar represents 500 µm

The average number of diffuse (smooth) and neuritic (core) plaques and the total number of plaques per tissue punch was determined for AD patients and controls revealing a significantly higher plaque load in all brain regions from AD patients compared to controls (frontal cortex: AD vs. control *P*<0.001, temporal cortex: AD vs. control *P*<0.005, entorhinal cortex: AD vs. control *P*<0.05) (Figure 12, Appendix 7). The distribution pattern of Testican-1 plaques was similar to that of total Aβ plaques, with a significantly higher Testican-1 positive

plaque count in the frontal ($P<0.001$), temporal region ($P<0.001$) and entorhinal cortex ($P<0.001$) (Figure 12, Appendix 7). The mean ratio of Aβ positive to Testican-positive plaques was 20.4:1 in the frontal, 5.6:1 in the temporal and 8.7:1 in the entorhinal cortex, revealing the highest relative and absolute number of Testican-1 plaques in the temporal cortex (Figure 12, Appendix 7).

Following these results we wanted to explore the molecular mechanism underlying the aggregation of Testican-1 in amyloid plaques. To achieve this aim, we used HEK293T cells to generate stable cell lines expressing the human wild type form of APP (APPwt) and the APP variant bearing the swedish double mutation K670N>M671L (APPsw) (Appendix 5). These cell lines were transiently transfected either with Testican-1 or empty vector (Mock) to evaluate the effect of this protein in the production of Aβ species (Aβ40/Aβ42). Wild type HEK293T cells were used as negative control due to the sparse expression of APP. The transfection efficiency as well as the levels of APP expressed by the cell lines was determined through Western blot (Appendix 6). The cells were transfected for 24 h and after that time the supernatant was collected and used to measure the production of Aβ40 and Aβ42 and proteins were isolated from the cells. An ELISA test was performed to determine the concentration of Aβ40 and Aβ42 in the supernatants. After quantification, it was found that the levels of both Aβ40 (Mean Concentration=623.1 pg/mL, SEM=6.507, P=0.0207) and Aβ42 (Mean Concentration=38.25 pg/mL, SEM=3.512, P=0.0011) were lower in APPsw cells transfected with Testican-1 compared with their levels in APPsw cells transfected with Mock (Aβ40 Mean Concentration=769.9 pg/mL, SEM=4.547; Aβ42 Mean Concentration=56.55 pg/mL, SEM=1.074) (Figure

13). In contrast, the transfection of Testican-1 or Mock in APPwt or wild type HEK293T cells did not produce statistical differences in the levels of Aβ40 and Aβ42 (Figure 13).
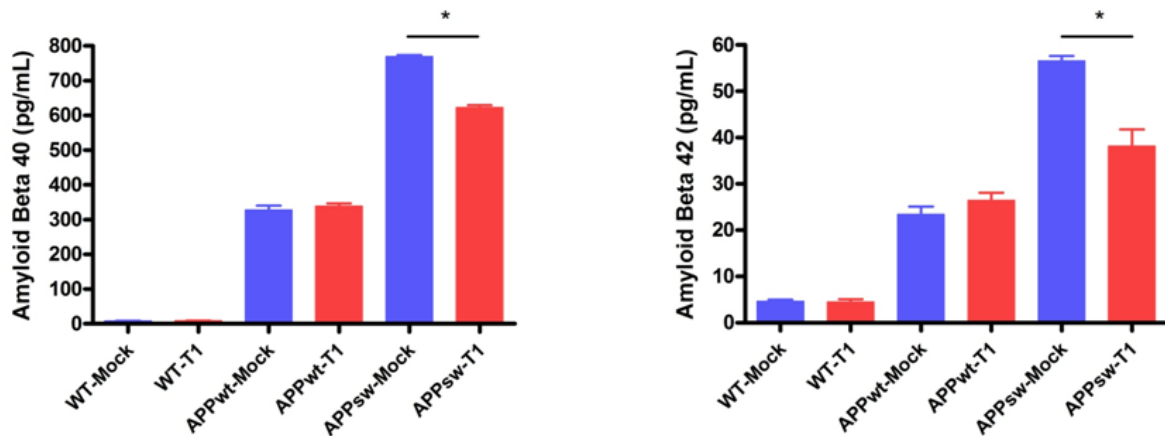
Figure 13. Levels of Aβ40 and Aβ42 in supernatant from HEK293T cells transfected with Testican-1. HEK cells expressing wild type, APPwt and APPsw were transfected with Mock or Testican-1. After 24h the levels of Aβ40 and Aβ42 present in the supernatant were measured by ELISA. A significant decrease in the concentration of Aβ40 ($P<0.0001$) and Aβ42 ($P=0.0006$) was observed in the HEK cells expressing APPsw. Results were analyzed using a t-test and a $P<0.05$ was adopted for statistical significance. Data are expressed as mean ± SEM.

We hypothesized that decreased levels of Aβ40 and Aβ42 in APPsw cells transfected with Testican-1 might be related to Testican-1 activity at different points during either the production or the degradation of Aβ. To examine whether Testican-1 could regulate Aβ production, we analyzed the relative activity of the enzymes involved in the processing of APP by monitoring levels of APP C-terminal fragments, C83 and C99, by Western blot. The first fragment serves as an indirect measure of the α-secretase activity and the second reflects the activity of the β-secretases. The analysis demonstrated that the transfection of Testican-1 did not alter the α- or β-secretase activity. No statistically significant differences were observed in the expression of the C83-

and C99-APP fragments in APPsw HEK293T cells when the cells transfected with Testican-1 were compared with the controls (Mock) (Figure 14). The same result was obtained when the ratio C83/APP-FL and C99/APP-FL was calculated (Figure 14). In APPwt cells the levels of the C83 and C99 fragments were elevated 4-fold and 2-fold respectively (Figure 14). However, when the expression of these fragments in Testican-1- and Mock-transfected APPwt cells was evaluated, no difference was found.

We looked for another alternative to explain the phenotype observed in APPsw cells. Since the activity of the secretases seemed to be unaltered by Testican-1 transfection, it is possible that expression of APP secretases was modified. Hence, BACE1, ADAM-10 and PS1 levels were analyzed in cell lysates. An increase in BACE1 expression was observed in all cells transfected with Testican-1 (WT, APPwt and APPsw) in comparison with Mock transfected cells, but this increment was not statistically significant (Figure 15). Regarding the levels of ADAM-10, a decrease in its levels was notable in APPwt and APPsw cells transfected with Testican-1 and no changes were observed in wild type cells expressing Testican-1 (Figure 15). These variations did not reach statistical significance. In comparison with ADAM-10, the expression of PS1 showed a tendency to increase in APPsw expressing Testican-1 and no variation was observed between Testican-1 and mock transfected wild type and APPwt cells (Figure 15).

Figure 14. Levels of APP and its fragments in HEK293T cells transfected with Testican-1. HEK cells expressing wild type, APPwt and APPsw were transfected with Mock or Testican-1. The levels of APP and APP-CTF were analyzed 24 h after transfection by Western blot. Data are expressed as mean ± SEM.
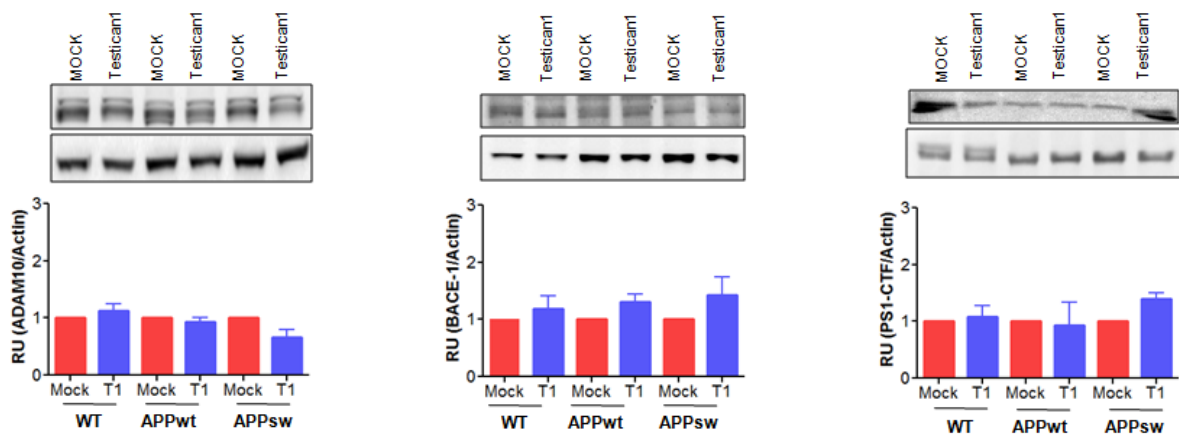
Figure 15. Expression of ADAM-10, BACE1 and PS1 in HEK293T cells transfected with Testican-1. HEK cells expressing wild type, APPwt and APPsw were transfected with Mock or Testican-1. The levels of ADAM-10, BACE1 and PS1 were analyzed 24 h after transfection by Western blot. Data are expressed as mean ± SEM.

Since the activity and the expression of the enzymes related to the processing of APP did not offer any molecular target explaining the variations of the Aβ levels in the APPsw cells transfected with Testican-1, we considered the possibility that degradation of Aβ was affected and decided to test the expression of IDE and cathepsin L in our cellular model. The expression of IDE was diminished in APPwt and APPsw cells transfected with Testican-1 (Figure 16). In contrast, IDE levels in the wild type HEK293T cells overexpressing Testican-1 were slightly augmented (Figure 16). The results of the statistical analysis did not show any difference among the experimental groups. Cathepsin L seemed to follow the same expression pattern as IDE. In both APPwt and APPsw cells, expression of Testican-1 led to decreased expression of cathepsin L when compared to controls (Figure 16). Unlike the other cell lines, the wild type cells showed increased levels of the protease, but in all cases the differences failed to reach statistical significance (Figure 16).
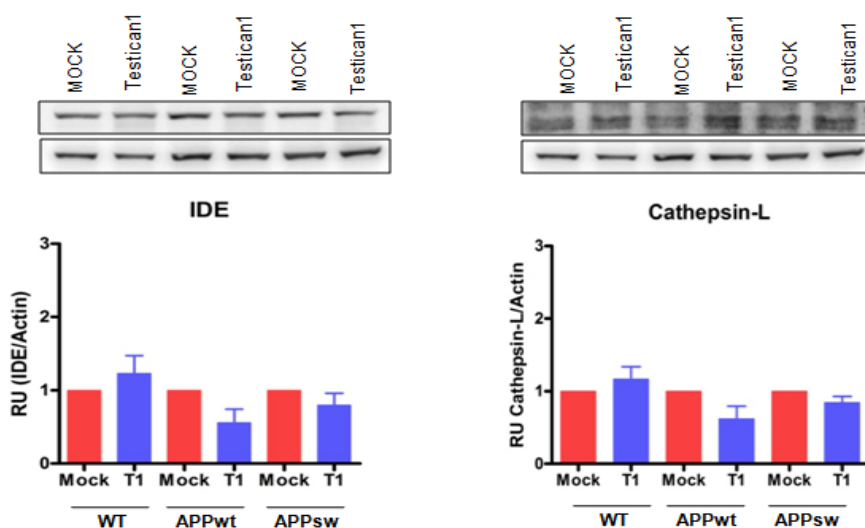
Figure 16. Expression of IDE and cathepsin L in HEK293T cells transfected with Testican-1. HEK cells expressing wild type, APPwt and APPsw were transfected with Mock or Testican-1. The levels of IDE and cathepsin L were analyzed 24 h after transfection by Western blot. Data are expressed as mean ± SEM.

In order to find an explanation for the phenotype observed in the APPsw cells transfected with Testican-1, we evaluated the colocalization and subcellular distribution of this proteoglycan in HEK293T cells (WT, APPwt and APPsw) using immunofluorescence and confocal microscopy. Initially, we analyzed the possible interaction between APP and Testican-1. In wild type HEK293T cells, Testican-1 had an intense perinuclear distribution corresponding to the ER. The protein was also distributed along the cytoplasm, but the intensity of the signal was very faint (Figure 17). Compared with APPwt cells transfected with the empty vector, the expression of APP and Testican-1 in APPwt cells showed a puncta-like pattern with very low colocalization of both proteins in the cytoplasmic region of the cells (Figure 17). In APPsw cells, the expression of APP and Testican-1 was diffuse and colocalization between both proteins was observed (Figure 17).
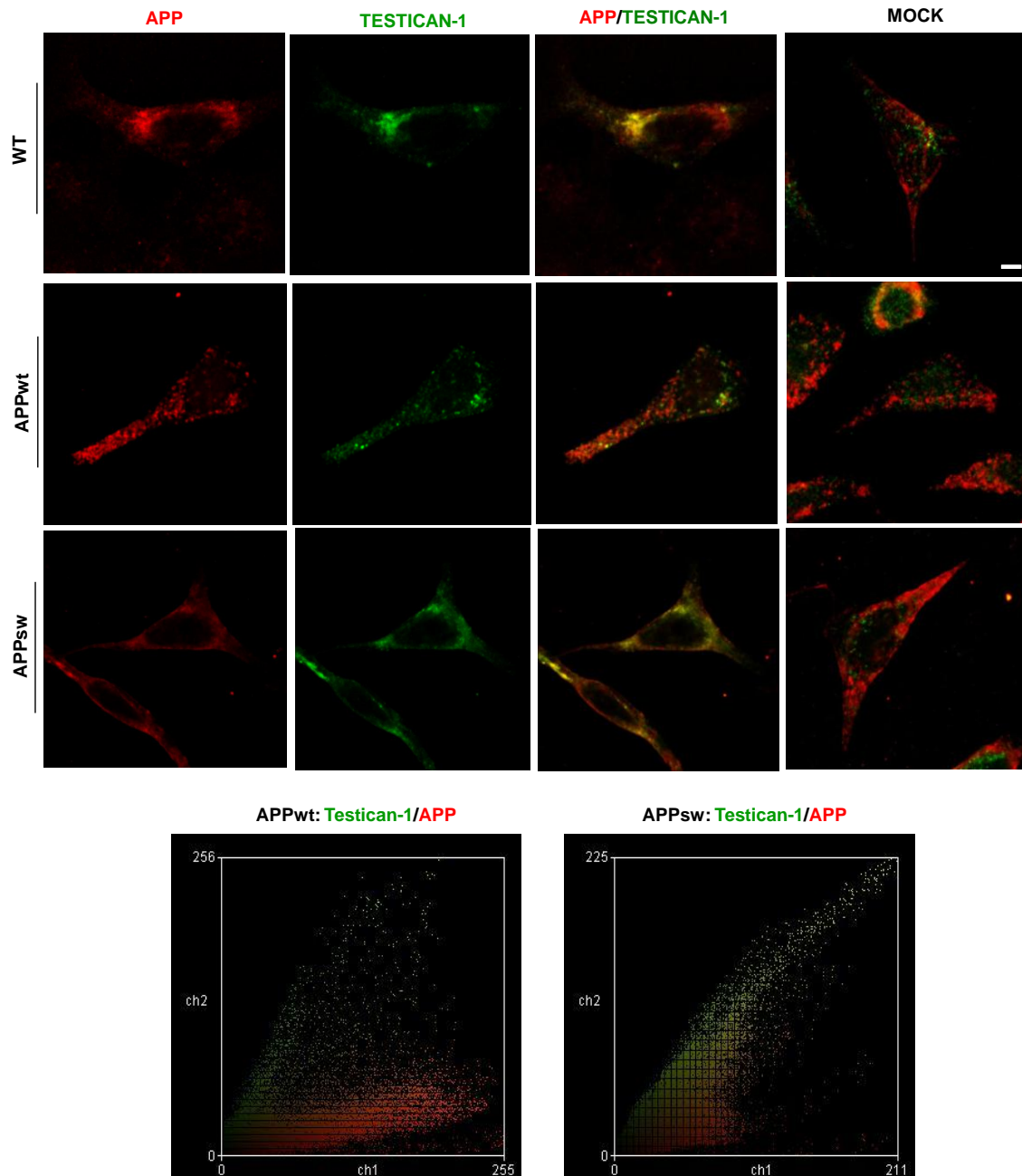
Figure 17. Subcellular distribution of APP and Testican-1 in HEK293T cells transfected with Testican-1. HEK cells expressing wild type, APPwt and APPsw were transfected with Mock or Testican-1. The distribution of APP (Red) and Testican-1 (Green) was analyzed 24 h after transfection using confocal microscopy. Colocalization profile of APP and Testican-1 in APPsw cells transfected with Mock or Testican-1. Scale bar represents 5 µm.

In order to investigate if the effect observed in the APPsw cells was due to alterations of ER or Golgi structure caused by Testican-1. Double staining for Testican-1 and KDEL, an ER marker, was carried out. Full colocalization and a dotted pattern of both proteins was observed in wild type cells (Figure 18) while

in APPwt cells the vesicle-like structures were observed, but the level of colocalization was lower compared with that of the wild type cells (Figure 18). The expression pattern of Testican-1 in the APPsw cells was diffuse, but at some extent localized in ER (Figure 18). Next, expression of Testican-1 in Golgi was analyzed using the marker GM130. Wild type cells showed perinuclear localization and well defined Golgi apparatus, while in the cells transfected with Testican-1, colocalization of both proteins was observed, but Testican-1 was also distributed along the cytoplasm (Figure 18). This was also the case in APPwt cells, but the intensity of the signal was higher and Testican-1 had a puncta-like pattern (Figure 18). Interestingly, the structure and the distribution of Golgi were highly altered in both APPsw cells, Mock- and Testican-1 transfected (Figure 18). The Golgi apparatus was not perinuclear, but distributed along the cell body. Some aggregates were observed in colocalization with Testican-1 (Figure 18).

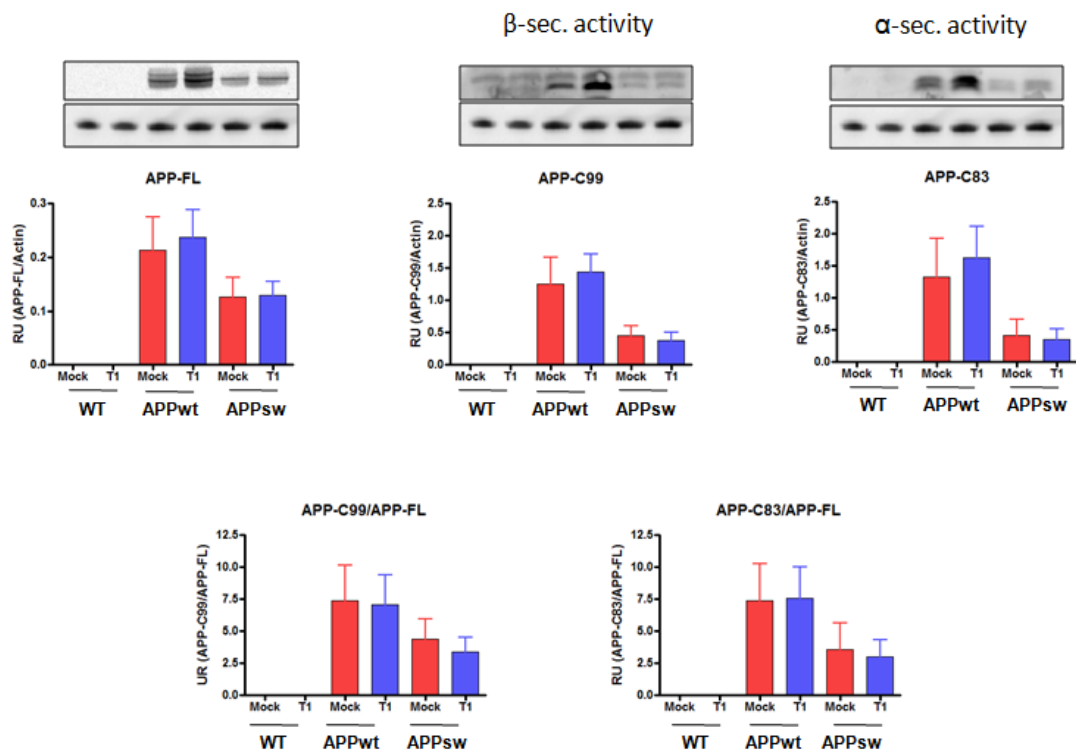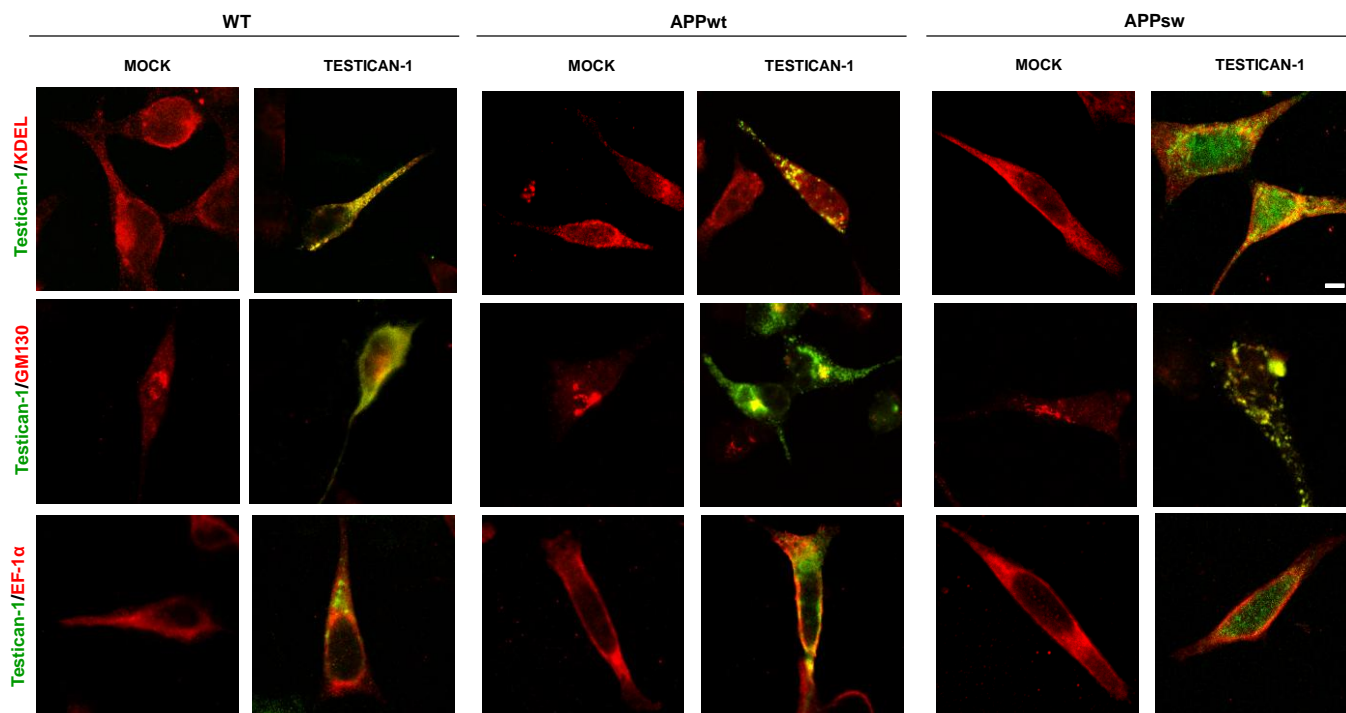**Figure 18. Localization of Testican-1 in subcellular compartments of HEK293T cells transfected with Testican-1.** HEK cells expressing wild type, APPwt and APPsw were transfected with Mock or Testican-1. Testican-1 (Green) localization in ER (KDEL: Red), Golgi (GM130: Red) and Exosomes (EF-1α: Red) was analyzed 24 h after transfection using confocal microscopy. Scale bar represents 5 µm.

Based on these results we hypothesized that the protein sorting machinery might be altered in the APPsw cells. We evaluated the subcellular distribution of Testican-1 and the Elongation factor-1α (EF-1α), a marker for exosomes, to test if secretion of Testican-1 was dysregulated. The staining revealed that the mean distribution of EF-1α was surrounding the nucleus in all cell lines and that there was no colocalization between this protein and Testican-1 (Figure 18). We also evaluated the formation of endosomes using Adaptin-γ as marker. Some aggregates were observed in wild type cells, but this could be due to the formation of multivesicular bodies (Figure 19). A colocalization between Adaptin-γ and Testican-1 was observed in these cells (Figure 19). Testican-1

and the endosomal marker were distributed through the cell body of the APPwt cells and some weak colocalization was observed around the nucleus (Figure 19). In the APPsw cells, the distribution of Adaptin-γ and Testican-1 was similar to that of the APPwt cells; however, these proteins were not located in the same subcellular compartment (Figure 19).

Finally, we studied the degradation system using cathepsin L as a lysosomal marker. In wild type cells, both cathepsin L and Testican-1 had a wide distribution throughout the cell and full colocalization was observed (Figure 20).
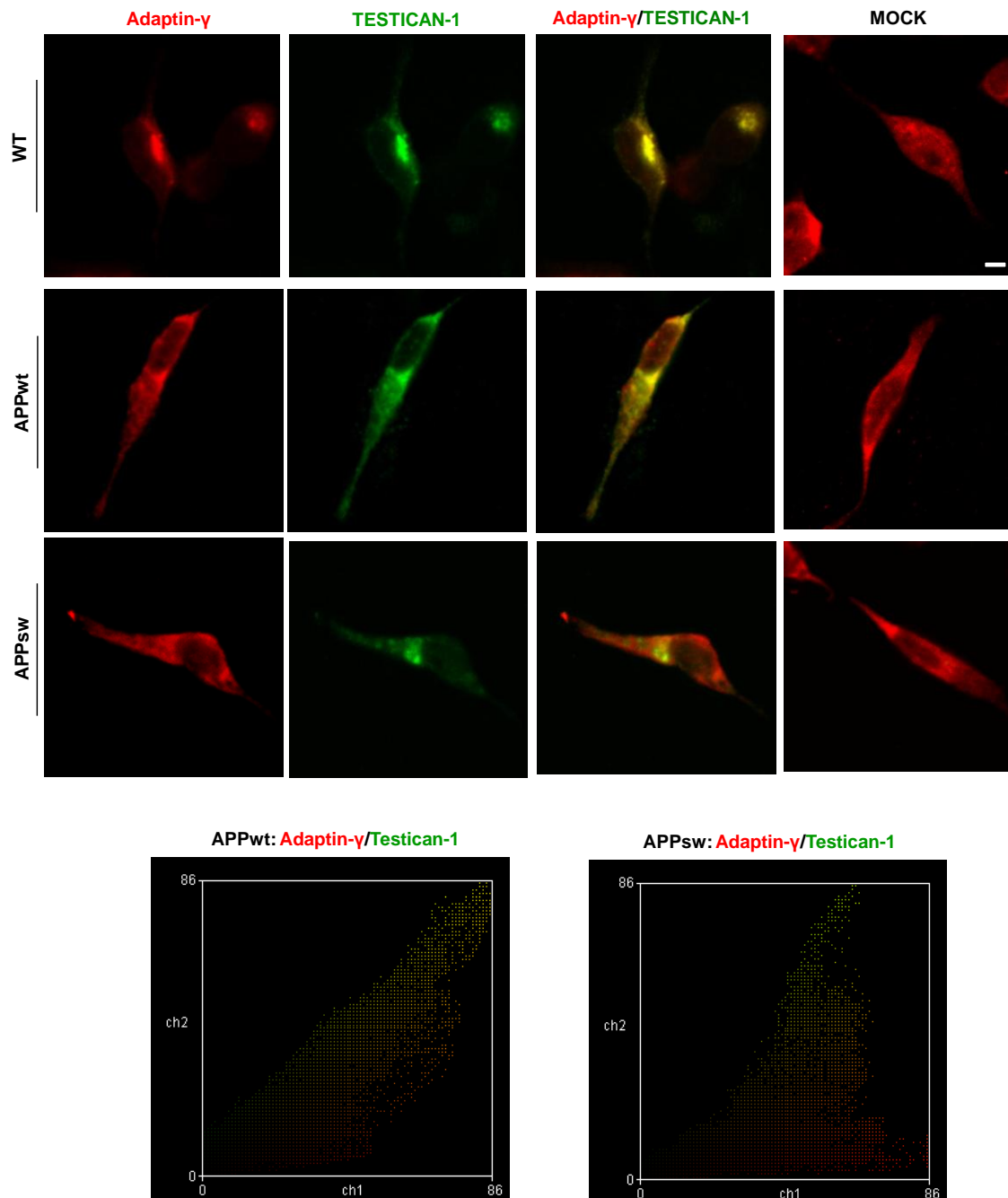
Figure 19. Localization of Testican-1 in Endosomes of HEK293T cells transfected with Testican-1. HEK cells expressing wild type, APPwt and APPsw were transfected with Mock or Testican-1. The localization of Testican-1 (Green) in Exosomes (Adaptin-γ: Red) was analyzed 24 h after transfection using confocal microscopy. Scale bar represents 5 µm.

The distribution of both proteins in APPwt cells behaved in the same way as in the wild type cell, but unlike these, the expression of Testican-1 showed the puncta-like pattern observed before (Figure 20). In APPsw cells, cathepsin L was widely distributed along the cell, but Testican-1 showed a discrete

expression surrounding the nucleus. In this case the colocalization observed between both proteins was higher than in APPwt cells (Figure 20).
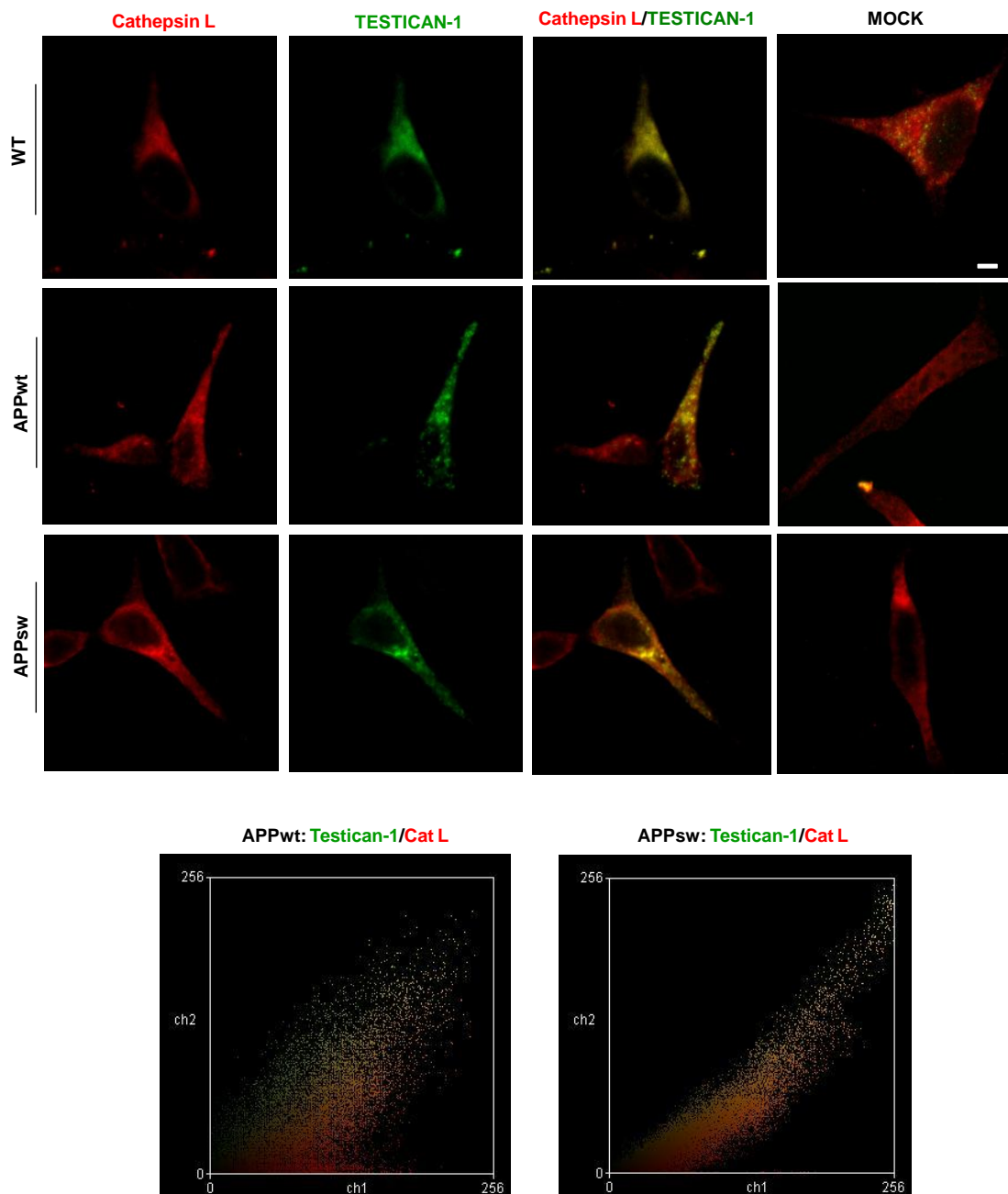
Figure 20. Subcellular distribution of cathepsin L and Testican-1 in HEK293T cells transfected with Testican-1. HEK cells expressing wild type, APPwt and APPsw were transfected with Mock or Testican-1. The distribution of cathepsin L (Red) and Testican-1 (Green) was analyzed 24 h after transfection using confocal microscopy. Colocalization profile of cathepsin L and Testican-1 in APPsw cells transfected with Mock or Testican-1. Scale bar represents 5 μm.

5. DISCUSSION

Alzheimer's disease affects more than 35 million people worldwide and it is a serious public health issue. Although most AD cases are due to unknown causes about 1% of them are caused by genetic mutations. Studies in FAD cohorts have provided valuable insights to understand the pathogenesis of the disease (128). The largest cohort of FAD with around 5000 members is a Colombian kindred carrying the E280A mutation in the PS1 gene. For several years the Neurosciences Group of Antioquia (Medellin, Colombia), in collaboration with its international partners, have been working in the genetic and clinical characterization of this family. Despite the progress reached so far to gain new insights into the disease many aspects are still unclear. For this reason a collaborative work was established with Institute of Neuropathology of the University Medical Center Hamburg-Eppendorf (Hamburg, Germany) to explore the neuropathological mechanisms of the disease in brain samples of FAD patients from Colombia and in this way obtain new knowledge about the disease.

The goal of this work was to characterize the expression of proteins that play an important role in the pathogenesis of AD and that could potentially be used as biomarkers for diagnosis or to differentiate between AD variants. We first evaluated the levels of APP in different brain regions, including frontal cortex, temporal cortex and cerebellum. Each of these areas has a particular function and may be affected by the progress of the disease in a specific way (27;129). Interestingly, we found that in FAD cases the expression of APP was decreased

when compared to SAD cases and controls in all the regions analyzed. This reduction could be caused by augmented processing of APP leading to increased levels of Aβ. The evaluation of the APP-CTFs showed less CTFs in FAD cases compared with SAD cases and controls in temporal cortex and cerebellum. This fact was confirmed when the ratio APP-CTF/APP-FL was analyzed indicating that in FAD cases the processing of APP is increased. The E280A PS1 mutation has been associated with a gain of function of the γ-secretase activity which could explain the elevated processing of APP observed in FAD patients (130). Furthermore, it has been proposed by Giliberto *et al.* that altered APP processing may be an indirect effect of the PS1 mutation on the expression and activity of BACE1. They demonstrated that different mutations in PS1 (M146V, S170F, and L392V) increased levels and activity of BACE1 in neuronal and non-neuronal cells and that this up-regulation was dependent on the expression of PS1 and the γ-secretase responsible of elevated Aβ42 formation (131). Although the E280A mutation was not evaluated, it is feasible that this mutation could modify the expression or activity of BACE1.

One important aspect in the processing of APP is related to the expression of levels of enzymes involved in this process. We evaluated the expression of ADAM-10, the most relevant metalloproteinase involved in the α-cleavage of APP, in the brain of FAD, SAD and control individuals. We found that in frontal cortex and cerebellum there was an unaltered expression of ADAM-10 in FAD cases compared with healthy individuals, but in SAD cases there was an elevation compared with the other two groups. ADAM-10 expression profile in SAD patients was different of that reported previously by Gatta *et al.* in which

they found increased levels of ADAM-10 mRNA in hippocampus and cerebellum of SAD patients (132). Another study demostrated that in platelets and CSF from SAD patients the levels of ADAM-10 were decreased (133). This interesting observation could be an indicator of accumulation or lack of degradation of this protease in the brain which could lead to the augmented amounts of ADAM-10. However, increased levels do not necessarily represent increased activity, further experiments for determining ADAM-10 activity would be necessary for clarifying this issue.

In further experiments where the expression of BACE1 was analyzed, we could establish that in the studied brain regions the levels of this protein were higher in SAD cases compared with FAD cases and controls; only in cerebellum SAD patients showed the same levels as the controls. Accordingly, earlier studies determined that the expression and activity of BACE1 is increased in the frontal cortex and temporal cortex, but not in the cerebellum of SAD patients (134-136). Recently it was found that the enzymatic activity of BACE1 was increased in CSF of SAD patients and that this was inversely correlated with the volume of the hippocampus (137). Immunohistochemical analysis showed elevated reactivity of BACE1 in frontal cortex and colocalization with Aβ labeling. Dystrophic axons close to blood vessels were labeled with BACE1 which could be related to axonal damage due to formation of Aβ deposition and give some evidence that might explain the formation of Aβ plaques surrounding the cerebral vasculature (123). These results support the idea that in SAD the modulation of BACE1 expression and activity is an important factor for the neuropathogenesis of the disease. Experiments performed in PS1/2 mouse

embryonic fibroblasts and SH-SY5Y cells transfected with PS1 suggest that the maturation and indirectly the activity of BACE1 may be regulated by PS1. The lack of PS1 decreased significantly the levels of BACE1 and its maturation was augmented when the cells were transfected with PS1 (138). However, in FAD patients this mechanism does not appear to be decisive for the progression of the disease. We found no alteration in our cases of the expression levels of BACE1 in FAD patients, in contrast to the findings discussed previously from Giliberto *et al.* Thus our results challenge the notion of an effect of PS1 mutations in BACE1 expression and APP processing that they proposed. BACE1 activity should be tested in this sample group in order to shed light on this issue.

The study of the expression of PS1 revealed that the frontal cortex of FAD and SAD cases presented higher levels of this protein compared to controls, while the cerebellar region showed less PS1 than SAD and control individuals. Markedly, no changes were observed in the temporal cortex (139). A recent study reported increased levels of PS1 mRNA and protein in frontal cortex of individuals with SAD, suggesting that the up-regulation of PS1 contributes to Aβ pathology. In contrast, some immunohistological studies have reported that the expression of PS1 seems to be unchanged or decreased in the frontal cortex of SAD individuals (138;139). The increased accumulation of PS1 in this region in both FAD and SAD cases could be due to a compensatory response to the increased activity of the γ-secretase complex or to an altered proteosome degradation of PS1 as suggested by experiments using neuronal cells (140). Using immunohistochemistry some authors have investigated the expression of

PS1 in the temporal cortex of SAD patients. They found a neuronal staining pattern labeling mainly the cell body of pyramidal, dystrophic neurites and Aβ plaques neurons; however, the data reveal that there is no difference in the immunoreactivity level of PS1 between SAD and control individuals (141). These data are in agreement with the results of the analysis of this area in FAD and SAD cases. Other researchers have also analyzed the levels of PS1 mRNA in the cerebellar region of SAD, but no differences were found relative to the control group (142). In the cerebellar region of E280A FAD samples, the decrease of PS1 expression might be due to the neuronal loss caused by the high Aβ load and the presence of NFTs as observed in previous work made in our group (129).

The alternative processing of APP has been matter of active research during the last years due to findings about enzymes with more affinity and specificity for APP than the classic proteases (84). We analyzed the expression pattern of cathepsin L, a cysteine protease related recently with the processing of APP. We could establish that the levels of this enzyme were slightly increased in the frontal cortex of FAD and SAD patients relative to controls. In comparison, the temporal cortex and the cerebellum did not show variations in the amounts of this protein. Cathepsin L belongs to the lysosomal system and its deficiency has shown to be involved in neurodegeneration in mice (143). Studies in human tissue have proposed that cathepsin L seems also to play an important role in the activation of microglia which is frequently seen in AD (144). So far, this is the first report about the expression of this cysteine protease in brain tissue from FAD, SAD and healthy individuals. Although no significative changes in the

expression levels of this enzyme were observed, further analysis of cathepsin L activity levels in this sample of patients will provide information not only about the involvement of this protein in the degradation of Aβ, but about its supposed β-secretase activity as proposed recently by Schechter *et al.* (84).

The balance between the production and degradation of Aβ is a determining feature for the pathogenesis of AD. The insulin degrading enzyme, a protein associated with the degradation of small peptides, has shown increased activity, but not expression in normal human brains (145). In SAD patients, IDE has been found in cortical, subcortical neurons and in senile plaques; the hippocampal region displayed a reduction of the enzyme levels as a function of the age while in cerebellum it remained mainly unchanged (146). Immunohistochemical characterization of IDE expression in frontal cortex from E280A FAD patients demostrated that this protein was present in the cytoplasmatic region of cortical neurons, it was linked to aggregated Aβ40 and it was present in activated astrocytes of white matter. This study reported also that the number of IDE-containing plaques was twofold increased in SAD compared to FAD patients suggesting that expression and activity of this enzyme is different between SAD and FAD (126). In the regions evaluated in our study only a slight decrease of IDE in FAD cases was observed, but there were no significant differences among groups. Although the total expression of IDE was unchanged in our samples, it would be necessary to evaluate the activity levels of this enzyme in the different brain regions in order to establish a correlation between the Aβ load and the degrading activity of IDE in AD.

Several studies have provided evidence for the involvement of PrP^c in the pathogenesis of AD. Immunohistochemical analysis of AD brains has shown that PrP^c colocalizes with diffuse plaques in a punctuated pattern while large PrP^c granules were observed in neuritic plaques. The deposition of this protein occurred in a filamentous and amorphous structures bond to Aβ plaques, but not the blood vessels (147). The expression of PrP^c in different brain regions of SAD patients has also been analyzed. These results indicate that while this protein was markedly overexpressed in frontal cortex, the occipital region showed a significant reduction (148). In contrast, recent studies have found no alterations of PrP^c levels in frontal and temporal cortices of individuals with no cognitive impairment, MCI, and SAD patients (149). When the expression levels of PrP^c were investigated in the brain regions of our sample of patients, we could observe that in SAD cases there were no changes in the expression of the protein as compared to healthy individuals, consistent with previous reports. However, in frontal and temporal cortices from FAD cases the amount of this protein was significantly decreased compared with SAD and controls. Conversely, in the cerebellar region the expression of PrP^c was highly increased. Whitehouse *et al.* found that PrP^c was reduced in hippocampus of SAD patients relative to controls, and no changes were observed between FAD and healthy individuals. In this study the authors evaluated six FAD cases with mutations in APP and two FAD patients carrying PS1 mutations. They reported that in FAD there were no modifications in the expression of PrP^c in comparison with the controls (150); however, no E280A carrier was included in this study and the effect observed should not be generalized for all FAD variants. A molecular mechanism that might explain the reduction of PrP^c observed in

frontal and temporal cortices of E280A FAD individuals could be proposed from the results obtained by Vincent *et al.* Using cell and animal models they demostrated that PS1 modulates the transcription of PrP^c by increasing AICD-induced p53 expression (151). Although the E280A PS1 mutation was not evaluated, it is possible to hypothesize that this mutation could produce a similar effect due to increased γ-secretase activity attributed to this mutation (130).

The formation of NFTs as consequence of the hyperphosphorylation of the Tau protein is a major event that contributes to the neurodegeneration in AD. Other authors have found decreased levels of basal GSK3β frontal cortex and hippocampus from SAD patients relative to controls (152;153). In our samples slight intergroup variations were observed, but without statistical significance. Since GSK3β phosphorylates Tau and the state of activity of this enzyme determines the function or aggregation of Tau, we analyzed the phosphorylation state of GSK3β as an indirect measurement of its activity. The study of GSK3β activated in frontal cortex of SAD cases showed a significant increase compared to FAD and control individuals. This effect was also found in temporal cortex and cerebellum, but without significance. The analysis of inhibited GSK3β revealed no significant alteration in the brain areas evaluated among groups. However, it is interesting that in frontal cortex from SAD cases there is a decrease of the GSK3β phosphorylated in serine 9 while in cerebellum the inverse tendency was observed. These findings suggest that the activation of GSK3β may be a particular event occurring in SAD, but not in FAD patients and therefore indicate that the formation of PHF and NFTs in FAD involves other

signaling cascades different that GSK3β. This finding is in agreement with a previous study of our group that reported differential Tau pathology in FAD patients when compared with SAD cases and differential kinase distribution and colocalization in Aβ plaques (129).

Looking for an explanation for this observation, we analyzed the expression and the activation of Erk1/2, another enzyme involved in the hyperphosphorylation of Tau and the formation of NTFs. Phosphorylated Erk in CSF from SAD patients suggested the activation of Erk signaling due to degenerative processes in AD (154). Some groups have found altered activation of Erk in temporal cortex from SAD cases. Immunohistochemical evaluation of Erk phosphorylated showed nuclear localization in SAD patients while this labeling was absent in control samples. This altered distribution was likely due to pathologic events characteristic of the disease like oxidative stress (155). In contrast, other studies showed that active Erk1/2 was up-regulated and had a cytoplasmatic distribution in neurons of enthorhinal, hippocampal and temporal cortices from SAD cases with neurofibrillary degeneration (115). In our study we could establish that in all the brain regions analyzed the phosphorylation of Erk1/2 was significantly augmented in FAD and SAD samples relative to controls and no differences were observed between FAD and SAD cases. These results confirm that in SAD alternative signaling to GSK3β participates in the Tau hyperphosphorylation and the production of NFTs, and suggest that the Tau pathology present in E280A FAD involves both kinases GSK3β and Erk1/2, but with differential activity.

Our results in the characterization of proteins involved in the pathophysiology of AD variants point to differential mechanisms in FAD and SAD that could be used for a better diagnosis in the early stages of the disease and that could lead to specific therapeutic strategies for each variant.

In our exploration of Testican-1 as a candidate biomarker in AD, we focused on its possible role in the neuropathogenesis of the disease. For this we analyzed by immunohistochemistry and immunofluorescence the expression of this proteoglycan in different brain areas of SAD and control individuals. Using different morphological methods we showed for the first time the presence of a plaque-like accumulation of Testican-1 in brain tissue of SAD patients in co-localization to Aβ plaques. We observed that the accumulation of Testican-1 was decreased in control compared to SAD individuals and the results of the MTA quantification revealed that the aggregation pattern of Testican-1 was comparable to that of Aβ. The amount of Testican-1 positive plaques was lower than the total amount of Aβ plaques and double staining showed that Testican-1 colocalized with Aβ plaques in ratios ranging between 6:1 (Aβ: Testican-1, temporal cortex) and 20:1 (Aβ: Testican-1, frontal cortex), a finding that may indicate that Testican-1 aggregation occurs secondary to Aβ accumulation. It has been shown that Testican-1 inhibits the cysteine protease cathepsin L which has been involved recently with the production of Aβ peptides. Testican-1 reduces the rate of enzymatic cleavage of substrates and stabilizes the mature form of cathepsin L increasing it half-live (120). Thus the overexpression of Testican-1 in human brain may be a compensatory effect of the neurons to the increased levels and activity of cathepsin L (156). The inhibition of cathepsin L

could lead to the production of Testican-1/CTF and augmented levels of Testican-1/CTF could be a reflection of an inhibitory mechanism in which the Testican-1/CTF is cleaved and the remaining protein stays attached to the enzyme, resulting in its inhibition. Previous data have demonstrated that Testican-1/CTF was elevated in SAD patients (118). To quantify the levels of Testican-1/CTF in AD patients, we designed an antibody directed to Testican-1/CTF in order to develop an ELISA test able to detect this fragment in CSF. Despite much effort and several strategies, it was not possible to detect Testican-1/CTF in samples from human CSF. Even though the antibody detected synthetic Testican-1/CTF, the test was not sensitive enough to measure the amount of the fragment in human samples. Due to the size of the fragment (22 amino acids) the number of available approaches for the quantification of this peptide was limited. For this reason, it will be necessary in the future to develop methods that allow the detection and accurate measurement of small peptides in human samples and in this way increase the possibility to find new biomarkers for AD.

In our search for the contribution of Testican-1 to the pathogenesis of AD, we investigated the expression levels of Testican-1 in brain tissue from SAD, FAD and healthy individuals. Western blot analysis did not reflect changes in the amount of this protein among groups in the regions evaluated. The lack of concordance between the histological and the biochemical analysis could be explained by the fact that most of Testican-1 found in the tissue was deposited in Aβ plaques. Tissue homogenates obtained during protein isolation from brain tissue did not contain Testican-1 associated to plaques and for this reason

western blot results just represent the Testican-1 expressed in neuronal cells, but not the total amount contained in the brain. It would be valuable to determine the ratio between the levels of intracellular Testican-1 and plaque-associated Testican-1 to know whether the elevation of protein levels showed by earlier studies and experiments is due to increased transcription or deficiencies of the degradation machinery and clearance of the protein. However, the amount of available tissue is a limiting factor for completing these results.

Using an *in vitro* approach, we proceeded to study the role of Testican-1 in AD. For this, HEK293T cells expressing APPwt and APPsw were transiently transfected with Testican-1. The analysis of the effect of Testican-1 in the production of Aβ40 and Aβ42 showed that in APPsw cells the overexpression of this protein led to decreased production of both Aβ species. In contrast, no changes were observed in wild type and APPwt cells. It is interesting that the reduction of the Aβ levels was only observed in APPsw cells which seem to produce higher amounts of Aβ than the APPwt cells. This effect could be due to increased activity or expression of α-secretases, decreased activity or expression of β- and γ-secretases or elevated expression of degrading enzymes such as IDE and cathepsin L. The results showed that neither the activity nor the levels of α-, β- or γ-secretases was altered by the transfection with Testican-1 and the expression of the degradation enzymes appeared unchanged. We decide to determine the subcellular distribution of Testican-1 and proteins related to the production, trafficking and degradation of APP, Aβ and Testican-1. These results showed that in APPwt, Testican-1 did not

colocalize with APP, which was apparently stored in vesicles. On the other hand, in APPsw cells Testican-1 and APP colocalized in the cytoplasm and no APP-bearing vesicles were observed. Since general APP shape and distribution was not different in cells transfected with empty vector, we conclude that the differences between APPwt and APPsw were due to the effect of APPsw mutation in APP processing (157). Testican-1 colocalized more with APPsw indicating that they might be occupying the same subcellular compartment. To define which compartment might be harboring both APPsw and Testican-1 we analyzed the subcellular distribution of Testican-1 with members of the exocytic and endocytic pathways (ER, Golgi, exosomes and endosomes). Only Adaptin-γ showed differences between APPwt and APPsw cells. Adaptin-γ distribution did not vary with APP or Testican-1 expression, but Testican-1 colocalization was less pronounced in APPsw compared with APPwt, indicating that Testican-1 might not be localized in endosomes in the presence of APPsw. Notably, the distribution analysis of Testican-1 and cathepsin L demostrated that the degree of colocalization of both proteins was higher in APPsw cells than in APPwt. These results taken together indicate that Testican-1 interacts with cathepsin L and that the subcellular localization of Testican-1 changes from the endosomal compartment to a different localization pattern in the presence of APPsw. We propose that both findings point to a role for Testican-1 in the processing of APPsw independently of the canonical secretases.

Testican-1's interaction with and inhibitory effect on cathepsin L has been already reported by different groups (119;120;158). Although cathepsin L belongs to the lysosomal system and is generally known for bulk proteolysis,

there is evidence suggesting that it also exhibits proteolytic functions similar to that of the APP secretases. However, it is not clear what kind of secretase actually may be. It has been reported that in primary hippocampal neurons and N2a cells the production of sAPPβ was decreased after administration of cathepsin L inhibitors. Furthermore, the levels of Aβ42 were elevated under the same treatment and kinetic assays showed that cathepsin L inhibitions reduced the α-secretase activity (125). So far these results pointed to cathepsin L as an α-secretase; however, recently a new report was published demonstrating that this enzyme displayed β-secretase activity, it had more affinity for APP and it was 74-fold faster than BACE1 in processing APP peptides (84). This evidence, together with the finding that cathepsin L being generally more abundant than BACE1 and that it is localized in both endosomal and lysosomal compartments, where Aβ formation likely takes place (83;84;86), offers a plausible explanation for the effect observed in our experiments. Accordingly, it is possible that the reduced production of Aβ species seen in APPsw cells was caused by the inhibitory action of Testican-1 on cathepsin L. However, more experiments evaluating the activity of this enzyme under our paradigm are necessary to confirm these findings.

6. CONCLUSION AND OUTLOOK

Alzheimer's disease shows a complex pathology and although different aspects of the disease have been clarified, there are still a number of questions to be answered. Several therapeutic approaches have been proposed and tried, but the cure for the disease remains elusive (159). This might be due to our incomplete knowledge about the cellular and molecular mechanisms involved in the pathogenesis of AD. This knowledge is still evolving and probably the strategies used so far need to be revised and redirected. Familial AD has been taken as a reference model to learn about the origin and development of the disease. The results generated from this study can be used to create new methodologies for diagnosis and eventually treatment of the disease.

The neuropathological characterization of samples from the largest family worldwide with hereditary AD is a significant challenge and a serious responsibility not only with the donors and their families, but with the patients and researchers around the world. In this study we evaluated for the first time some of the most relevant proteins known to be involved in the neurodegenerative process of the disease in this population, and compared this to sporadic cases. Although the sample size limits the statistical power of our results, the set of data generated with this research makes an important contribution to the knowledge about AD and sets the basis for future projects.

Based on the results obtained in our study we can conclude that:

- In FAD, the expression of APP was altered in the evaluated brain regions, as a consequence of its increased processing. Although no major changes were observed in the expression profile of α- and β-secretases, variations in PS1 indicated that this protein is a determinant factor for the development of the disease in both AD variants. Dysregulation of the activity of these proteases is certainly a contributing factor to pathogenesis.

- Except for the increased levels of APP observed in frontal cortex and BACE1 in temporal cortex, there is no evidence of altered processing of APP in SAD. These facts suggest a fundamental difference between both variants of AD and deserve further analysis with a larger number of individuals to establish the consistency of these findings.

- In FAD, the expression of PrP^c was modified among the brain areas analyzed, while in SAD no changes were observed. Variations of the levels of this protein may be a key factor during the aggregation process of Aβ in regions like cerebellum. In addition, the effect of PS1 in the transcription and expression of PrP^c could be a relevant factor to study the role of PrP^c as receptor for oligomers and the formation of Aβ aggregates. The differential expression of this protein in FAD and SAD is another point of divergence between both forms of AD and may help to explain the dynamics of Aβ accumulation and the production of Aβ plaques.

- In FAD, the activation level of GSK3β was decreased in the analyzed areas, while in SAD the activation of this kinase was elevated. This

activation profile indicates that the steady-state of this enzyme is regulated in a differential fashion in both AD forms.

- The activation profile of Erk1/2 was increased in both forms of AD among the different brain regions evaluated. Based on these facts we propose that Erk1/2 may be involved in the hyperphosphorylation of Tau and the formation of NFTs in FAD and SAD while GSK3β contributes to this process in SAD, but not in FAD.

- Testican-1 seems to be involved in the pathogenesis of AD since it associates with Aβ plaques. The development of more sensitive methods for the measurement of small peptides will help to establish the potential of Testican-1/CTF as a biomarker for AD. *In vitro* analysis revealed that this proteoglycan may regulate the β-secretase activity of cathepsin L and in this way modulate the production of Aβ. Further studies are required to determine the detailed molecular mechanisms and their relevance *in vivo*.

REFERENCES

1. Querfurth,H.W. and LaFerla,F.M. 2010. Alzheimer's disease. *N.Engl.J.Med.* 362:329-344.

2. Brookmeyer,R., Johnson,E., Ziegler-Graham,K., and Arrighi,H.M. 2007. Forecasting the global burden of Alzheimer's disease. *Alzheimers.Dement.* 3:186-191.

3. Ballard,C., Gauthier,S., Corbett,A., Brayne,C., Aarsland,D., and Jones,E. 2011. Alzheimer's disease. *Lancet* 377:1019-1031.

4. van der Flier,W.M., Pijnenburg,Y.A., Fox,N.C., and Scheltens,P. 2011. Early-onset versus late-onset Alzheimer's disease: the case of the missing APOE varepsilon4 allele. *Lancet Neurol.* 10:280-288.

5. Lautenschlager,N.T., Cupples,L.A., Rao,V.S., Auerbach,S.A., Becker,R., Burke,J., Chui,H., Duara,R., Foley,E.J., Glatt,S.L. *et al.* 1996. Risk of dementia among relatives of Alzheimer's disease patients in the MIRAGE study: What is in store for the oldest old? *Neurology* 46:641-650.

6. Coon,K.D., Myers,A.J., Craig,D.W., Webster,J.A., Pearson,J.V., Lince,D.H., Zismann,V.L., Beach,T.G., Leung,D., Bryden,L. *et al.* 2007. A high-density whole-genome association study reveals that APOE is the major susceptibility gene for sporadic late-onset Alzheimer's disease. *J.Clin.Psychiatry* 68:613-618.

7. Petersen,R.C., Smith,G.E., Waring,S.C., Ivnik,R.J., Tangalos,E.G., and Kokmen,E. 1999. Mild cognitive impairment: clinical characterization and outcome. *Arch.Neurol.* 56:303-308.

8. Kivipelto,M., Ngandu,T., Fratiglioni,L., Viitanen,M., Kareholt,I., Winblad,B., Helkala,E.L., Tuomilehto,J., Soininen,H., and Nissinen,A. 2005. Obesity and vascular risk factors at midlife and the risk of dementia and Alzheimer disease. *Arch.Neurol.* 62:1556-1560.

9. Plassman,B.L., Havlik,R.J., Steffens,D.C., Helms,M.J., Newman,T.N., Drosdick,D., Phillips,C., Gau,B.A., Welsh-Bohmer,K.A., Burke,J.R. *et al.* 2000. Documented head injury in early adulthood and risk of Alzheimer's disease and other dementias. *Neurology* 55:1158-1166.

10. Lye,T.C. and Shores,E.A. 2000. Traumatic brain injury as a risk factor for Alzheimer's disease: a review. *Neuropsychol.Rev.* 10:115-129.

11. DeKosky,S.T. and Orgogozo,J.M. 2001. Alzheimer disease: diagnosis, costs, and dimensions of treatment. *Alzheimer Dis.Assoc.Disord.* 15 Suppl 1:S3-S7.

12. Voisin,T. and Vellas,B. 2009. Diagnosis and treatment of patients with severe Alzheimer's disease. *Drugs Aging* 26:135-144.

13. McKhann,G.M., Knopman,D.S., Chertkow,H., Hyman,B.T., Jack,C.R., Jr., Kawas,C.H., Klunk,W.E., Koroshetz,W.J., Manly,J.J., Mayeux,R. *et al.* 2011. The diagnosis of dementia due to Alzheimer's disease: recommendations from the National Institute on Aging-Alzheimer's Association workgroups on diagnostic guidelines for Alzheimer's disease. *Alzheimers.Dement.* 7:263-269.

14. Bertram,L. and Tanzi,R.E. 2004. Alzheimer's disease: one disorder, too many genes? *Hum.Mol.Genet.* 13 Spec No 1:R135-R141.

15. Goate,A. and Hardy,J. 2012. Twenty years of Alzheimer's disease-causing mutations. *J.Neurochem.* 120 Suppl 1:3-8.

16. Cruchaga,C., Chakraverty,S., Mayo,K., Vallania,F.L., Mitra,R.D., Faber,K., Williamson,J., Bird,T., Diaz-Arrastia,R., Foroud,T.M. *et al.* 2012. Rare Variants in APP, PSEN1 and PSEN2 Increase Risk for AD in Late-Onset Alzheimer's Disease Families. *PLoS.One.* 7:e31039.

17. Larner,A.J. and Doran,M. 2006. Clinical phenotypic heterogeneity of Alzheimer's disease associated with mutations of the presenilin-1 gene. *J.Neurol.* 253:139-158.

18. Citron,M., Westaway,D., Xia,W., Carlson,G., Diehl,T., Levesque,G., Johnson-Wood,K., Lee,M., Seubert,P., Davis,A. *et al.* 1997. Mutant presenilins of Alzheimer's disease increase production of 42-residue amyloid beta-protein in both transfected cells and transgenic mice. *Nat.Med.* 3:67-72.

19. Lopera,F., Ardilla,A., Martinez,A., Madrigal,L., Arango-Viana,J.C., Lemere,C.A., Arango-Lasprilla,J.C., Hincapie,L., Arcos-Burgos,M., Ossa,J.E. *et al.* 1997. Clinical features of early-onset Alzheimer disease in a large kindred with an E280A presenilin-1 mutation. *JAMA* 277:793-799.

20. Acosta-Baena,N., Sepulveda-Falla,D., Lopera-Gomez,C.M., Jaramillo-Elorza,M.C., Moreno,S., Aguirre-Acevedo,D.C., Saldarriaga,A., and Lopera,F. 2011. Pre-dementia clinical stages in presenilin 1 E280A familial early-onset Alzheimer's disease: a retrospective cohort study. *Lancet Neurol.* 10:213-220.

21. Sherrington,R., Froelich,S., Sorbi,S., Campion,D., Chi,H., Rogaeva,E.A., Levesque,G., Rogaev,E.I., Lin,C., Liang,Y. *et al.* 1996. Alzheimer's disease associated with mutations in presenilin 2 is rare and variably penetrant. *Hum.Mol.Genet.* 5:985-988.

22. Jayadev,S., Leverenz,J.B., Steinbart,E., Stahl,J., Klunk,W., Yu,C.E., and Bird,T.D. 2010. Alzheimer's disease phenotypes and genotypes associated with mutations in presenilin 2. *Brain* 133:1143-1154.

23. Lindquist,S.G., Hasholt,L., Bahl,J.M., Heegaard,N.H., Andersen,B.B., Norremolle,A., Stokholm,J., Schwartz,M., Batbayli,M., Laursen,H. *et al.* 2008. A novel presenilin 2 mutation (V393M) in early-onset dementia with profound language impairment. *Eur.J.Neurol.* 15:1135-1139.

24. Perl,D.P. 2010. Neuropathology of Alzheimer's disease. *Mt.Sinai J.Med.* 77:32-42.

25. Hardy,J. and Selkoe,D.J. 2002. The amyloid hypothesis of Alzheimer's disease: progress and problems on the road to therapeutics. *Science* 297:353-356.

26. Wilcock,G.K. and Esiri,M.M. 1982. Plaques, tangles and dementia. A quantitative study. *J.Neurol.Sci.* 56:343-356.

27. Braak,H. and Braak,E. 1991. Neuropathological stageing of Alzheimer-related changes. *Acta Neuropathol.* 82:239-259.

28. Lambert,M.P., Barlow,A.K., Chromy,B.A., Edwards,C., Freed,R., Liosatos,M., Morgan,T.E., Rozovsky,I., Trommer,B., Viola,K.L. *et al.* 1998. Diffusible, nonfibrillar ligands derived from Abeta1-42 are potent central nervous system neurotoxins. *Proc.Natl.Acad.Sci.U.S.A* 95:6448-6453.

29. Haass,C. and Selkoe,D.J. 2007. Soluble protein oligomers in neurodegeneration: lessons from the Alzheimer's amyloid beta-peptide. *Nat.Rev.Mol.Cell Biol.* 8:101-112.

30. Walsh,D.M. and Selkoe,D.J. 2007. A beta oligomers - a decade of discovery. *J.Neurochem.* 101:1172-1184.

31. Thal,D.R., Rub,U., Orantes,M., and Braak,H. 2002. Phases of A beta-deposition in the human brain and its relevance for the development of AD. *Neurology* 58:1791-1800.

32. Buckner,R.L., Snyder,A.Z., Shannon,B.J., LaRossa,G., Sachs,R., Fotenos,A.F., Sheline,Y.I., Klunk,W.E., Mathis,C.A., Morris,J.C. *et al.* 2005. Molecular, structural, and functional characterization of Alzheimer's disease: evidence for a relationship between default activity, amyloid, and memory. *J.Neurosci.* 25:7709-7717.

33. Braak,H. and Del Tredici,K. 2011. The pathological process underlying Alzheimer's disease in individuals under thirty. *Acta Neuropathol.* 121:171-181.

34. Klunk,W.E. and Mathis,C.A. 2008. The future of amyloid-beta imaging: a tale of radionuclides and tracer proliferation. *Curr.Opin.Neurol.* 21:683-687.

35. Villemagne,V.L., Pike,K.E., Chetelat,G., Ellis,K.A., Mulligan,R.S., Bourgeat,P., Ackermann,U., Jones,G., Szoeke,C., Salvado,O. *et al.* 2011. Longitudinal assessment of Abeta and cognition in aging and Alzheimer disease. *Ann.Neurol.* 69:181-192.

36. Selkoe,D.J. 2000. Toward a comprehensive theory for Alzheimer's disease. Hypothesis: Alzheimer's disease is caused by the cerebral accumulation and cytotoxicity of amyloid beta-protein. *Ann.N.Y.Acad.Sci.* 924:17-25.

37. Zhang,H., Ma,Q., Zhang,Y.W., and Xu,H. 2012. Proteolytic processing of Alzheimer's beta-amyloid precursor protein. *J.Neurochem.* 120 Suppl 1:9-21.

38. Lee,J., Retamal,C., Cuitino,L., Caruano-Yzermans,A., Shin,J.E., van Kerkhof,P., Marzolo,M.P., and Bu,G. 2008. Adaptor protein sorting nexin 17 regulates amyloid precursor protein trafficking and processing in the early endosomes. *J.Biol.Chem.* 283:11501-11508.

39. Koo,E.H., Sisodia,S.S., Archer,D.R., Martin,L.J., Weidemann,A., Beyreuther,K., Fischer,P., Masters,C.L., and Price,D.L. 1990. Precursor of amyloid protein in Alzheimer disease undergoes fast anterograde axonal transport. *Proc.Natl.Acad.Sci.U.S.A* 87:1561-1565.

40. Ehehalt,R., Keller,P., Haass,C., Thiele,C., and Simons,K. 2003. Amyloidogenic processing of the Alzheimer beta-amyloid precursor protein depends on lipid rafts. *J.Cell Biol.* 160:113-123.

41. Thinakaran,G. and Koo,E.H. 2008. Amyloid precursor protein trafficking, processing, and function. *J.Biol.Chem.* 283:29615-29619.

42. Fahrenholz,F., Gilbert,S., Kojro,E., Lammich,S., and Postina,R. 2000. Alpha-secretase activity of the disintegrin metalloprotease ADAM 10. Influences of domain structure. *Ann.N.Y.Acad.Sci.* 920:215-222.

43. Asai,M., Hattori,C., Szabo,B., Sasagawa,N., Maruyama,K., Tanuma,S., and Ishiura,S. 2003. Putative function of ADAM9, ADAM10, and ADAM17 as APP alpha-secretase. *Biochem.Biophys.Res.Commun.* 301:231-235.

44. Esch,F.S., Keim,P.S., Beattie,E.C., Blacher,R.W., Culwell,A.R., Oltersdorf,T., McClure,D., and Ward,P.J. 1990. Cleavage of amyloid beta peptide during constitutive processing of its precursor. *Science* 248:1122-1124.

45. Zhang,Y.W., Thompson,R., Zhang,H., and Xu,H. 2011. APP processing in Alzheimer's disease. *Mol.Brain* 4:3.

46. Vassar,R., Bennett,B.D., Babu-Khan,S., Kahn,S., Mendiaz,E.A., Denis,P., Teplow,D.B., Ross,S., Amarante,P., Loeloff,R. *et al.* 1999. Beta-secretase cleavage of Alzheimer's

amyloid precursor protein by the transmembrane aspartic protease BACE. *Science* 286:735-741.

47. Selkoe,D.J. and Wolfe,M.S. 2007. Presenilin: running with scissors in the membrane. *Cell* 131:215-221.

48. George-Hyslop,P. and Fraser,P.E. 2012. Assembly of the presenilin gamma-/epsilon-secretase complex. *J.Neurochem.* 120 Suppl 1:84-88.

49. Zheng,H. and Koo,E.H. 2011. Biology and pathophysiology of the amyloid precursor protein. *Mol.Neurodegener.* 6:27.

50. Clarris,H.J., Nurcombe,V., Small,D.H., Beyreuther,K., and Masters,C.L. 1994. Secretion of nerve growth factor from septum stimulates neurite outgrowth and release of the amyloid protein precursor of Alzheimer's disease from hippocampal explants. *J.Neurosci.Res.* 38:248-258.

51. Ohsawa,I., Takamura,C., Morimoto,T., Ishiguro,M., and Kohsaka,S. 1999. Amino-terminal region of secreted form of amyloid precursor protein stimulates proliferation of neural stem cells. *Eur.J.Neurosci.* 11:1907-1913.

52. Roch,J.M., Masliah,E., Roch-Levecq,A.C., Sundsmo,M.P., Otero,D.A., Veinbergs,I., and Saitoh,T. 1994. Increase of synaptic density and memory retention by a peptide representing the trophic domain of the amyloid beta/A4 protein precursor. *Proc.Natl.Acad.Sci.U.S.A* 91:7450-7454.

53. Taylor,C.J., Ireland,D.R., Ballagh,I., Bourne,K., Marechal,N.M., Turner,P.R., Bilkey,D.K., Tate,W.P., and Abraham,W.C. 2008. Endogenous secreted amyloid precursor protein-alpha regulates hippocampal NMDA receptor function, long-term potentiation and spatial memory. *Neurobiol.Dis.* 31:250-260.

54. Treiber,C., Simons,A., Strauss,M., Hafner,M., Cappai,R., Bayer,T.A., and Multhaup,G. 2004. Clioquinol mediates copper uptake and counteracts copper efflux activities of the amyloid precursor protein of Alzheimer's disease. *J.Biol.Chem.* 279:51958-51964.

55. Kuhn,P.H., Wang,H., Dislich,B., Colombo,A., Zeitschel,U., Ellwart,J.W., Kremmer,E., Rossner,S., and Lichtenthaler,S.F. 2010. ADAM10 is the physiologically relevant, constitutive alpha-secretase of the amyloid precursor protein in primary neurons. *EMBO J.* 29:3020-3032.

56. Seals,D.F. and Courtneidge,S.A. 2003. The ADAMs family of metalloproteases: multidomain proteins with multiple functions. *Genes Dev.* 17:7-30.

57. Hartmann,D., de Strooper,B., Serneels,L., Craessaerts,K., Herreman,A., Annaert,W., Umans,L., Lubke,T., Lena,I.A., von Figura,K. *et al.* 2002. The disintegrin/metalloprotease ADAM 10 is essential for Notch signalling but not for alpha-secretase activity in fibroblasts. *Hum.Mol.Genet.* 11:2615-2624.

58. Six,E., Ndiaye,D., Laabi,Y., Brou,C., Gupta-Rossi,N., Israel,A., and Logeat,F. 2003. The Notch ligand Delta1 is sequentially cleaved by an ADAM protease and gamma-secretase. *Proc.Natl.Acad.Sci.U.S.A* 100:7638-7643.

59. Marambaud,P., Shioi,J., Serban,G., Georgakopoulos,A., Sarner,S., Nagy,V., Baki,L., Wen,P., Efthimiopoulos,S., Shao,Z. *et al.* 2002. A presenilin-1/gamma-secretase cleavage releases the E-cadherin intracellular domain and regulates disassembly of adherens junctions. *EMBO J.* 21:1948-1956.

60. Marambaud,P., Wen,P.H., Dutt,A., Shioi,J., Takashima,A., Siman,R., and Robakis,N.K. 2003. A CBP binding transcriptional repressor produced by the PS1/epsilon-cleavage of N-cadherin is inhibited by PS1 FAD mutations. *Cell* 114:635-645.

61. Georgakopoulos,A., Litterst,C., Ghersi,E., Baki,L., Xu,C., Serban,G., and Robakis,N.K. 2006. Metalloproteinase/Presenilin1 processing of ephrinB regulates EphB-induced Src phosphorylation and signaling. *EMBO J.* 25:1242-1252.

62. Taylor,D.R., Parkin,E.T., Cocklin,S.L., Ault,J.R., Ashcroft,A.E., Turner,A.J., and Hooper,N.M. 2009. Role of ADAMs in the ectodomain shedding and conformational conversion of the prion protein. *J.Biol.Chem.* 284:22590-22600.

63. Bremer,J., Baumann,F., Tiberi,C., Wessig,C., Fischer,H., Schwarz,P., Steele,A.D., Toyka,K.V., Nave,K.A., Weis,J. *et al.* 2010. Axonal prion protein is required for peripheral myelin maintenance. *Nat.Neurosci.* 13:310-318.

64. Klingeborn,M., Race,B., Meade-White,K.D., Rosenke,R., Striebel,J.F., and Chesebro,B. 2011. Crucial role for prion protein membrane anchoring in the neuroinvasion and neural spread of prion infection. *J.Virol.* 85:1484-1494.

65. Altmeppen,H.C., Prox,J., Puig,B., Kluth,M.A., Bernreuther,C., Thurm,D., Jorissen,E., Petrowitz,B., Bartsch,U., de Strooper,B. *et al.* 2011. Lack of a-disintegrin-and-metalloproteinase ADAM10 leads to intracellular accumulation and loss of shedding of the cellular prion protein in vivo. *Mol.Neurodegener.* 6:36.

66. Pruessmeyer,J. and Ludwig,A. 2009. The good, the bad and the ugly substrates for ADAM10 and ADAM17 in brain pathology, inflammation and cancer. *Semin.Cell Dev.Biol.* 20:164-174.

67. Kandalepas,P.C. and Vassar,R. 2012. Identification and biology of beta-secretase. *J.Neurochem.* 120 Suppl 1:55-61.

68. Eggert,S., Paliga,K., Soba,P., Evin,G., Masters,C.L., Weidemann,A., and Beyreuther,K. 2004. The proteolytic processing of the amyloid precursor protein gene family members APLP-1 and APLP-2 involves alpha-, beta-, gamma-, and epsilon-like cleavages: modulation of APLP-1 processing by n-glycosylation. *J.Biol.Chem.* 279:18146-18156.

69. Wong,H.K., Sakurai,T., Oyama,F., Kaneko,K., Wada,K., Miyazaki,H., Kurosawa,M., de Strooper,B., Saftig,P., and Nukina,N. 2005. beta Subunits of voltage-gated sodium channels are novel substrates of beta-site amyloid precursor protein-cleaving enzyme (BACE1) and gamma-secretase. *J.Biol.Chem.* 280:23009-23017.

70. von Arnim,C.A., Kinoshita,A., Peltan,I.D., Tangredi,M.M., Herl,L., Lee,B.M., Spoelgen,R., Hshieh,T.T., Ranganathan,S., Battey,F.D. *et al.* 2005. The low density lipoprotein receptor-related protein (LRP) is a novel beta-secretase (BACE1) substrate. *J.Biol.Chem.* 280:17777-17785.

71. Willem,M., Garratt,A.N., Novak,B., Citron,M., Kaufmann,S., Rittger,A., DeStrooper,B., Saftig,P., Birchmeier,C., and Haass,C. 2006. Control of peripheral nerve myelination by the beta-secretase BACE1. *Science* 314:664-666.

72. Griffiths,H.H., Whitehouse,I.J., Baybutt,H., Brown,D., Kellett,K.A., Jackson,C.D., Turner,A.J., Piccardo,P., Manson,J.C., and Hooper,N.M. 2011. Prion protein interacts with BACE1 protein and differentially regulates its activity toward wild type and Swedish mutant amyloid precursor protein. *J.Biol.Chem.* 286:33489-33500.

73. Roberds,S.L., Anderson,J., Basi,G., Bienkowski,M.J., Branstetter,D.G., Chen,K.S., Freedman,S.B., Frigon,N.L., Games,D., Hu,K. *et al.* 2001. BACE knockout mice are healthy despite lacking the primary beta-secretase activity in brain: implications for Alzheimer's disease therapeutics. *Hum.Mol.Genet.* 10:1317-1324.

74. Kobayashi,D., Zeller,M., Cole,T., Buttini,M., McConlogue,L., Sinha,S., Freedman,S., Morris,R.G., and Chen,K.S. 2008. BACE1 gene deletion: impact on behavioral function in a model of Alzheimer's disease. *Neurobiol.Aging* 29:861-873.

75. Hitt,B.D., Jaramillo,T.C., Chetkovich,D.M., and Vassar,R. 2010. BACE1-/- mice exhibit seizure activity that does not correlate with sodium channel level or axonal localization. *Mol.Neurodegener.* 5:31.

76. Kaether,C., Lammich,S., Edbauer,D., Ertl,M., Rietdorf,J., Capell,A., Steiner,H., and Haass,C. 2002. Presenilin-1 affects trafficking and processing of betaAPP and is targeted in a complex with nicastrin to the plasma membrane. *J.Cell Biol.* 158:551-561.

77. Loetscher,H., Deuschle,U., Brockhaus,M., Reinhardt,D., Nelboeck,P., Mous,J., Grunberg,J., Haass,C., and Jacobsen,H. 1997. Presenilins are processed by caspase-type proteases. *J.Biol.Chem.* 272:20655-20659.

78. Leissring,M.A., Akbari,Y., Fanger,C.M., Cahalan,M.D., Mattson,M.P., and LaFerla,F.M. 2000. Capacitative calcium entry deficits and elevated luminal calcium content in mutant presenilin-1 knockin mice. *J.Cell Biol.* 149:793-798.

79. Jo,D.G., Chang,J.W., Hong,H.S., Mook-Jung,I., and Jung,Y.K. 2003. Contribution of presenilin/gamma-secretase to calsenilin-mediated apoptosis. *Biochem.Biophys.Res.Commun.* 305:62-66.

80. Zhang,Z., Hartmann,H., Do,V.M., Abramowski,D., Sturchler-Pierrat,C., Staufenbiel,M., Sommer,B., van de,W.M., Clevers,H., Saftig,P. *et al.* 1998. Destabilization of beta-catenin by mutations in presenilin-1 potentiates neuronal apoptosis. *Nature* 395:698-702.

81. Naruse,S., Thinakaran,G., Luo,J.J., Kusiak,J.W., Tomita,T., Iwatsubo,T., Qian,X., Ginty,D.D., Price,D.L., Borchelt,D.R. *et al.* 1998. Effects of PS1 deficiency on membrane protein trafficking in neurons. *Neuron* 21:1213-1221.

82. de Strooper,B., Iwatsubo,T., and Wolfe,M.S. 2012. Presenilins and gamma-Secretase: Structure, Function, and Role in Alzheimer Disease. *Cold Spring Harb.Perspect.Med.* 2:a006304.

83. Turk,V., Stoka,V., Vasiljeva,O., Renko,M., Sun,T., Turk,B., and Turk,D. 2012. Cysteine cathepsins: From structure, function and regulation to new frontiers. *Biochim.Biophys.Acta* 1824:68-88.

84. Schechter,I. and Ziv,E. 2011. Cathepsins S, B and L with aminopeptidases display beta-secretase activity associated with the pathogenesis of Alzheimer's disease. *Biol.Chem.* 392:555-569.

85. Turk,B., Turk,D., and Turk,V. 2000. Lysosomal cysteine proteases: more than scavengers. *Biochim.Biophys.Acta* 1477:98-111.

86. Brix,K., Dunkhorst,A., Mayer,K., and Jordans,S. 2008. Cysteine cathepsins: cellular roadmap to different functions. *Biochimie* 90:194-207.

87. Colby,D.W. and Prusiner,S.B. 2011. Prions. *Cold Spring Harb.Perspect.Biol.* 3:a006833.

88. Chen,S., Yadav,S.P., and Surewicz,W.K. 2010. Interaction between human prion protein and amyloid-beta (Abeta) oligomers: role OF N-terminal residues. *J.Biol.Chem.* 285:26377-26383.

89. Nygaard,H.B. and Strittmatter,S.M. 2009. Cellular prion protein mediates the toxicity of beta-amyloid oligomers: implications for Alzheimer disease. *Arch.Neurol.* 66:1325-1328.

90. Parkin,E.T., Watt,N.T., Hussain,I., Eckman,E.A., Eckman,C.B., Manson,J.C., Baybutt,H.N., Turner,A.J., and Hooper,N.M. 2007. Cellular prion protein regulates beta-

secretase cleavage of the Alzheimer's amyloid precursor protein. *Proc.Natl.Acad.Sci.U.S.A* 104:11062-11067.

91. Schwarze-Eicker,K., Keyvani,K., Gortz,N., Westaway,D., Sachser,N., and Paulus,W. 2005. Prion protein (PrPc) promotes beta-amyloid plaque formation. *Neurobiol.Aging* 26:1177-1182.

92. Shaw,L.M., Vanderstichele,H., Knapik-Czajka,M., Clark,C.M., Aisen,P.S., Petersen,R.C., Blennow,K., Soares,H., Simon,A., Lewczuk,P. *et al.* 2009. Cerebrospinal fluid biomarker signature in Alzheimer's disease neuroimaging initiative subjects. *Ann.Neurol.* 65:403-413.

93. Steinerman,J.R., Irizarry,M., Scarmeas,N., Raju,S., Brandt,J., Albert,M., Blacker,D., Hyman,B., and Stern,Y. 2008. Distinct pools of beta-amyloid in Alzheimer disease-affected brain: a clinicopathologic study. *Arch.Neurol.* 65:906-912.

94. Mawuenyega,K.G., Sigurdson,W., Ovod,V., Munsell,L., Kasten,T., Morris,J.C., Yarasheski,K.E., and Bateman,R.J. 2010. Decreased clearance of CNS beta-amyloid in Alzheimer's disease. *Science* 330:1774.

95. Malito,E., Hulse,R.E., and Tang,W.J. 2008. Amyloid beta-degrading cryptidases: insulin degrading enzyme, presequence peptidase, and neprilysin. *Cell Mol.Life Sci.* 65:2574-2585.

96. Qiu,W.Q., Walsh,D.M., Ye,Z., Vekrellis,K., Zhang,J., Podlisny,M.B., Rosner,M.R., Safavi,A., Hersh,L.B., and Selkoe,D.J. 1998. Insulin-degrading enzyme regulates extracellular levels of amyloid beta-protein by degradation. *J.Biol.Chem.* 273:32730-32738.

97. Farris,W., Mansourian,S., Chang,Y., Lindsley,L., Eckman,E.A., Frosch,M.P., Eckman,C.B., Tanzi,R.E., Selkoe,D.J., and Guenette,S. 2003. Insulin-degrading enzyme regulates the levels of insulin, amyloid beta-protein, and the beta-amyloid precursor protein intracellular domain in vivo. *Proc.Natl.Acad.Sci.U.S.A* 100:4162-4167.

98. Leissring,M.A., Farris,W., Chang,A.Y., Walsh,D.M., Wu,X., Sun,X., Frosch,M.P., and Selkoe,D.J. 2003. Enhanced proteolysis of beta-amyloid in APP transgenic mice prevents plaque formation, secondary pathology, and premature death. *Neuron* 40:1087-1093.

99. Kanemitsu,H., Tomiyama,T., and Mori,H. 2003. Human neprilysin is capable of degrading amyloid beta peptide not only in the monomeric form but also the pathological oligomeric form. *Neurosci.Lett.* 350:113-116.

100. Authier,F., Posner,B.I., and Bergeron,J.J. 1996. Insulin-degrading enzyme. *Clin.Invest Med.* 19:149-160.

101. Kirschner,R.J. and Goldberg,A.L. 1983. A high molecular weight metalloendoprotease from the cytosol of mammalian cells. *J.Biol.Chem.* 258:967-976.

102. Misbin,R.I. and Almira,E.C. 1989. Degradation of insulin and insulin-like growth factors by enzyme purified from human erythrocytes. Comparison of degradation products observed with A14- and B26-[125I]monoiodoinsulin. *Diabetes* 38:152-158.

103. Perez,A., Morelli,L., Cresto,J.C., and Castano,E.M. 2000. Degradation of soluble amyloid beta-peptides 1-40, 1-42, and the Dutch variant 1-40Q by insulin degrading enzyme from Alzheimer disease and control brains. *Neurochem.Res.* 25:247-255.

104. Iqbal,K., Liu,F., Gong,C.X., and Grundke-Iqbal,I. 2010. Tau in Alzheimer disease and related tauopathies. *Curr.Alzheimer Res.* 7:656-664.

105. Higuchi,M., Lee,V.M., and Trojanowski,J.Q. 2002. Tau and axonopathy in neurodegenerative disorders. *Neuromolecular.Med.* 2:131-150.

106. Mattsson,N., Zetterberg,H., Hansson,O., Andreasen,N., Parnetti,L., Jonsson,M., Herukka,S.K., van der Flier,W.M., Blankenstein,M.A., Ewers,M. *et al.* 2009. CSF biomarkers and incipient Alzheimer disease in patients with mild cognitive impairment. *JAMA* 302:385-393.

107. Sengupta,A., Kabat,J., Novak,M., Wu,Q., Grundke-Iqbal,I., and Iqbal,K. 1998. Phosphorylation of tau at both Thr 231 and Ser 262 is required for maximal inhibition of its binding to microtubules. *Arch.Biochem.Biophys.* 357:299-309.

108. Liu,F., Li,B., Tung,E.J., Grundke-Iqbal,I., Iqbal,K., and Gong,C.X. 2007. Site-specific effects of tau phosphorylation on its microtubule assembly activity and self-aggregation. *Eur.J.Neurosci.* 26:3429-3436.

109. Hooper,C., Killick,R., and Lovestone,S. 2008. The GSK3 hypothesis of Alzheimer's disease. *J.Neurochem.* 104:1433-1439.

110. Hernandez,F., de Barreda,E.G., Fuster-Matanzo,A., Goni-Oliver,P., Lucas,J.J., and Avila,J. 2009. The role of GSK3 in Alzheimer disease. *Brain Res.Bull.* 80:248-250.

111. Cohen,P. and Frame,S. 2001. The renaissance of GSK3. *Nat.Rev.Mol.Cell Biol.* 2:769-776.

112. Leroy,K., Boutajangout,A., Authelet,M., Woodgett,J.R., Anderton,B.H., and Brion,J.P. 2002. The active form of glycogen synthase kinase-3beta is associated with granulovacuolar degeneration in neurons in Alzheimer's disease. *Acta Neuropathol.* 103:91-99.

113. Zhu,X., Lee,H.G., Raina,A.K., Perry,G., and Smith,M.A. 2002. The role of mitogen-activated protein kinase pathways in Alzheimer's disease. *Neurosignals.* 11:270-281.

114. Pearson,G., Robinson,F., Beers,G.T., Xu,B.E., Karandikar,M., Berman,K., and Cobb,M.H. 2001. Mitogen-activated protein (MAP) kinase pathways: regulation and physiological functions. *Endocr.Rev.* 22:153-183.

115. Pei,J.J., Braak,H., An,W.L., Winblad,B., Cowburn,R.F., Iqbal,K., and Grundke-Iqbal,I. 2002. Up-regulation of mitogen-activated protein kinases ERK1/2 and MEK1/2 is associated with the progression of neurofibrillary degeneration in Alzheimer's disease. *Brain Res.Mol.Brain Res.* 109:45-55.

116. Spitzer,P., Schieb,H., Kamrowski-Kruck,H., Otto,M., Chiasserini,D., Parnetti,L., Herukka,S.K., Schuchhardt,J., Wiltfang,J., and Klafki,H.W. 2011. Evidence for Elevated Cerebrospinal Fluid ERK1/2 Levels in Alzheimer Dementia. *Int.J.Alzheimers.Dis.* 2011:739847.

117. Holtzman,D.M. 2011. CSF biomarkers for Alzheimer's disease: current utility and potential future use. *Neurobiol.Aging* 32 Suppl 1:S4-S9.

118. Jahn,H., Wittke,S., Zurbig,P., Raedler,T.J., Arlt,S., Kellmann,M., Mullen,W., Eichenlaub,M., Mischak,H., and Wiedemann,K. 2011. Peptide fingerprinting of Alzheimer's disease in cerebrospinal fluid: identification and prospective evaluation of new synaptic biomarkers. *PLoS.One.* 6:e26540.

119. Edgell,C.J., BaSalamah,M.A., and Marr,H.S. 2004. Testican-1: a differentially expressed proteoglycan with protease inhibiting activities. *Int.Rev.Cytol.* 236:101-122.

120. Bocock,J.P., Edgell,C.J., Marr,H.S., and Erickson,A.H. 2003. Human proteoglycan testican-1 inhibits the lysosomal cysteine protease cathepsin L. *Eur.J.Biochem.* 270:4008-4015.

121. Sepulveda-Falla,D., Matschke,J., Bernreuther,C., Hagel,C., Puig,B., Villegas,A., Garcia,G., Zea,J., Gomez-Mancilla,B., Ferrer,I. *et al.* 2011. Deposition of hyperphosphorylated tau in cerebellum of PS1 E280A Alzheimer's disease. *Brain Pathol.* 21:452-463.

122. Li,R., Lindholm,K., Yang,L.B., Yue,X., Citron,M., Yan,R., Beach,T., Sue,L., Sabbagh,M., Cai,H. *et al.* 2004. Amyloid beta peptide load is correlated with increased beta-secretase activity in sporadic Alzheimer's disease patients. *Proc.Natl.Acad.Sci.U.S.A* 101:3632-3637.

123. Cai,Y., Xiong,K., Zhang,X.M., Cai,H., Luo,X.G., Feng,J.C., Clough,R.W., Struble,R.G., Patrylo,P.R., Chu,Y. *et al.* 2010. beta-Secretase-1 elevation in aged monkey and Alzheimer's disease human cerebral cortex occurs around the vasculature in partnership with multisystem axon terminal pathogenesis and beta-amyloid accumulation. *Eur.J.Neurosci.* 32:1223-1238.

124. Hook,V., Schechter,I., Demuth,H.U., and Hook,G. 2008. Alternative pathways for production of beta-amyloid peptides of Alzheimer's disease. *Biol.Chem.* 389:993-1006.

125. Klein,D.M., Felsenstein,K.M., and Brenneman,D.E. 2009. Cathepsins B and L differentially regulate amyloid precursor protein processing. *J.Pharmacol.Exp.Ther.* 328:813-821.

126. Dorfman,V.B., Pasquini,L., Riudavets,M., Lopez-Costa,J.J., Villegas,A., Troncoso,J.C., Lopera,F., Castano,E.M., and Morelli,L. 2010. Differential cerebral deposition of IDE and NEP in sporadic and familial Alzheimer's disease. *Neurobiol.Aging* 31:1743-1757.

127. Marr,H.S., BaSalamah,M.A., Bouldin,T.W., Duncan,A.W., and Edgell,C.J. 2000. Distribution of testican expression in human brain. *Cell Tissue Res.* 302:139-144.

128. Bekris,L.M., Yu,C.E., Bird,T.D., and Tsuang,D.W. 2010. Genetics of Alzheimer disease. *J.Geriatr.Psychiatry Neurol.* 23:213-227.

129. Sepulveda-Falla,D., Matschke,J., Bernreuther,C., Hagel,C., Puig,B., Villegas,A., Garcia,G., Zea,J., Gomez-Mancilla,B., Ferrer,I. *et al.* 2011. Deposition of hyperphosphorylated tau in cerebellum of PS1 E280A Alzheimer's disease. *Brain Pathol.* 21:452-463.

130. de Strooper,B. 2007. Loss-of-function presenilin mutations in Alzheimer disease. Talking Point on the role of presenilin mutations in Alzheimer disease. *EMBO Rep.* 8:141-146.

131. Giliberto,L., Borghi,R., Piccini,A., Mangerini,R., Sorbi,S., Cirmena,G., Garuti,A., Ghetti,B., Tagliavini,F., Mughal,M.R. *et al.* 2009. Mutant presenilin 1 increases the expression and activity of BACE1. *J.Biol.Chem.* 284:9027-9038.

132. Gatta,L.B., Albertini,A., Ravid,R., and Finazzi,D. 2002. Levels of beta-secretase BACE and alpha-secretase ADAM10 mRNAs in Alzheimer hippocampus. *Neuroreport* 13:2031-2033.

133. Colciaghi,F., Borroni,B., Pastorino,L., Marcello,E., Zimmermann,M., Cattabeni,F., Padovani,A., and Di Luca,M. 2002. [alpha]-Secretase ADAM10 as well as [alpha]APPs is reduced in platelets and CSF of Alzheimer disease patients. *Mol.Med.* 8:67-74.

134. Holsinger,R.M., McLean,C.A., Beyreuther,K., Masters,C.L., and Evin,G. 2002. Increased expression of the amyloid precursor beta-secretase in Alzheimer's disease. *Ann.Neurol.* 51:783-786.

135. Fukumoto,H., Cheung,B.S., Hyman,B.T., and Irizarry,M.C. 2002. Beta-secretase protein and activity are increased in the neocortex in Alzheimer disease. *Arch.Neurol.* 59:1381-1389.

136. Yang,L.B., Lindholm,K., Yan,R., Citron,M., Xia,W., Yang,X.L., Beach,T., Sue,L., Wong,P., Price,D. *et al.* 2003. Elevated beta-secretase expression and enzymatic activity detected in sporadic Alzheimer disease. *Nat.Med.* 9:3-4.

137. Ewers,M., Cheng,X., Zhong,Z., Nural,H.F., Walsh,C., Meindl,T., Teipel,S.J., Buerger,K., He,P., Shen,Y. *et al.* 2011. Increased CSF-BACE1 activity associated with decreased hippocampus volume in Alzheimer's disease. *J.Alzheimers.Dis.* 25:373-381.

138. Kuzuya,A., Uemura,K., Kitagawa,N., Aoyagi,N., Kihara,T., Ninomiya,H., Ishiura,S., Takahashi,R., and Shimohama,S. 2007. Presenilin 1 is involved in the maturation of beta-site amyloid precursor protein-cleaving enzyme 1 (BACE1). *J.Neurosci.Res.* 85:153-165.

139. Borghi,R., Piccini,A., Barini,E., Cirmena,G., Guglielmotto,M., Tamagno,E., Fornaro,M., Perry,G., Smith,M.A., Garuti,A. *et al.* 2010. Upregulation of presenilin 1 in brains of sporadic, late-onset Alzheimer's disease. *J.Alzheimers.Dis.* 22:771-775.

140. Viswanathan,J., Haapasalo,A., Bottcher,C., Miettinen,R., Kurkinen,K.M., Lu,A., Thomas,A., Maynard,C.J., Romano,D., Hyman,B.T. *et al.* 2011. Alzheimer's disease-associated ubiquilin-1 regulates presenilin-1 accumulation and aggresome formation. *Traffic.* 12:330-348.

141. Hendriks,L., De Jonghe,C., Lubke,U., Woodrow,S., Vanderhoeven,I., Boons,J., Cras,P., Martin,J.J., and Van Broeckhoven,C. 1998. Immunoreactivity of presenilin-1 and tau in Alzheimer's disease brain. *Exp.Neurol.* 149:341-348.

142. Takami,K., Terai,K., Matsuo,A., Walker,D.G., and McGeer,P.L. 1997. Expression of presenilin-1 and -2 mRNAs in rat and Alzheimer's disease brains. *Brain Res.* 748:122-130.

143. Stahl,S., Reinders,Y., Asan,E., Mothes,W., Conzelmann,E., Sickmann,A., and Felbor,U. 2007. Proteomic analysis of cathepsin B- and L-deficient mouse brain lysosomes. *Biochim.Biophys.Acta* 1774:1237-1246.

144. Yoshiyama,Y., Arai,K., Oki,T., and Hattori,T. 2000. Expression of invariant chain and pro-cathepsin L in Alzheimer's brain. *Neurosci.Lett.* 290:125-128.

145. Miners,J.S., van Helmond,Z., Kehoe,P.G., and Love,S. 2010. Changes with age in the activities of beta-secretase and the Abeta-degrading enzymes neprilysin, insulin-degrading enzyme and angiotensin-converting enzyme. *Brain Pathol.* 20:794-802.

146. Caccamo,A., Oddo,S., Sugarman,M.C., Akbari,Y., and LaFerla,F.M. 2005. Age- and region-dependent alterations in Abeta-degrading enzymes: implications for Abeta-induced disorders. *Neurobiol.Aging* 26:645-654.

147. Ferrer,I., Blanco,R., Carmona,M., Puig,B., Ribera,R., Rey,M.J., and Ribalta,T. 2001. Prion protein expression in senile plaques in Alzheimer's disease. *Acta Neuropathol.* 101:49-56.

148. Rezaie,P., Pontikis,C.C., Hudson,L., Cairns,N.J., and Lantos,P.L. 2005. Expression of cellular prion protein in the frontal and occipital lobe in Alzheimer's disease, diffuse

Lewy body disease, and in normal brain: an immunohistochemical study. *J.Histochem.Cytochem.* 53:929-940.

149. Saijo,E., Scheff,S.W., and Telling,G.C. 2011. Unaltered prion protein expression in Alzheimer disease patients. *Prion.* 5:109-116.

150. Whitehouse,I.J., Jackson,C., Turner,A.J., and Hooper,N.M. 2010. Prion protein is reduced in aging and in sporadic but not in familial Alzheimer's disease. *J.Alzheimers.Dis.* 22:1023-1031.

151. Vincent,B., Sunyach,C., Orzechowski,H.D., George-Hyslop,P., and Checler,F. 2009. p53-Dependent transcriptional control of cellular prion by presenilins. *J.Neurosci.* 29:6752-6760.

152. Baum,L., Hansen,L., Masliah,E., and Saitoh,T. 1996. Glycogen synthase kinase 3 alteration in Alzheimer disease is related to neurofibrillary tangle formation. *Mol.Chem.Neuropathol.* 29:253-261.

153. Causevic,M., Farooq,U., Lovestone,S., and Killick,R. 2010. beta-Amyloid precursor protein and tau protein levels are differently regulated in human cerebellum compared to brain regions vulnerable to Alzheimer's type neurodegeneration. *Neurosci.Lett.* 485:162-166.

154. Klafki,H.W., Lewczuk,P., Kamrowski-Kruck,H., Maler,J.M., Muller,K., Peters,O., Heuser,I., Jessen,F., Popp,J., Frolich,L. *et al.* 2009. Measurement of ERK 1/2 in CSF from patients with neuropsychiatric disorders and evidence for the presence of the activated form. *J.Alzheimers.Dis.* 18:613-622.

155. Zhu,X., Sun,Z., Lee,H.G., Siedlak,S.L., Perry,G., and Smith,M.A. 2003. Distribution, levels, and activation of MEK1 in Alzheimer's disease. *J.Neurochem.* 86:136-142.

156. Boland,B. and Campbell,V. 2004. Abeta-mediated activation of the apoptotic cascade in cultured cortical neurones: a role for cathepsin-L. *Neurobiol.Aging* 25:83-91.

157. Haass,C., Lemere,C.A., Capell,A., Citron,M., Seubert,P., Schenk,D., Lannfelt,L., and Selkoe,D.J. 1995. The Swedish mutation causes early-onset Alzheimer's disease by beta-secretase cleavage within the secretory pathway. *Nat.Med.* 1:1291-1296.

158. Meh,P., Pavsic,M., Turk,V., Baici,A., and Lenarcic,B. 2005. Dual concentration-dependent activity of thyroglobulin type-1 domain of testican: specific inhibitor and substrate of cathepsin L. *Biol.Chem.* 386:75-83.

159. Carlsson,C.M. 2008. Lessons learned from failed and discontinued clinical trials for the treatment of Alzheimer's disease: future directions. *J.Alzheimers.Dis.* 15:327-338.

APPENDICES

Appendix 1. The demographic and neuropathological data of FAD, SAD patients and control individuals included in the protein expression analysis

Group	Source	Gender	Age of onset	Age of death	Disease duration	Braak	CERAD score	ApoE	FC	TC	Crb
Ctr	GNA	F	----	61	----	ND	----	ND			X
Ctr	GNA	M	----	60	----	ND	----	ND			X
Ctr	GNA	F	----	60	----	ND	----	ND			X
Ctr	NBB	F	----	54	----	ND	----	3/3			X
Ctr	NBB	F	----	50	----	ND	----	ND			X
Ctr	UKE	M	----	63	----	II	----	ND	X	X	
Ctr	UKE	F	----	69	----	ND	----	ND	X	X	
Ctr	UKE	F	----	75	----	II	----	ND	X	X	
Ctr	UKE	M	----	86	----	III	----	ND	X	X	
Ctr	UKE	M	----	61	----	ND	----	ND	X	X	
FAD	GNA	F	47	54	7	VI	C	3/3	X	X	X
FAD	GNA	F	39	59	20	VI	C	3/4	X	X	X
FAD	GNA	F	46	66	20	VI	C	3/4	X	X	X
FAD	GNA	F	48	64	16	VI	C	3/3	X	X	X
FAD	GNA	F	37	47	10	VI	C	3/3	X	X	X
SAD	GNA	M	80	86	6	IV	C	ND	X	X	X
SAD	GNA	F	82	91	9	VI	C	3/3	X	X	X
SAD	GNA	F	65	74	9	IV	C	3/3	X	X	X
SAD	GNA	F	65	76	11	VI	C	4/4	X	X	X
SAD	GNA	F	69	76	7	VI	C	3/4	X	X	X

FC: Frontal cortex; TC: Temporal cortex; Crb:Cerebellum; ND. Not defined
GNA: Neuroscience Group of Antioquia
NBB: The Netherlands Brain Bank
UKE: Institute for Neuropathology - UKE

Appendix 2. The demographic and neuropathological data of patients and controls included in TMA-analysis

	AD	Controls
Number of patients	n = 38	n = 34
Age at death	80.4 ± 11.2	75.9 ± 12.5
Ratio male: female	15:23	17:17
CERAD-Classification		
Normal	0	34
Possible	5	0
Probable	9	0
Definite	24	0
Braak-Stages		
0	0	31
I	5	1
II	3	1
III	5	1
IV	8	0
V	13	0
VI	4	0

Appendix 3. Cloning of Testican-1
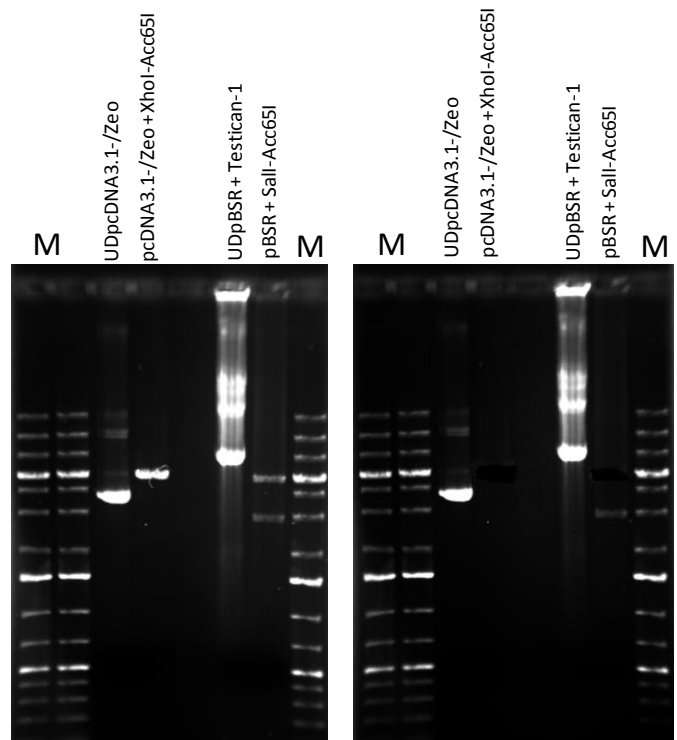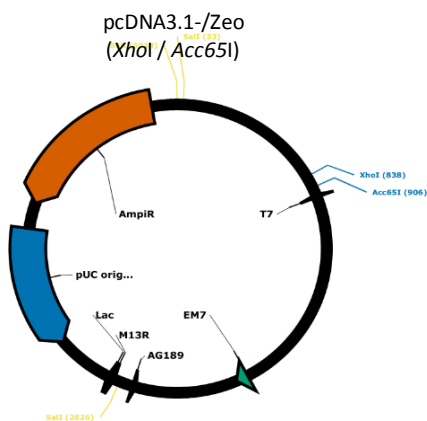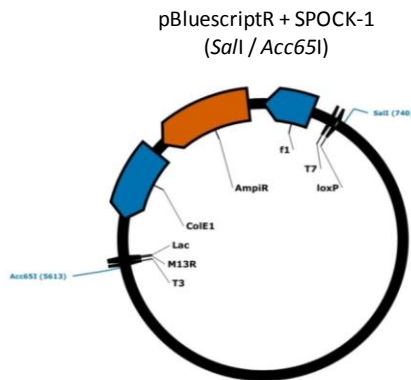
Appendix 4. Primers used for Testican-1 sequencing

Name	Sequence (5'… - …3')	Tm (°C)	Base Count
T1_1Fn	CTCGAGCAACTCGGACTA	59.3	18
T1_2Fn	AGCCCTCACAAAGTGTGT	58.2	18
T1_3Fn	AACAGAGTCATCAAGCCC	57.6	18
T1_4Fn	AAGCTGAGTAAGGGGAAA	56.4	18
T1_5Fn	TCACTTCCTATTCCTGCA	56.7	18
T1_6Fn	CCCTTTTTGATTACCCAC	56.8	18
T1_5F	AGAAAGACTGTATGTGTGTGC	56.8	21
T1_6F	TCCCCTTCTACTGACAAATC	58.2	20
T1_7F	AGCAAGAAATATGTTCAGCC	58.4	20
T1_8F	CCACTGATTTTAATTTGCCT	58.2	20
T1_9F	CACTTAGAAAAACTTCTAGGAA	53.8	22
T1_10F	GAATGTTTGCTTTCTTCTTC	55.6	20
T1_11F	ACAGCAGCAAATGACAAC	57.2	18

Appendix 5. Characterization of HEK293T cells stably transfected with APPwt and APPsw
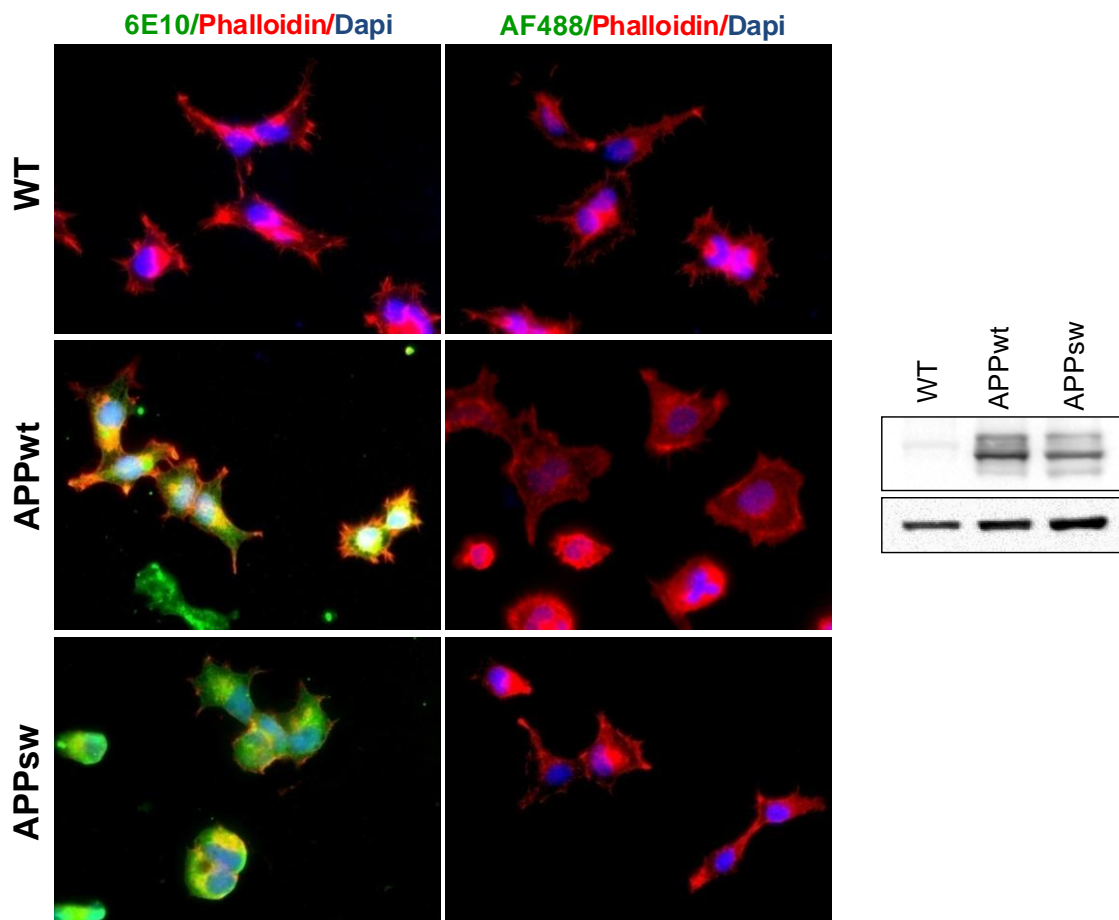
Appendix 6. Characterization of HEK293T cells stably transfected with APPwt and APPsw

HEK293T
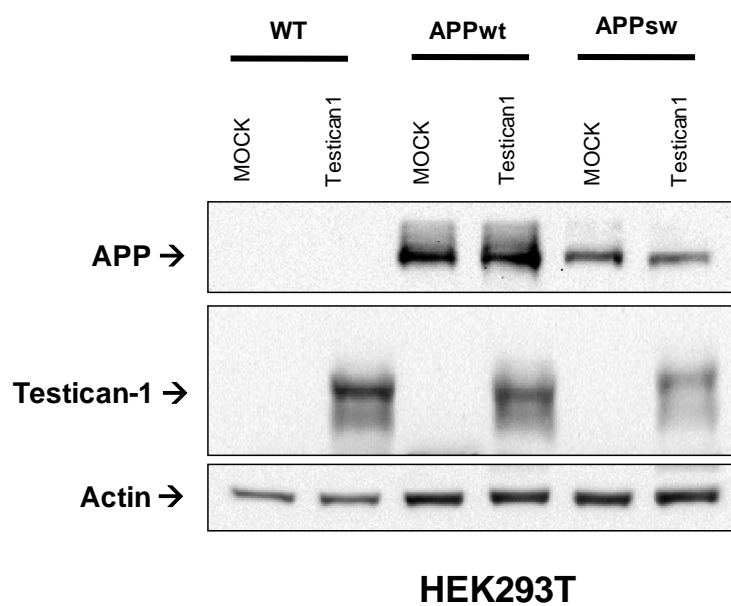
Appendix 7. Results of the Tissue Microarrays plaque count for Testican-1 and Aβ

	Testican-1					Beta-Amyloid															
						Total Plaques					Neuritic Plaques					Diffuse Plaques					
	AD		Controls			AD		Controls			AD		Controls			AD		Controls		
Brain region	mean	SD	mean	SD	p	mean	SD	mean	SD	p	mean	SD	mean	SD	p	mean	SD	mean	SD	p
Frontal cortex	3.3	3.0	0.3	0.5	<0.001	18.7	16.8	0.7	2.4	<0.001	0.6	0.7	0.0	0.1	<0.001	18.1	16.4	0.7	2.4	<0.001
Temporal cortex	3.6	2.7	0.4	0.4	<0.001	12.0	9.8	3.5	11.9	<0.005	0.5	0.5	0.1	0.1	<0.001	11.5	9.6	3.5	11.8	<0.005
Entorhinal cortex	1.4	1.2	0.3	0.4	<0.001	6.6	7.2	2.3	7.5	<0.05	0.1	0.2	0.1	0.3	0.29	6.5	7.1	2.2	7.2	<0.05

Appendix 8. Equipment used during this study

Product	Company, City
8-channel pipette 20-200	Eppebdorf, Hamburg
ASP300S tissue processor	Leica, Wetzlar
Autoclave	Memmert, Schwabach
Bacteria incubator	Heraeus electronic, Hanau
Balance	Vibra, Tokyo
Balance, precision	Sartorius, Göttingen
Centrifuge 5415 R, refrigerated, rotor F45-24-11	Eppebdorf, Hamburg
Centrifuge 5430 R, refrigerated, rotor F45-24-11 HS	Eppebdorf, Hamburg
Centrifuge 5810 R, refrigerated, rotor A-4-62	Eppebdorf, Hamburg
Centrifuge, mini MC6	Sarstedt, Nümbrecht
Cryostat CM 1950	Leica, Wetzlar
Electrophoresis, horizontal mini-sub cell GT	BioRad, München
Electrophoresis, vertical mini-protean cell	BioRad, München
Gel caster & combs	BioRad, München
Gel documentation De Vision G	Decon Science Tec GmbH, Hohengandern
Imaging system Chemi Doc XRS	BioRad, München
Incubator (cell culture)	Heraeus electronic, Hanau
Incubator (immunohistochemistry)	Memmert, Schwabach
Cabinet, horizontal flow HERAsafe	Heraeus electronic, Hanau
Magnetic stirrer with heating RCT basic IKAMAG	IKA Werke GmbH&Co. KG, Staufen
Microscope Axioskop40	Zeiss, Göttingen
Microscope, confocal TCS SP2	Leica, Wetzlar
Micropipette 0.1 - 2.5 µL	Eppebdorf, Hamburg
Micropipette 1 - 10 µL	Eppebdorf, Hamburg
Micropipette 10 - 100 µL	Eppebdorf, Hamburg
Micropipette 100 - 1000 µL	Eppebdorf, Hamburg
Microtome SM2000R	Leica, Wetzlar
Microwave Micromat	AEG, Frankfurt am Main
Neubauer counting chamber, 0.1mm	Assistent, Sondheim
pH meter CG 840	Schott, Mainz
Photometer, Biophotometer plus	Eppebdorf, Hamburg
Pipette boy	Integra Bioscience, Fernwald
Powersupply, easy volt	Stratagene, Waldbronn
Printer P93D	Mitsubishi, Ratingen
Shaker, overhead rotationbar	Hartenstein, Würzburg
Shaker, platform STR6	Stuart Scientific, Essex
Spectrophotometer µQuant	Biotek, Bad Friedrichshall
Thermal cycler MyCycler	BioRad, München
Thermomixer	Eppebdorf, Hamburg
Ventana Benchmark XT	Ventana, Tucson
Vortex	IKA Werke GmbH&Co. KG, Staufen
Waterbath	P-D Industriegesell. mbH, Dresden

Appendix 9. Reagents used during this study

Product	Company, City	DNA	Protein	IHC/ICC	Cells
1 Kb DNA Plus-ladder	Fermentas, St. Leon-Rot	X			
10-20% Tricine gels	Invitrogen, Darmstadt		X		
2-mercaptoethanol	Merck, Darmstadt		X		
2-propanol	Riedel-de Haen, Seelze	X	X		
4',6-diamidino-2-phenylindole (DAPI)	Sigma, Munich			X	
acetone	Roth, Karlsruhe				X
acrylamide/bisacrylamide , Mix 37,5:1	Roth, Karlsruhe		X		
agarose	Invitrogen, Darmstadt	X			
ammoniumperoxidesulfate (APS)	Roth, Karlsruhe		X		
antibody diluent solution	Zytomed, Berlin			X	
autoclaved aqua bidest	UKE, Hamburg	X			
BCA Protein Assay Kit	Thermo Scientific, Bremen		X		
bovine serum albumin (BSA)	PAA, Pasching		X		
bromophenol blue	Merck, Darmstadt	X	X		
cell culture dish, 10 cm, sterile	Nunc, Langenselbold				X
cell culture dish, 6 wells, sterile	Nunc, Langenselbold				X
Complete Mini, EDTA-free, prot. inhibitor	Roche, Munich		X		
coverslips Glaswarenfabrik	K. Hecht, Sondheim			X	
Cryovial-cryotubes, sterile	Roth, Karlsruhe				X
diaminiobenzidine (DAB)	Sigma, Munich			X	
di-Sodium hydrogen phosphate dihydrate	Roth, Karlsruhe		X		
DMEM	PAA, Pasching				X
DMSO (Dimethyl sulfoxide)	Sigma, Munich				X
Dulbecco's PBS (1x)	PAA, Pasching				X
ECL Western Blotting Substrate	Thermo Scientific, Bremen		X		
ELISA kit human Aβ40 quantification	Invitrogen, Darmstadt		X		
ELISA kit human Aβ42 quantification	Invitrogen, Darmstadt		X		
eosin	Merck, Darmstadt			X	
ethanol	UKE, Hamburg	X		X	
ethidium bromide	Sigma, Munich	X			
ethylendiaminetetraacetat (EDTA)	Sigma, Munich	X	X		
Fetal Bovine Sera (FBS), standard quality	PAA, Pasching				X
Fluoromount-G	Southern Biotech, Birmingham		X		
G418 (Gentamycin)	PAA, Pasching				X
Gene GeLIPCR purification Kit	Fermentas, St. Leon-Rot	X			
glas pipette 230 mm AdvantageTM, sterile	BD Labware, Heidelberg				X
glycerol	Merck, Darmstadt	X	X		
glycine	Sigma, Munich		X		
Harri's Hämatoxylin	ROTH, Karlsruhe			X	
hydrogen peroxide	Sigma, Munich			X	
Lipofectamine 2000	Invitrogen				
Mayer's Hämalaun	Merck, Darmstadt			X	
methanol	J.T.Baker, Griesheim		X	X	
mounting media GLC	Sakura Finetek GmbH, Staufen			X	
multiply PCR plate natural 96-well	Sarstedt, Nümbrecht	X			
N',N'-tetramethylethylenediamine (TEMED)	Sigma-Aldrich, Hamburg		X		
Nitrocellulose membran (0.2 µm)	Biorad, Munich		X		
object slide Superfrost Glaswarenfabrik	K. Hecht, Sondheim			X	
Oligonucleotides (0.025 µmol HPLC pur)	Sigma, Munich	X			

Opti-MEM® reduced serum medium (1x)	Invitrogen, Darmstadt			X
Page RulerTM , Prestained Protein Ladder	Fermentas, St. Leon.Rot	X		
paraformaldehyd	Büfa Chemikalien, Hude		X	
Penicillin/Streptomycin (100x)	PAA, Pasching			X
Phalloidin	Invitrogen, Darmstadt			
pipettes Serol 2 ml, 5 ml, 10 ml, 25 ml	BD Labware, Heidelberg			X
plasmid DNA purification kit (Midi prep)	Macherey-Nagel, Düren	X		
plasmid DNA purification kit (Mini prep)	Invitek, Berlin	X		
ponceau S	Sigma-Aldrich, Hamburg		X	
potassium chloride	Fluka Biochemika, Deisenhofen		X	
potassium dihydrogen phosphate	Merck, Darmstadt		X	
restriction enzymes	Fermentas, St. Leon-Rot	X		
safeseal tips premium from Biozym	Biozym, Hessisch Ohlendorf	X		
skimmed milk powder instant ,,Frema"	Granovita GmbH, Lüneburg		X	
sodium azide	Fluka Biochemika, Deisenhofen		X	
sodium chloride	Sigma, Munich		X	
sodium hydroxide	Roth, Karlsruhe		X	
sodiumdodecyl sulfate (SDS)	Sigma, Munich		X	
sulfuric acid 6 M	Roth, Karlsruhe		X	
SuperSignal West Femto	Thermo Scientific, Bremen		X	
SuperSignal West Pico	Thermo Scientific, Bremen		X	
T4 ligase	Fermentas, St. Leon-Rot	X		
tetramethyl benzidine reagent (TMB kit)	Thermo Scientific, Bremen		X	
Tissue Tek	Sakura Finetek GmbH, Staufen			X
Triton X 100	Roth, Karlsruhe			X
trizma base, minimum, 99.9 % titration	Sigma, Munich	X		
Trypsin-EDTA (1x)	PAA, Pasching			X
Tween 20	Roth, Karlsruhe		X	
UVette® for spectrophotometer	Eppendorf, Hamburg	X		
Whatman® Paper 3MM (blotting-paper)	Schleicher&Schuell, Dassel		X	
XL10-Gold competent cells	Stratgene, Waldbronn	X		
Xylol	Fischer, Wiesbaden			X

Appendix 10. Primary antibodies used during this study

Name	Host	Reactivity	Mol. Weight	Type/Isotype	Manufacturer	Method	Dilution
Anti-APP (6E10)	Mouse	H	100-140 kDa	Monoclonal, IgG1	Covance	WB, ICC	WB(1:1000), ICC(1:100)
Anti-APP C-Terminal	Rabbit	H, M, R	11/95-100 kDa	Polyclonal, IgG	Sigma	WB	WB(1:500)
Anti-ADAM10	Rabbit	H, M, R	84 kDa	Polyclonal	Dr. Paul Saftig	WB	WB(1:1000)
Anti-BACE C-Terminal	Mouse	H, M, R	60-75 kDa	Monoclonal, IgG1	Millipore	WB	WB(1:1000)
Anti-Presenilin 1 (CTF)	Rabbit	H, M, R, MK	22-55 kDa	Polyclonal	Cell Signaling Tech	WB	WB(1:500)
Anti-Cathepsin L	Goat	H, M, R	25/42 kDa	Polyclonal, IgG	Santa Cruz Biotech	WB	WB(1:1000)
Anti-Cathepsin L	Mouse	H, M, R	25/42 kDa	Monoclonal, IgG1	Abcam	ICC	ICC(1:100)
Anti-Prion Protein (POM1)	Mouse	H, M, R	25-35 kDa	Monoclonal, IgG1	Dr. Adriano Aguzzi	WB	WB(1:1000)
Anti-IDE	Rabbit	H, M, R	118 kDa	Polyclonal, IgG	Abcam	WB	WB(1:1000)
Anti-pGSK3beta (Tyr216)	Mouse	H, M, R	46 kDa	Monoclonal, IgG1	BD Biosciences	WB	WB(1:1000)
Anti-pGSK3beta (Ser9)	Rabbit	H, M, R, MK	46 kDa	Monoclonal, IgG	Cell Signaling Tech	WB	WB(1:1000)
Anti-GSK3beta	Rabbit	H, M, R, MK	46 kDa	Monoclonal, IgG	Cell Signaling Tech	WB	WB(1:1000)
Anti-Erk 1/2	Rabbit	H, M, R, MK	42/44 kDa	Polyclonal	Cell Signaling Tech	WB	WB(1:1000)
Anti-pErk 1/2	Mouse	H, M, R, MK	42/44 kDa	Monoclonal, IgG1	Cell Signaling Tech	WB	WB(1:1000)
Anti-Testican-1	Rabbit	H	50 kDa	Polyclonal	Sigma-Prestige antibodies	WB, ICC	WB(1:1000), ICC(1:100)
Anti-Testican-1/CTF	Rabbit	H	2.6/50 kDa	Polyclonal	Biogenes - NP UKE	ELISA	ELISA(1:100)
Anti-βActin	Rabbit	H, M, R	42 kDa	Polyclonal	Sigma	WB	WB(1:5000)
Anti-GAPDH	Mouse	H, M, R	38 kDa	Monoclonal, IgG1	Millipore	WB	WB(1:5000)
Anti-KDEL	Mouse	H, M, R	94 kDa	Monoclonal, IgG2b	Enzo Life Sci	ICC	ICC(1:100)
Anti-GM130	Mouse	H, M, R	130 kDa	Monoclonal, IgG1 kappa	BD Biosciences	ICC	ICC(1:100)
Anti-EF-1 alfa	Mouse	H, M, R	53 kDa	Monoclonal, IgG kappa	Millipore	ICC	ICC(1:100)
Anti-Adaptin gamma	Mouse	H, M, R	104 kDa	Monoclonal, IgG1	BD Biosciences	ICC	ICC(1:100)

H: Human; M: Mouse; R: Rat, MK: Monkey
WB: Western blot
ICC: Immunocytochemistry, immunohistochemistry or immunofluorescence

Appendix 11. Secondary antibodies used during this study

Name	Host	Reactivity	Type/Isotype	Manufacturer	Method	Dilution
Anti-Mouse-HRP	Goat	M	IgG (H+L)	Invitrogen	WB	WB(1:2500)
Anti-Rabbit-HRP	Goat	R	IgG (H+L)	Invitrogen	WB	WB(1:2500)
Anti-Goat-HRP	Rabbit	G	IgG (H+L)	Thermo - Pierce	WB	WB(1:2500)
Anti-Mouse Alexa Fluor 488	Donkey	M	IgG (H+L)	Invitrogen	ICC	WB(1:5000)
Anti-Rabbit Alexa Fluor 488	Donkey	R	IgG (H+L)	Invitrogen	ICC	WB(1:5000)
Anti-Mouse Alexa Fluor 555	Goat	M	IgG1 gamma1	Invitrogen	ICC	WB(1:5000)
Anti-Human FITC	Mouse	H	IgG	Sigma	ICC	WB(1:5000)

M: Mouse; R: Rabbit, G: Goat
WB: Western blot
ICC: Immunocytochemistry, immunohistochemistry or immunofluorescence

Appendix 12. Preparation of solutions used during this study

1x TAE

Tris base	40 mM
Acetic acid	40 mM
EDTA	1 mM
pH 8	

10X DNA loading buffer

Tris HCl pH 7.6	10 mM
EDTA	60 mM
Glycerol	60 %
Bromophenol blue	0.002 %

NZY$^+$ broth

Bacto-Tryptone	10 g
Bacto-yeast extract	5 g
NaCl	5 g
Distilled water to	1 L

HSG medium

Casein-peptone	13.5 g
NaCl	12.5 g
Yeast extract	7 g
Glycerin (87%)	17 g
K_2HPO_4	2.3 g
KH_2PO_4	1.5 g
$MgSO_4x7H_2O$	0.25 g
Water to	1 L
pH 7.4	

Lysis buffer (Protein isolation)

NaCl	150 mM
Tris pH 7.4	20 mM
EDTA	1 mM
Glycerol	10%
NP40	1%

6X Protein loading buffer

Tris pH 6.8	0.375 M
Glycerol	50%
SDS	10%
DTT	0.5 M
Bromophenol blue	0.002%

5x SDS running buffer

Tris Base pH 8.3	15.1 g
Glycine	72 g
SDS	5 g
Deionized water to	1 L

Transfer buffer (Tobwin)

5x SDS running buffer	200 mL
Methanol	20%
Deionized water to	1 L

Preparation of SDS-PA stacking and running gels for protein analysis

SDS-PAGE Gel (30% Acrylamide - 29:1 or 37.5:1 ratio)

6% Running Gel

Reagent	5	7	10	15	20	25	30	40	50
Water	2,6	3,7	5,3	7,9	10,6	13,2	15,9	21,2	26,5
30%Acrylamide/Bis mL	1,0	1,4	2,0	3,0	4,0	5,0	6,0	8,0	10,0
1.5 M Tris-HCl pH 8.8 mL	1,25	1,75	2,50	3,75	5,00	6,25	7,50	10,00	12,50
10% SDS uL	50	70	100	150	200	250	300	400	500
10% APS uL	50	70	100	150	200	250	300	400	500
TEMED uL	5	7	10	15	20	25	30	40	50

8% Running Gel

Reagent	5	7	10	15	20	25	30	40	50
Water	2,3	3,2	4,6	6,9	9,2	11,6	13,9	18,5	23,1
30%Acrylamide/Bis mL	1,33	1,87	2,67	4,00	5,33	6,67	8,00	10,67	13,33
1.5 M Tris-HCl pH 8.8 mL	1,25	1,75	2,50	3,75	5,00	6,25	7,50	10,00	12,50
10% SDS uL	50	70	100	150	200	250	300	400	500
10% APS uL	50	70	100	150	200	250	300	400	500
TEMED uL	5	7	10	15	20	25	30	40	50

10% Running Gel

Reagent	5	7	10	15	20	25	30	40	50
Water	2,0	2,8	4,0	5,9	7,9	9,9	11,9	15,8	19,8
30%Acrylamide/Bis mL	1,67	2,33	3,33	5,00	6,67	8,33	10,00	13,33	16,67
1.5 M Tris-HCl pH 8.8 mL	1,25	1,75	2,50	3,75	5,00	6,25	7,50	10,00	12,50
10% SDS uL	50	70	100	150	200	250	300	400	500
10% APS uL	50	70	100	150	200	250	300	400	500
TEMED uL	5	7	10	15	20	25	30	40	50

12% Running Gel

Reagent	5	7	10	15	20	25	30	40	50
Water	1,6	2,3	3,3	4,9	6,6	8,2	9,9	13,2	16,5
30%Acrylamide/Bis mL	2,00	2,80	4,00	6,00	8,00	10,00	12,00	16,00	20,00
1.5 M Tris-HCl pH 8.8 mL	1,25	1,75	2,50	3,75	5,00	6,25	7,50	10,00	12,50
10% SDS uL	50	70	100	150	200	250	300	400	500
10% APS uL	50	70	100	150	200	250	300	400	500
TEMED uL	5	7	10	15	20	25	30	40	50

15% Running Gel

Reagent	5	7	10	15	20	25	30	40	50
Water	1,1	1,6	2,3	3,4	4,6	5,7	6,9	9,2	11,5
30%Acrylamide/Bis mL	2,50	3,50	5,00	7,50	10,00	12,50	15,00	20,00	25,00
1.5 M Tris-HCl pH 8.8 mL	1,25	1,75	2,50	3,75	5,00	6,25	7,50	10,00	12,50
10% SDS uL	50	70	100	150	200	250	300	400	500
10% APS uL	50	70	100	150	200	250	300	400	500
TEMED uL	5	7	10	15	20	25	30	40	50

5% Stacking Gel

Reagent	5	7	10	15	20	25	30	40	50
Water	2,8	3,9	5,6	8,4	11,2	14,0	16,8	22,4	28,0
30%Acrylamide/Bis mL	0,83	1,17	1,67	2,50	3,33	4,17	5,00	6,67	8,33
0.5 M Tris-HCl pH 6.8 mL	1,26	1,76	2,52	3,78	5,04	6,30	7,56	10,08	12,60
10% SDS uL	50	70	100	150	200	250	300	400	500
10% APS uL	50	70	100	150	200	250	300	400	500
TEMED uL	5	7	10	15	20	25	30	40	50

6X Protein loading buffer for tricine gels

Tris pH 6.8	0.15 M
Glycerol	36%
SDS	12%
DTT	0.3 M
Coomasie Blue	0.002%

10X Cathode buffer

Tris base	1M
Tricine	1M
SDS	1%

10X Anode buffer

Tris base	1M
HCl	0.225 M

1X TBS

Tris HCl pH 7.5	100 mM
NaCl	500 mM

1X TTBS

Tris HCl pH 7.5	100 mM
NaCl	500 mM
Tween 20	0.02%

Appendix 13. Abbreviations

%	percentage
°C	degree Celcius
AD	Alzheimer's disease
ADAM	desintegrin and metalloproteinase domain proteins
AICD	amino-terminal APP intracellular domain
APLP1/2	amyloid precursor-like proteins 1 and 2
APOE- ε4	Apolipoprotein E-ε4
APP	amyloid precursor protein
APS	ammoniumperoxidsulfat
Aβ	amyloid beta
BACE1	beta-site APP cleaving enzyme 1
bp	base pair
BSA	bovine serum albumin
CDK5	cyclin dependent kinase 2
cDNA	complementary deoxyribonucleic acid
CNS	central nervous system
CSF	cerebrospinal fluid
CTF	C-terminal fragment
DAB	diaminiobenzidine
DMEM	Dulbecco's Modified Eagle's Medium
DMSO	dimethylsulfoxid
DNA	deoxyribonucleic acid

dNTPs	desoxynucleotide triphosphate (s)
DTT	dithiothreitol
ECL	enhanced chemiluminiscence
EDTA	ethylendiamintetraacetat
ELISA	enzyme-linked immunosorbent assay
ER	endoplasmic reticulum
Erk1/2	Extracellular signal related kinase 1 and 2
FAD	familial Alzheimer's disease
FBS	fetal bovine sera
FL	full lenght
g	accelaration
g	gram
GSK3β	Glycogen synthase kinase 3β
h	hour
HRP	horse radish peroxidase
IDE	insulin degrading enzyme
JNK	c-Jun NH2-terminal kinases
kb	kilo base (= 1000 bp)
kDa	kilo Dalton (= 1000 Da)
L	liter
LTP	long-term potentiation
M	molar
mA	mili amper
mg	miligram
min	minute
mL	mililitre
mM	milimolar
mRNA	messenger RNA
Nct	nicastrin
ng	nanogram
nm	nanometer
NFT	neurofibrillary tangles
OD	optical densitiy
PAGE	polyacrylamide gel electrophoresis
PBS	phosphate buffered saline
pH	potentia hydrogenii
PKA	cAMP-dependent protein kinase
PrP^c	Prion protein
PS1	presenilin-1
PS2	presenilin-2

RNA	ribonucleic acid
rpm	round per minute
SAD	sporadic Alzheimer's disease
SDS	sodiumdodecyl sulfate
SDS-PAGE	Sodium dodecyl sulfate polyacrylamide gel electrophoresis
sec	seconds
TBS	tris buffered saline
TEMED	N',N'-tetramethylethylenediamine
TMA	Tissue microarray
TMB	3,3´,5,5´-Tetramethylbenzidine
TNG	trans-Golgi network
TTBS	tris buffered saline with Tween
U	unit
V	volt
WT	wild-type
µg	microgram
µL	microlitre

ACKNOWLEDGMENTS

I must also acknowledge to my friends and colleagues from the Institute for Neuropathology for their support and the moments shared during my time in the lab. Especially, I would like to express my gratitude to Dr. Berta Puig-Martorell and Beata Szalay for their friendship and technical support during my PhD.

I am particularly indebted to my wife and best friend Carmen, who with her love and patience was my source of motivation and hope, and to my son Simon for filling my live with happiness and smiles.

Finally, I thank my mother for instilling in me confidence and a drive for pursuing my PhD.